Copyright Undertaking

This thesis is protected by copyright, with all rights reserved.

By reading and using the thesis, the reader understands and agrees to the following terms:

1. The reader will abide by the rules and legal ordinances governing copyright regarding the use of the thesis.

2. The reader will use the thesis for the purpose of research or private study only and not for distribution or further reproduction or any other purpose.

3. The reader agrees to indemnify and hold the University harmless from and against any loss, damage, cost, liability or expenses arising from copyright infringement or unauthorized usage.

Pao Yue-kong Library, The Hong Kong Polytechnic University, Hung Hom, Kowloon, Hong Kong

http://www.lib.polyu.edu.hk

SYSTEMATIC STUDY OF INDUSTRIAL SCALE SUSTAINABLE COLOUR FADING PROCESS OF COTTON FABRIC

LIU SENBIAO

PhD

The Hong Kong Polytechnic University

2023

The Hong Kong Polytechnic University

School of Fashion and Textiles

Systematic Study of Industrial Scale Sustainable Colour Fading Process of Cotton Fabric

LIU Senbiao

A thesis submitted in partial fulfilment of the requirements for the degree of Doctor of Philosophy

February 2023

CERTIFICATE OF ORIGINALITY

I hereby declare that this thesis is my own work and that, to the best of my knowledge and belief, it reproduces no material previously published or written, nor material that has been accepted for the award of any other degree or diploma, except where due acknowledgement has been made in the text.

_____   _____ (Signed)

_____LIU Senbiao (刘森标)_____ (Name of student)

Abstract

Plasma treatment is an environmentally friendly fading method that requires constant adjustment to obtain accurate fading results. However, the mechanism by which variations in plasma treatment parameters affect fading results is still unclear. Through a systematic review of how artificial intelligence techniques had been applied to the textile colour fading field, it had been found that the application of artificial intelligence techniques might be able to predict well what fading results would result from different plasma treatment parameters.

This study used a Bayesian Regulated Neural Network (BRNN) with 10-fold cross-validation to accurately predict the fading effect of plasma treatment on cotton fabrics for given parameters. This prediction system used a modular approach, with multiple independent models trained to avoid the effects of small sample sizes further. The inputs included plasma treatment parameters and colour measurements of the cotton fabric before fading, while the outputs included colour measurements after fading. Plasma treatment parameters included colour depth, air (oxygen) concentration, water content and treatment time. Colour measurements included CIE L*a*b*C*h values and K/S values. The datasets collected for model training in this study were divided into three categories, namely 216 datasets of reactive dye-dyed cotton fabrics, 216 datasets of sulphur-dyed cotton fabrics and 162 datasets of two-colour mixed-dyed cotton fabrics. The coefficient of determination R^2 of the model fit was close to 1. Moreover, the difference between the predicted and actual colours was negligible or within acceptable limits for the different colour difference formulas for 82.35% to 95.83% of the test set samples.

In addition, polynomial regression models were used in this study to investigate the relationship between the single-colour fading effect and the two-colour mixed fading effect of plasma-

treated cotton fabrics. In most cases, the colour characteristics of the two-colour mixed fading effect of plasma-treated cotton fabrics might be predicted from the known single-colour fading effect of plasma-treated cotton fabrics. It was found that the relatively low R^2 of the polynomial regression model on the CIE L* values might reflect the relatively poor relationship between the lightness levels of the single-colour fading effect and the two-colour mixed fading effect of plasma-treated cotton fabrics. In contrast, the R^2 of the polynomial regression models for CIE a* values, CIE b* values and K/S values were all above 0.99, suggesting that the relationship between the single-colour fading effect and the two-colour mixed fading effect might be more reflected in the colour-related CIE a* and CIE b* values, or in the K/S values related to the dyeing level.

Acknowledgements

Table of Contents

List of Figures

List of Tables

XVI

List of Publications

Liu, S., Lo, C. K., & Kan, C. W. (2022). Application of artificial intelligence techniques in textile wastewater decolorisation fields: A systematic and citation network analysis review. *Coloration Technology*, *138*(2), 117-136. https://doi.org/10.1111/cote.12589

Liu, S., Liu, Y. H., & Kan, C. W. (2023). Using Bayesian Regulated Neural Network (BRNN) to predict the effect of plasma treatment on the fading effect of cotton fabric. *The Journal of the Textile Institute*, 1-11. https://doi.org/10.1080/00405000.2023.2220218

Liu, S., Liu, Y. H., & Kan, C. W. (2022). Predicting the effect of plasma treatment on the fading of sulphur-dyed cotton fabric using Bayesian Regulated Neural Network (BRNN). *Fashion and Textiles*, reply to comments

Liu, S., Liu, Y. H., Lo, C. K., & Kan, C. W. (2022). Analyzing the effects of plasma treatment process parameters on fading of cotton fabrics dyed with two-color mix dyes using Bayesian conditioning neural networks (BRNNs). *Journal of Natural Fibers*, reply to comments

Liu, S., Liu, Y. H., Lo, C. K., & Kan, C. W. (2023). Intelligent Techniques and Optimization Algorithms in Textile Colour Management: A Systematic Review of Applications and Prediction Accuracy. *Fashion and Textiles*, under review

Chapter 1 Introduction

1.1 Background

Chemical processing can add value to textiles from the perspective of fashion and functionality, and ensure the necessary visual appeal and comfort (Samanta et al., 2017). Recently, fashion and apparel trends focused on the visual effect of fading. An important example is fading blue jeans (Hung et al., 2011) because fading effects are particularly popular among young adults. These fading effects are achieved through a series of physical, chemical, and mechanical finishing (Venkatraman & Liauw, 2019).

Moreover, faded effects are also a viable way for garment manufacturers to increase the value of their products, as consumers may be more inclined to purchase if textile products have a faded effect (Samanta et al., 2017). Therefore, the fading treatment of cotton fabric is essential to the value addition of final garment products (Samanta et al., 2017). For faded jeans, in some areas, they are even more expensive than bright blue jeans that look brand new. With the addition of some design and texture to the fabric surface, fabric manufacturers are able to change the aesthetics of the fabric and achieve a higher profit margin, which is an ideal method for the fabric sector to respond to the consumer's demand, thereby improving the added value of the product (Samanta et al., 2017).

Therefore, in recent years, companies have been trying to develop various technologies to fade out the colour of fabrics, such as laser fading process (Dascalu et al., 2000; Ortiz-Morales et al., 2003). The fading effects can be achieved through traditional fading technologies, such as stone washing, sand washing, enzyme washing, etc. (Kan et al., 2010). However, these methods have problems, such as inconsistent surface effects (Kan et al., 2010), and may cause serious

environmental and health risks (Venkatraman & Liauw, 2019). In addition, these labour-intensive and traditional procedures are difficult to scale up since they raise costs and degrade quality, which leads to insufficient supply and cannot meet the huge demand for fading effect in the jeans market (Kan et al., 2010). There are many limitations in using traditional methods to create fading effects. For example, the durability of the fabric is reduced with these types of methods (Samanta et al., 2017). In addition, using traditional techniques to produce fading effects on fabrics involves considerable water consumption, much of which is severely polluted by the chemicals applied during the fading process (Kan et al., 2016). Thus, after considering the implementation of strict emission law (Samanta et al., 2017) and the high cost of chemical waste treatment, alternative methods should be developed to reduce the production cost (Samanta et al., 2017) and replace the traditional method of applying design and texture on the surface of textiles.

Recently, people have studied the fading methods of cotton fabrics which have little harm to the environment. These methods include plasma, laser, and ozone treatment (Venkatraman & Liauw, 2019). Therefore, in this research, we propose non-aqueous technology as an alternative, as it is not only an entirely dry treatment method but also an environmentally friendly process as well as able to make the fading effect in low health risk conditions (Venkatraman & Liauw, 2019). At present, research in the textile field is developing towards the technology of no water or less water (Samanta et al., 2017). With the help of a new plasma treatment method on the colour fading of textile materials, the drawbacks involved in conventional technologies could be tackled, including (1) difficulties in establishing repeatable and standardized designs by using chemical methods due to problems of measurement accuracy (Kan et al., 2016); and (2) inconsistent fading effects of the product (Samanta et al., 2017); and (3) water consumed in large quantities and effluents generated that are highly contaminated (Kan et al., 2016); and (4)

it is time-consuming and difficult to meet the market demand of producing fading jeans in large quantities (Samanta et al., 2017).

1.2 Critical issues

For the plasma, its ionization properties can be used for altering the surface of the fabric (Samanta et al., 2017). Faster fading can be achieved by adjusting the plasma treatment parameters (Haji & Naebe, 2020; Liu et al., 2019), and the principle is based on breaking the dye-molecule bonding in fabric surface, with an ionized gas (Morent et al., 2008; Samanta et al., 2017). Plasma can also reduce the amount of dye in plasma-treated fabrics, thus imparting higher reflectivity and producing lighter colours while providing the required fading effect (Kan et al., 2016). Plasma can fade reactive dye-dyed cotton fabrics by inducing oxygen in the air to produce ozone (Kan et al., 2016; Kan et al., 2017). Since ozone is unstable and self-decomposing, it is also broken down into oxygen at the end of fading process (Liu et al., 2019). Moreover, plasma treatment requires fewer treatment steps than conventional processes, resulting in effective water and chemical savings and better quality (Kan et al., 2016). Thus, plasma treatment is an environmentally friendly alternative to conventional fading treatments. However, the interaction of plasma with the fabric surface is complicated by a number of factors, such as plasma treatment operating parameters, chemical composition of the plasma gas and fabric properties, which has resulted in plasma treatment still not being widely used in the textile industry (Jelil, 2015; Zille et al., 2015). Among the parameters, water content, treatment time and air concentration are the main factors that affect the fading effect (Kan et al., 2016). Since it is difficult to know the right plasma treatment parameters quickly and accurately, achieving a specific fading effect requires several attempts and observations to ensure the best possible treatment.

Therefore, in order to ensure the continued development of textile manufacturing and cotton material processing industry (Samanta et al., 2017), it is necessary to develop sustainable processing technology, which can be combined with artificial intelligence (AI) techniques to quickly find the processing parameters of plasma treatment for specific fading effect. These technologies are more cost-effective and environmentally friendly when considering water, energy, cost, and wastewater, while keeping pace with environmental protection policies and the needs of modern consumers (Samanta et al., 2017). Specifically, for textile processing, sustainability means that it does not damage the environment and the workers in the production process and controls the production cost at a low level (Samanta et al., 2017). Sustainability also includes the focus on the health and safety of labourers employed by textile and garment manufacturers, such as how to reduce their exposure time to chemicals during bleaching and dyeing (Samanta et al., 2017).

1.3 Research objectives

The overarching objective of this research project encapsulates the investigation and validation of the feasibility of integrating plasma treatment technology with artificial intelligence in industrial-scale applications. This goal encompasses addressing potential complexities and unpredictable outcomes arising from the multifaceted interaction between plasma and fabric surfaces within such applications. Employing this amalgamated approach aims to enhance the quality of textiles, minimize production costs, optimize the manufacturing environment, and mitigate environmental impact.

The specific objectives are as follows.

(1) To systematically review the application of artificial intelligence techniques in the field of textile colour fading and to summarise the relevant research trends.

(2) To simulate the relationship between the plasma treatment process and the fading effect of reactive dye-dyed fabric samples by means of AI techniques and to propose a reliable model.

(3) To simulate the relationship between the plasma treatment process and the fading effect of sulphur-dyed fabric samples by means of AI techniques and to propose a reliable model.

(4) To simulate the relationship between the plasma treatment process and the fading effect of two-colour mixed-dyed fabric samples by means of AI techniques and to present a reliable model.

(5) To investigate the relationship between the single-colour fading effect and the two-colour mixed fading effect of plasma-treated cotton fabrics by means of polynomial regression models.

(6) To provide a tool for manufacturers when using AI techniques in combination with plasma treatment for fading.

1.4 Significance and Value

Plasma technology is a sustainable technology which is a completely dry process. In textile industry, this technology has been brought up in the last decade but its effect on textile colour fading process is seldom reported. Its difficulties lie in the complexity and difficulty to predict the interaction of the plasma treatment with the textile surface, and the surface changes caused by the treatment can be influenced by many factors. Therefore, by systematic investigation of this novel colour fading process, technical and theoretical aspect of this process can be well explored, which have both industrial and academic benefits. Besides, this research can lead to a breakthrough of development in dry colour fading process in fashion and textile industry. For example, by combining the application of artificial intelligence techniques in the plasma

treatment process, it is possible to predict the fading effect after treatment with different plasma parameters and to find the right plasma treatment parameters faster in order to achieve a specific fading effect. Thus, this technology also helps to increase the competitiveness of local manufacturers in the rapidly expanding global apparel. Furthermore, the purposed research can provide guideline references to the textile finishing industry for using this technology.

1.5 The thesis structure

This thesis was organized into five parts. The first part was the introduction to the effect of plasma treatment on fading under industrial conditions. The second part was a literature review, which focused on previous applications of plasma treatment of textile samples in combination with AI techniques as well as a systematic review of specific applications of AI techniques in the field of textile colour fading and a summary of relevant research trends. The third part proposed the research methodology of this study, i.e., how AI techniques were employed to develop a model of the relationship between the plasma treatment process and the fading effect of cotton fabrics and to investigate the relationship between the single-colour fading effect and the two-colour mixed fading effect of plasma-treated cotton fabrics. The fourth part was to simulate the relationship between the plasma treatment process and the fading effect of reactive dye-dyed fabric samples by artificial intelligence techniques and to propose a reliable BRNN model. The fifth part was to simulate the relationship between the plasma treatment process and the fading effect of sulphur-dyed fabric samples using artificial intelligence techniques and to propose a reliable BRNN model. The sixth part was to simulate the relationship between the plasma treatment process and the fading effect of two-colour mixed dyed fabric samples using artificial intelligence techniques and to propose a suitable BRNN model. The seventh part was to investigate the relationship between the single-colour fading effect and the two-colour mixed

dyed fading effect of plasma-treated cotton fabrics by means of a polynomial regression model.

The eighth part was the conclusion and recommendations of this thesis.

Chapter 2 Literature Review

This chapter consists of nine parts. The first part described and analysed the advantages and disadvantages of traditional chemical or mechanical methods of fading. The second part illustrated the advantages and disadvantages of plasma treatment of textile fading and its future directions for improvement. The third part was a brief description of the mechanism of colour fading of cotton textiles by plasma-induced ozone. The fourth part described the working principle of the G2 plasma machine. The fifth part explained the colour measurement process for faded cotton fabrics. The sixth part was a study of applications related to the combination of AI techniques and plasma treatment. The seventh and eighth parts were a brief introduction to the application of AI techniques in (1) colour matching and colour prediction as well as (2) colour difference detection and evaluation, respectively. These research articles might provide relevant inspiration for the study of plasma treatment combined with AI techniques for fading cotton materials. The ninth part was a summary of the chapter.

2.1 Traditional fading methods

Traditionally, the desired fading effect can be achieved in certain areas of the fabric by using various chemical or mechanical methods such as sanding, sandblasting, brushing and pre-washing (Liu et al., 2019; Samanta et al., 2017). During the production process, however, a number of challenges have arisen, such as (1) chemical or mechanical methods are difficult to establish repeatable and standardized designs (Kan et al., 2016); and (2) there are inconsistent fading effects on the products (Samanta et al., 2017); and (3) in addition to consuming a large amount of water, highly polluted effluent is also generated (Kan et al., 2016); and (4) it is difficult to produce large quantities of fading jeans (Samanta et al., 2017).

In general, chemicals or physical methods are capable of fading, but they may cause environmental pollution. As shown in Table 2.1, traditional chemical and physical methods have both advantages and disadvantages. Therefore, in light of the increasing concern of society to protect the environment, the fashion and textile industry needs to address associated health and environmental issues (Kan et al., 2016).

Table 2.1 Advantages and disadvantages of traditional fading methods

Traditional chemical or physical methods	Advantages and Disadvantages	References
Strong oxidising agents such as sodium hypochlorite, potassium permanganate, enzyme preparations	Advantages: • It is possible to achieve rapid colour fading. • Simple. Disadvantages: • Bleaching results depend on the strength of the chemical and the dose used • There are dangerous components in sodium hypochlorite, and it can react with flammable compounds • There is difficulty in reproducing and standardizing bleaching results. • In order to prevent excessive bleaching of cotton, the process must be controlled and held for an appropriate period of time • The machine's life expectancy might be reduced. • The improper use of strong oxidizing agents may pose a health risk to workers • The strength of the fabric may be compromised by improper bleaching.	(Cheung, 2018; Farooq et al., 2013; Kan et al., 2016; Kan & Yuen, 2012; Liu et al., 2019; Mundadaa & Brighub, 2016; Radetić et al., 2009; Samanta et al., 2017)

	• In order to minimize yellowing or wrinkles caused by bleaching, pre-treating the fabric with chlorine resistance is required after bleaching	
Mechanical methods such as pumice, sandblasting process, and abrasion by grinding machine	Advantages: • Fabric is soft, lubricated and flexible Disadvantages: • It is inevitable that there will be variations in quality in mass production. As a result, standardization becomes a problem. • There is a high workload, so the process might not be cost-effective. • The sandblasting process is potentially hazardous to the worker's health	(Kan et al., 2016) (Cheung, 2018; Liu et al., 2019; Robinson et al., 2001; Samanta et al., 2017)

As a result, new fading methods have been gradually developed. Plasma treatment is one method that does not require the use of water and does not emit any pollutants (Bulut & Sana, 2018; Kan et al., 2016; Kan et al., 2014; Paul, 2015). In addition, no adverse effects will be observed with regard to the bulk properties of cotton fabrics following plasma treatment (Jelil, 2015; Kan et al., 2016; Kan et al., 2017). As a result, plasma treatment may be suitable for addressing the limitations and difficulties associated with conventional fading techniques, such as inconsistency, quality loss, and difficulty in reproducing the same results over time (Cheung et al., 2013; Kan et al., 2016).

2.2 Colour fading by plasma treatment

In the cotton material processing industry, using water-based finishing systems for textile drying is energy-intensive, and the treatment of effluent is costly and environmentally hazardous (Stegmaier et al., 2009). In contrast, plasma is classified as a dry treatment, and it is a mixture of gases produced by partial ionization and then energized by an external source to

produce electrons, free radicals, and atoms (Kan, 2014; Stegmaier et al., 2009; Tonks & Langmuir, 1929). The primary strengths of plasma treatment are that textiles remain dry during treatment, no wastewater is produced, fewer chemicals are required, and the treatment is faster than conventional techniques (Stegmaier et al., 2009). This is because plasma species can crack covalent chemical bonds without changing the fibre properties, thus producing chemical and physical changes to the treated surface (Kan, 2014; Stegmaier et al., 2009). Therefore, there is room for "sustainable", "greener" and "cleaner" improvement of existing cotton processing processes (Kan, 2014), and plasma treatment can be used to complement existing wet processing methods. It means that plasma treatment can be applied as an energy-saving and economical alternative to different methods of wet processing in textiles (Stegmaier et al., 2009). However, the disadvantage of plasma treatment is that due to the complexity and difficulty to know exactly the process of interaction between the plasma and the surface(Chan et al., 1996; Kan, 2014). Therefore, it is very necessary to find the appropriate plasma treatment parameters, such as the duration of the treatment, the concentration and the nature of the gas used (Kan & Yuen, 2007), to achieve the purpose of the plasma treatment.

In addition, it has been proposed that the fading effect of denim can be obtained by plasma (Ghoranneviss et al., 2006; Stegmaier et al., 2009), for example, low-temperature argon plasma can produce a more suitable fading effect on the decolourisation of denim within 15 minutes (Ghoranneviss et al., 2006). It reflects that plasma treatment has been used mainly to fade indigo denim and to determine the colour difference of denim before and after treatment with plasma by using the CIE L*a*b* colourimetric system (Radetic et al., 2007). Plasma treatment has the benefits that the process does not use a great deal of water and chemicals, the energy cost is low, the treatment time is short, and it can be performed at low or atmospheric pressure (Lam et al., 2011; Radetic et al., 2007; Stegmaier et al., 2009). Besides, the fading of plasma-

treated denim is more pronounced than with conventional enzyme treatment techniques, probably due to the oxidative fading of the indigo dye in the presence of plasma (Stegmaier et al., 2009). For example, plasma-induced ozone treatment for colour fading is an environmentally friendly method that uses very little energy for the treatment process and does not require water or chemicals (Srikrishnan & Jyoshitaa, 2022). Plasma treatment produces highly energetic electrons and UV light also produces ·OH radicals (Srikrishnan & Jyoshitaa, 2022). Indigo dye molecules (RH) can be oxidized by the hydroxyl radicals, which release the extremely active organic radical R·, which can be further oxidized (Srikrishnan & Jyoshitaa, 2022). Thus, the fading effect of indigo textiles is obtained (Srikrishnan & Jyoshitaa, 2022).

At the same time, the modification is fairly uniform over the entire surface (Kan & Yuen, 2007) and allows for a greater improvement in the wettability of the textile (Morent et al., 2008) as well as a greater increase in stain removal and dyeability (Correia et al., 2021; Gotoh & Yasukawa, 2011). However, the disadvantage is that the denim has a rougher feel after treatment, so some additional treatment is required (Radetic et al., 2007). Moreover, it has been found that the treatment speed can control the degree of modification on the surface of cotton material, for example, the treatment speed as the main factor can provide the right time of plasma accumulation on the fabric surface to prevent damage to the material (Lam et al., 2011). In addition, similar to other chemical reactions, the parameters that affect the results of plasma treatment are the nature of the gas used, the flow rate of the gas, and the discharge power, and so on (Kan & Yuen, 2007). For practical applications in industry, in addition to the gas concentration used for plasma treatment, two other factors are the moisture content in the fabric and the treatment time (Hu et al., 2021). For example, variation in the ozone treatment time can adjust the degree of fading when using plasma-induced ozone to fade reactive dyes (Atav et al., 2022). Furthermore, different colours of reactive dyes require different fading times

(Atav et al., 2022). The yellow colour fades more slowly and the blue colour fades more quickly when using plasma-induced ozone (Atav et al., 2022). It is recommended to keep the ozone treatment time to five minutes or less for blues, which fade easily (Atav et al., 2022).

In general, plasma-substrate interactions are chemical and physical interactions between surfaces generated by external energy excitation of a mixture of partially ionized gases (Morent et al., 2008). To fade cotton fabrics through plasma-induced ozone, certain bonds in the dye molecule are broken, which results in the dye fading from the textile (Ben & Jaouachi, 2021). Thus, it is necessary to explore the appropriate plasma treatment parameters, such as gas type and concentration, moisture content in the fabric and treatment time (Hu et al., 2021; Morent et al., 2008). For example, if the plasma treatment time is too long, the modification of the material surface can be significant and may have a detrimental effect on the material (Kan & Yuen, 2007). At the same time, the utilization of this technology has matured from a large number of applications of plasma treatment on different textile materials (Morent et al., 2008). It can be used to obtain a large number of beneficial environmental and economic impacts, such as high efficiency and environmental friendliness (Gotoh & Yasukawa, 2011), thus achieving significant environmental benefits in terms of emission reduction (Stegmaier et al., 2009). Its main drawback is that plasma treatment cannot completely replace water-based processes, but offers a promising and sustainable alternative, while some studies point out that the initial investment in plasma equipment is still relatively expensive and that challenges remain in industrial applications (Periyasamy & Periyasami, 2023; Radetic et al., 2007). For further development of plasma treatment, it is possible to combine numerical simulation software and hardware to simulate the plasma treatment process and find suitable plasma treatment parameters to make the plasma equipment achieve better results after further

optimization (Stegmaier et al., 2009) and accelerate the progress of industrial-scale plasma treatment (Morent et al., 2008).

Overall, plasma treatment is a dry and sustainable textile processing method that provides faster processing and improved textile wetting while achieving economical (e.g., using fewer chemicals and no need to treat the wastewater) and environmentally friendly effect. Currently, the key to plasma treatment on an industrial scale is to find the right plasma treatment parameters to achieve specific textile processing effects, such as fading effects. Due to the complex interaction of the plasma with the substrate surface, adjusting the plasma treatment parameters in a conventional way may be time and cost-consuming, Therefore, the plasma treatment can be considered in combination with AI techniques.

2.3 Mechanisms for fading cotton fabrics with plasma-induced ozone

There are 12 equations explaining how cotton fabrics fade when exposed to plasma-induced ozone. The first step is the release of high-energy electrons through electron impact due to plasma treatment (Kan et al., 2016; Zhang et al., 2008). Mixed radicals are produced when electrons with high energy interact with air moisture (Cheung, 2018; Kan et al., 2016; Zhang et al., 2008). This process can be explained by Equation (2.1).

$$5H_2O \xrightarrow{e^-} \cdot 2OH + e_{aq}^- + \cdot H + H_2O_2 + H_3^+O + H_2 \qquad (2.1)$$
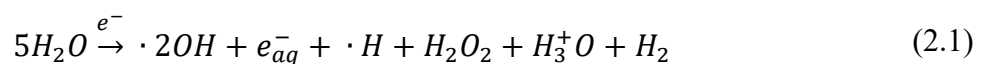
Meanwhile, some electrons with a high energy level interact with oxygen molecules in the air. During this reaction, $O \cdot$ and O_3 are formed (Zhang et al., 2008). Equations (2.2) and (2.3) describe this process.

$$O_2 + O \cdot \rightarrow O_3 \qquad (2.2)$$

$$O_2 \xrightarrow{e^-} 2O \cdot \xrightarrow{H_2O} 2 \cdot OH \qquad (2.3)$$

Besides, it is possible to introduce ozone into the water. When injected into the water, ozone can be held for between three and twenty minutes (Cheung, 2018). As ozone is highly soluble in water, ozone produced previously is easily absorbed by airborne moisture, which serves as a powerful oxidant (Kan et al., 2016). It has been reported that the radical $\cdot OH$ formed following ozone dissolution is an important cause of colour fading (Kan et al., 2016; Zhang et al., 2008). A description of this process can be found in Equations (2.4) to (2.7).

$$O_3 \rightarrow O_2 + O \cdot \qquad (2.4)$$

$$O \cdot + H^+ + e^- \rightarrow \cdot OH \qquad (2.5)$$

$$O_3 + H_2O_2 \rightarrow \cdot OH + O_2 + HO_2 \cdot \qquad (2.6)$$

$$O_3 + HO_2 \cdot \rightarrow \cdot OH + 2O_2 \qquad (2.7)$$
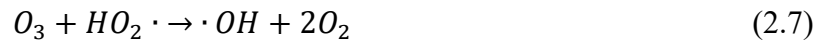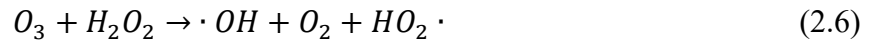
During ozone plasma generation, charged particles, free radicals, and ultraviolet (UV) light are produced (Kan et al., 2016; Srikrishnan & Jyoshitaa, 2022). Additionally, UV rays, which are produced by the plasma treatment process, are also responsible for generating $\cdot OH$ radicals (Kan et al., 2016; Srikrishnan & Jyoshitaa, 2022). Despite this, the efficiency of $\cdot OH$ production in water via UV is rather low, while the efficiency of the production of $\cdot OH$ radical is relatively high when ozone is present (Zhang et al., 2008). A description of this process can be found in Equations (2.8) and (2.9).

$$O_3 + H_2O \xrightarrow{hv} H_2O_2 + O_2 \qquad (2.8)$$

$$H_2O_2 \xrightarrow{hv} 2 \cdot OH \qquad (2.9)$$

Among the oxidation radicals produced during the plasma process, the hydroxyl radical $\cdot OH$ is most prevalent, mainly contributing to the degradation of dyes in textiles (Kan et al., 2016). $\cdot OH$ can promote the oxidation of dye molecules (RH) to produce organic radicals $R \cdot$, capable of increasing the reaction rate and can be used to further oxidise dye molecules (Kan et al., 2016; Khan et al., 2010; Srikrishnan & Jyoshitaa, 2022). In this manner, the dyed fabric was able to achieve a fading effect (Srikrishnan & Jyoshitaa, 2022). This process is described in equations (2.10) to (2.12).

$$RH + \cdot OH \rightarrow H_2O + R \cdot \qquad (2.10)$$

$$R \cdot \rightarrow fragmentation\ of\ R \cdot \qquad (2.11)$$

$$R \cdot + O_2 \rightarrow ROO \cdot \qquad (2.12)$$

Therefore, plasma-induced ozone might be utilized as a suitable technique for colour fading of textiles (Carneiro et al., 2001; Kan et al., 2016; Morent et al., 2008; Srikrishnan & Jyoshitaa, 2022).

2.4 G2 plasma machine

The G2 plasma machine is a water-free washing machine that removes colour by using a controlled high concentration of ozone plasma (Cheung, 2018; Kan et al., 2016). In comparison to conventional processes, the G2 plasma machine saves 62% of energy (kW/h), 67% of water, 85% of chemicals, and reduces the amount of time required for production by 85% (Kan et al., 2016). Using electric currents to ionize oxygen molecules within the incoming air, the G2 creates ozone plasma to fade textiles (Kan et al., 2016). Before being returned to the

atmosphere, residual plasma ozone undergoes a transformation into purified air (Kan et al., 2016). Figure 2.1 demonstrates how the G2 plasma machine works.
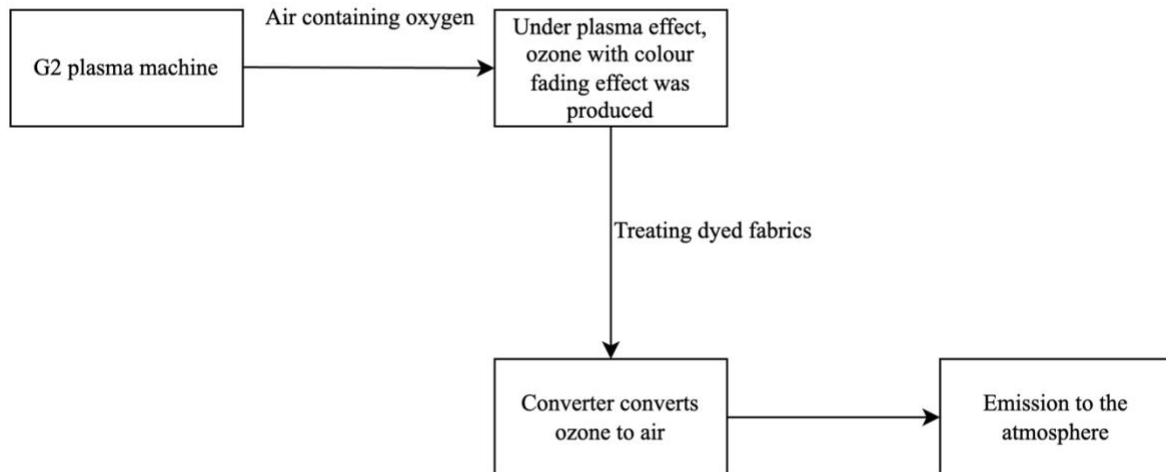
Figure 2.1. The working principle of the G2 plasma machine (Kan et al., 2016)

2.5 Colour measurement of faded cotton fabrics

In this study, it is necessary to study the fading effects of plasma treatment on cotton fabrics. Prior to the measurement of colour, fabric samples were conditioned at 65±2% relative humidity and 20±2°C for at least 24 hours. Several types of samples were measured with a Macbeth Colour-Eye 7000A (CE-7000A) spectrophotometer. Colours were measured in terms of CIE L*a* b*C*h and K/S values.

The CIE L* value represents the lightness level of the fabric sample and the CIE a* value represents the magnitude of red and green, i.e., +a* indicates red and -a* indicates green (Hunt & Pointer, 2011). Besides, the degree of yellow and blue of a fabric sample is determined by the b* value, i.e. +b* values represent yellow and -b* values represent blue (Hunt & Pointer, 2011). As for the CIE L*a*b*C*h value, it is composed of two different expressions, CIE L*a*b* and CIE L*C*h. CIE C* value and CIE h value can be derived from the CIE a* value

and the CIE b* value (Hunt & Pointer, 2011), as shown in Equation (2.13) and Equation (2.14) below.

$$C^* = \sqrt{a^{*2} + b^{*2}} \qquad (2.13)$$

$$h = arctan\frac{b^*}{a^*} \qquad (2.14)$$

Besides, for calculating K/S values, Equation (2.15), the Kubelka-Munk dyeing depth equation is applied (Brinkworth, 1972). The greater the K/S value as determined by calculation, the darker the surface colour of the fabric samples, indicating better dyeing results (Brinkworth, 1972).

$$K/S = \frac{(1-R)^2}{2*R} \qquad (2.15)$$

The Macbeth colour eye 7000A was used to measure colour with an illuminant D65, a large aperture value, and a 10° observer angle. Additionally, black traps and white traps were used to calibrate the colour-measuring device. In order to improve the accuracy of the colour measurement, several fabric samples of each type and four uniformly coloured areas of each fabric sample were tested. The final measurement of colour was also derived by averaging these data.

2.6 Combination of AI techniques and plasma treatment

Plasma treatment technology can provide a sustainable and alternative approach to textile processing. However, its shortcoming is that the interaction of the plasma with the textile surface is more complex and difficult to predict, as the surface changes induced by plasma

treatment can be influenced by many factors, such as plasma treatment parameters and textile structure (Leroux et al., 2006). Therefore, one of the keys for applying plasma treatment to textile processing processes is to find the appropriate plasma treatment parameters, in which the application of AI techniques can be combined to effectively reduce the time and cost spent (Abd Jelil et al., 2013). Besides, it can predict what effect different plasma treatment parameters will have, and evaluate the most suitable plasma treatment parameters required for a particular processing effect.

One of the more prevalent types of intelligent techniques is the neural network model, which has a better surface in terms of accuracy and predictive power than traditional statistical models. Meanwhile, it has the ability to model complex nonlinear multidimensional functional relationships, learning and deriving good approximations from less experimental data (Coit et al., 1998). The ability to generalize well to multiple nonlinear variables with unknown interactions eliminates the need to assume the nature of the relationship in advance (Coit et al., 1998). Moreover, neural network models are often superior to statistical models when it comes to modelling complicated data sets, and for example, no detailed understanding of the chemical or physical characteristics of the process is necessary to develop a powerful nonparametric simulation model (Gadekar & Ahammed, 2019). However, one of its drawbacks is that it is like an "empirical black box", i.e., it is difficult to explicitly explain the weighted connectivity part of the network model, and therefore the model needs to be validated by testing the data set so as to ensure the credibility of the model (Coit et al., 1998). Therefore, when using neural networks to optimize a process, the integrity of the training and test data sets will determine the quality of the neural network model (Coit et al., 1998). In addition, two methods that help enhance the generalizability of neural networks or the tendency of overfitting, i.e., to prevent trained neural network models from performing poorly on top of unseen datasets, are (1) early

stopping and (2) Bayesian regularization methods respectively (Doan & Liong, 2004). For the early stopping method, it is used to stop the whole training process when the neural network shows overtraining characteristics, such as poor prediction accuracy when the trained network is applied to the test set (Doan & Liong, 2004). For the Bayesian regularization method, it minimizes the overfitting problem by considering the degree of fit and network structure (Doan & Liong, 2004). Between them, Bayesian regularization methods perform better in most cases (Abd Jelil et al., 2013; Doan & Liong, 2004).

Besides, the Adaptive Neuro-Fuzzy Inference System (ANFIS) introduced by Jang (1993) incorporates fuzzy if-then rules derived from expertise and prescribed input-output data pairs to construct input-output mappings, i.e., combining the concepts of neural networks and Fuzzy Logic (FL) (Jang, 1993), which allows this intelligent techniques to be used in many engineering-related applications because it can produce better predictions than using only one of these two methods (Haji & Payvandy, 2020; Jang, 1993). It is a model that correctly connects input and target values and a network structure that implements a fuzzy inference system, and it is trained using hybrid learning rules (Haji & Payvandy, 2020; Jang, 1993).

Abd Jelil et al. (2013) used a neural network approach to construct a nonlinear model to analyze the effect of plasma processing parameters on fabric surface wettability. In this neural network, plasma parameters and fabric structure characteristics serve as input variables, while factors that respond to the wettability of the fabric surface, such as the cosine of the water contact angle as well as fabric capillary height, are used as output variables (Abd Jelil et al., 2013). The complexity of the model is reduced by combining a FL approach to find the most effective parameters, allowing the neural network to learn its structure efficiently with limited data, and enhancing the generalizability of the neural network by early stopping and Bayesian

Regularization (Abd Jelil et al., 2013), thus identifying the effect of the input variables during prediction without conducting costly and time-consuming experiments. Results showed that Bayesian Regularization Neural Networks (BRNN) provided a more accurate prediction, where the root mean square error (RMSE) was 0.0137, which was lower than that of Levenberg-Marquardt Neural Networks (LMNN). The value of the correlation coefficient (R) is 0.9957, which is higher than that of the LMNN during the testing process. In addition, the study of Mitrović et al. (2020) pointed out that plasma treatment can be used to decolourise textile dyes in aqueous solution (Mitrović et al., 2020). In this process, a general regression neural network (GRNN) was used to fit a complex system with a limited training data set to predict the plasma treatment parameters related to decolourisation effectiveness, such as treatment time, inlet flow rate, and gas composition, to achieve optimal decolourisation and to discover the most critical factors affecting decolourisation efficacy (Mitrović et al., 2020). For the design of the neural network, a four-layer generalized regression neural network was chosen. This neural network is suitable for sparse data sets with a multidimensional measurement space and for regression problems in which the linearity assumptions do not hold, where the training process between the input and hidden layers as well as between the hidden and output layers consists of unsupervised and supervised learning respectively (Mitrović et al., 2020; Specht, 1991). The structure of this neural network was chosen to enable it to adapt to multidimensional data sets (Mitrović et al., 2020; Specht, 1991). According to this neural network model, the decolourisation effect can be predicted with satisfactory accuracy ($R^2 >$ 0.95 and the low values of RMSE) (Mitrović et al., 2020).

In addition, Haji and Payvandy (2020) used two computational intelligence techniques, ANN and ANFIS to investigate the effects of plasma treatment parameters, such as oxygen flow rate, power, and treatment time, on the colour strength (K/S) of wool samples. It was found that

ANFIS predicted the colour strength (K/S) with better accuracy than the conventional response surface method (RSM) or simple ANN model, because the R-value of 0.997 for ANFIS is higher than that of ANN (0.986) and RSM (0.902) (Haji & Payvandy, 2020).

In summary, relatively few studies combining plasma treatment with intelligent techniques have been conducted to analyse the influence of plasma treatment parameters on sample colour intensity, textile dye removal from aqueous solutions, and fabric surface wettability. Among the main intelligent techniques used are artificial neural networks (ANNs), or general regression neural networks based on neural networks and ANFIS with links to neural networks. Moreover, results show that better performance can be achieved using BRNN than using LMNN, as well as the prediction performance of ANFIS can be somewhat better than ANN. There are few studies related to the fading effect of plasma treatment in combination with AI techniques on cotton materials. Therefore, the application of AI techniques for (1) colour matching and colour prediction, (2) colour difference detection and assessment can be further explored to gain inspiration related to the study of the fading effect of plasma treatment in combination with AI techniques on cotton materials. This is because, on the one hand, it is possible to draw on available intelligent techniques. On the other hand, intelligent techniques have the ability to transfer learning in similar situations, i.e., knowledge accumulated from existing data in similar domains with large amounts of data can be used to facilitate predictive modelling of the target domain (Lu et al., 2015). Meanwhile, the intelligent techniques and optimisation algorithms mentioned in the study for transfer learning include neural networks, Bayesian and fuzzy logic, and genetic algorithms (GAs) (Lu et al., 2015).

2.7 Application of AI techniques in colour matching and colour prediction

As there is a need to predict the colour of plasma-treated cotton fabrics after fading, the application of AI techniques for colour matching and colour prediction needs to be further explored for inspiration related to the study of the fading effect of plasma treatment combined with artificial intelligence techniques on cotton materials. The relevant 34 research articles were selected through an advanced search in Web of Science using the keywords "TS=(textile OR fabric) AND TS=(colour fading OR colour prediction OR colour recipe) AND TS=(ANN OR neural network OR intelligent techniques OR optimisation algorithms)". The time span is set to the last decade, i.e., from 2013 to 2022. The 34 research articles are classified according to the AI techniques (including intelligent techniques and optimisation algorithms) used, as shown in Table 2.2.

Table 2.2. AI techniques applied to colour matching and colour prediction in the last decade

AI techniques	Publications	Total occurrences	Percentage
ANN	(Almodarresi et al., 2013; Chakraborty et al., 2019; Farooq et al., 2021; Farooq et al., 2020; Furferi et al., 2016; Haji & Payvandy, 2020; Haji & Vadood, 2021; Hajipour & Shams-Nateri, 2019; Hasanzadeh et al., 2013; Hemingray & Westland, 2016; Hossain et al., 2017; Hung et al., 2014; Hwang et al., 2015; Jawahar et al., 2015; Kan & Song, 2016; Liu & Liang, 2018; Nateri et al., 2017; Rosa et al., 2021; Şahin et al., 2022; Shen & Zhou, 2017; Vadood & Haji, 2022a, 2022b)	22	64.7%

Fuzzy Logic (FL) & ANFIS	(Haji & Payvandy, 2020; Haji & Vadood, 2021; Hossain et al., 2017; Hossain et al., 2015; Hossain, Hossain, Choudhury, et al., 2016)	5	14.7%
Support Vector Machine (SVM), Least Squares SVM (LSSVM)	(Rahaman et al., 2020; Yu et al., 2021; Yu et al., 2020)	3	8.8%
Recurrent Neural Network (RNN)	(Zhang et al., 2021)	1	2.9%
Genetic Algorithm (GA)	(Boukouvalas et al., 2021; Chaouch et al., 2020, 2022; Vadood & Haji, 2022a, 2022b)	5	14.7%
Particle Swarm Optimisation (PSO), a combination of PSO and FMINCON (PSO-FMIN)	(Boukouvalas et al., 2021; Vadood & Haji, 2022a; Yu et al., 2021; Yu et al., 2020)	4	11.7%
Ant Colony Optimisation (ACO)	(Chaouch et al., 2019a, 2019b, 2022)	3	8.8%
Multi-objective Evolutionary Algorithms (MOEA), Non-dominated Sorting Genetic Algorithm (NSGAII)	(Boukouvalas et al., 2021; Vadood & Haji, 2022b)	2	5.8%
Response Surface Methodology (RSM)	(Hasanzadeh et al., 2013; Rosa et al., 2021)	2	5.8%
Gray Wolf Optimisation (GWO)	(Vadood & Haji, 2022a)	1	2.9%
Taguchi method	(Hossain, Hossain, & Choudhury, 2016)	1	2.9%

As can be seen from Table 2.2, the main intelligent techniques applied to colour matching and colour prediction were ANN, FL & ANFIS, which accounted for 64.7% and 14.7% of the 34 research articles on colour matching and colour prediction, respectively, and the less frequently used intelligent techniques were SVM, LSSVM and RNN. the main optimisation algorithms applied on colour matching and colour prediction were GA, PSO, PSO-FIMIN, and ACO, which accounted for 14.7%, 11.7%, and 8.8% of the 34 research articles on colour matching and colour prediction, respectively, and the less frequently used optimisation algorithms were MOEA, NSGAII, RSM, GWO, and Taguchi's method.

In terms of colour matching and colour prediction, the ANN model could provide more accurate prediction results than the RSM model in the study of Hasanzadeh et al. (2013), with a relative error of 1.67% for the ANN model, which was lower than the relative error of 1.80% for the RSM model. In the studies of Hossain et al. (2017) and Haji and Vadood (2021), the ANN model provided higher prediction accuracy than the FL, i.e. the ANN model had a higher R^2 (Hossain et al., 2017), and smaller RSE (Hossain et al., 2017), MAE (Hossain et al., 2017), MAPE (Haji & Vadood, 2021). In contrast, in the study of Haji and Payvandy (2020), ANFIS provided higher prediction accuracy than the ANN model, and the correlation coefficient of ANFIS was higher than that of the ANN model. In the study of Vadood and Haji (2022a), using the PSO-FMIN algorithm to weight the ANN provided better prediction results than the BPNN, i.e. smaller MSE. For the optimisation algorithm, in the study of Chaouch et al. (2022), ACO can provide better predictions and higher computational efficiency than GA, as reflected by the lower mean MSE and the shorter computational time required for ACO. It is worth noting that different modulation methods and different application contexts and data structures may provide different prediction accuracy results. From the above-mentioned research articles, it can be found that different intelligent techniques can provide different prediction accuracies

when applied to colour matching and colour prediction. Thus, the application of AI techniques for colour matching and colour prediction might provide inspiration related to the study of the fading effect of plasma treatment combined with AI techniques on cotton materials.

2.8 Application of AI techniques in colour difference detection and assessment

Due to the need to predict the colour of plasma-treated cotton fabrics after fading, there is a need to further explore the application of AI techniques to colour difference detection and assessment. This will provide inspiration for the study of the fading effect of plasma treatments in conjunction with AI techniques on cotton fabrics.

Using the keywords mentioned above, 15 relevant articles were selected from an advanced search on the Web of Science. It covers the period from 2013 to 2022, which is the last decade. In Table 2.3, the 15 research articles were categorized according to the AI techniques (including intelligent techniques and optimisation algorithms) applied.

Table 2.3. Intelligent techniques and optimisation algorithms applied to colour difference detection and assessment in the last decade

AI techniques	Publications	Total occurrences	Percentage
Extreme Learning Machine (ELM), Online Sequential ELM (OSLEM), Kernel ELM (KELM), Regularisation ELM (RELM)	(Li et al., 2020; Zhou, Gao, Zhang, et al., 2019; Zhou, Gao, Zhu, et al., 2019; Zhou et al., 2021; Zhou, Wang, et al., 2019; Zhou et al., 2016)	6	40.0%
SVM, LSSVM, Support Vector Regression (SVR),	(Li et al., 2022; Zhang & Yang, 2014; Zhang et al., 2017; Zhou, Gao, Zhang, et al., 2019; Zhou,	6	40.0%

Least Squares SVR (LSSVR)	Gao, Zhu, et al., 2019; Zhou, Wang, et al., 2019)		
ANN	(Li et al., 2015; Xie et al., 2021; Zhou, Gao, Zhang, et al., 2019; Zhou, Gao, Zhu, et al., 2019; Zhou, Wang, et al., 2019)	5	33.3%
Random Vector Functional-link net (RVFL)	(Liu & Yang, 2021; Zhang & Zhou, 2022)	2	13.3%
K-means	(Xie et al., 2020)	1	6.7%
Takagi-Sugeno Fuzzy Neural Network (T-S FNN)	(Li et al., 2017)	1	6.7%
Differential Evolution (DE)	(Li et al., 2020; Zhou, Gao, Zhang, et al., 2019; Zhou et al., 2021; Zhou, Wang, et al., 2019)	4	26.7%
PSO	(Li et al., 2022; Zhou, Gao, Zhu, et al., 2019; Zhou et al., 2016)	3	20.0%
Rotation Forest (RF)	(Zhou, Gao, Zhang, et al., 2019; Zhou, Gao, Zhu, et al., 2019)	2	13.3%
Bagging	(Zhou et al., 2016)	1	6.7%
Dynamic Parameter Selection (DPS)	(Zhou et al., 2021)	1	6.7%
Hunger Games Search (HGS)	(Zhang & Zhou, 2022)	1	6.7%
GA	(Zhang & Yang, 2014)	1	6.7%
GM (1,1)	(Zhang et al., 2017)	1	6.7%
Grasshopper Optimisation Algorithm (GOA)	(Li et al., 2020)	1	6.7%
GWO	(Zhang & Zhou, 2022)	1	6.7%
Marine Predators Algorithm (MPA)	(Liu & Yang, 2021)	1	6.7%
Sine and Cosine Algorithm (SCA)	(Liu & Yang, 2021)	1	6.7%

Principal Component Analysis (PCA)	(Zhang & Yang, 2014)	1	6.7%
Whale Optimisation Algorithm (WOA)	(Zhou, Wang, et al., 2019)	1	6.7%

As can be seen from Table 2.3, the main intelligent techniques applied to colour difference detection and assessment were ELM (e.g. ELM, OSLEM, KELM, RELM), SVM (e.g. SVM, LSSVM, SVR, LSSVR) and ANN, which accounted for 40.0%, 40.0% and 33.3% of the 15 research articles on colour difference detection and colour difference evaluation respectively, and the less frequently used intelligent techniques were RVFL, K-means algorithms and T-S FNN. The main optimisation algorithms applied to colour difference detection and assessment were DE, PSO and RF, which accounted for 26.7%, 20.0% and 13.3% of the 15 research articles on colour difference detection and colour difference evaluation respectively, with less frequently used optimisation algorithms being Bagging, DPS, HGS, GA, GM (1,1) and GOA.

In terms of colour difference detection and assessment, in the study of Zhang and Yang (2014), the GA-optimised SVM approach was used to build an evaluation model that could provide higher prediction accuracy and lower relative error than the traditional Naive Bayesian algorithm, resulting in a better evaluation of the quality of dyed fabrics. In the study of Zhou, Gao, Zhang, et al. (2019), DE-OSELM could provide higher prediction accuracy than traditional textile colour correction models based on SVR and ELM algorithms, and the models also had better generalisation and greater robustness. In the study of Zhou, Wang, et al. (2019), the DE-WOA-ELM model could provide a higher average classification accuracy than ELM, SVM, BPNN and KELM, with an improvement ranging from 0.47% to 12.11%. In the study of Zhou, Gao, Zhu, et al. (2019), the RF-PSO-SLSSVR model could provide lower RMSE values than the traditional SVR and ELM algorithms. In the study of Li et al. (2020), the DE-

GOA-KELM could provide higher classification accuracy than the traditional KELM model, i.e. an improvement of about 8%. In the study of Zhou et al. (2021), the DPS-DE-RELM model could provide higher classification accuracy, faster convergence and higher robustness than the traditional ELM model. From the above description, it can be found that by combining intelligent techniques and optimisation algorithms, the prediction effectiveness of traditional methods or single intelligent techniques can be improved, further improving prediction accuracy and enhancing robustness. Thus, the application of AI techniques for colour difference detection and assessment might provide inspiration related to the study of the fading effect of plasma treatment combined with AI techniques on cotton materials.

2.9 Summary

This chapter, encompassing sections 2.1 to 2.5, provides an overview of the merits and demerits of conventional fading techniques, elucidates the need for sustainable fading methods like plasma treatment, and elaborates on the advantages of such treatment in the context of cotton material discolouration. Utilizing numerical simulation software, it becomes feasible to pinpoint optimal plasma treatment parameters to achieve anticipated results. Additionally, this chapter delineates the mechanism by which ozone, generated via plasma, alters the hues of cotton fabrics, including the working principles of eco-friendly G2 plasma machines and the colorimetric assessment methods for faded cotton fabrics.

Moreover, section 2.6 encapsulates the application of intelligent techniques in plasma treatment, spanning three key areas: (1) The use of optimized neural network models in analysing the relationship between treatment parameters and fabric wettability; (2) The employment of generalized regression neural networks in dye removal; (3) The utilization of ANFIS to predict the colour strength (K/S) of dyed wool.

In sections 2.7 and 2.8, the exploration extends to the application of AI technology in (1) colour matching and colour prediction, and (2) the detection and evaluation of colour differences. Findings indicate that distinct AI techniques offer differing predictive accuracies in terms of colour matching and prediction. By amalgamating intelligent technologies and optimization algorithms, the predictive accuracy and robustness of traditional methods or singular intelligent technologies can be enhanced.

In summary, AI technologies, as described in the relevant literature, have potential applicability in predicting the fading effects of plasma-treated cotton materials, thereby facilitating the selection of appropriate plasma treatment parameters. In the succeeding sections, detailed experiments, data analysis, and discussion will be presented.
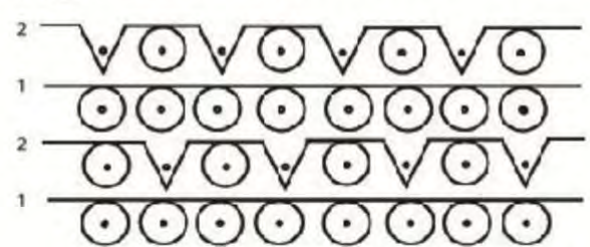
Chapter 3 Methodology

Firstly, this chapter described the material, specification and dyeing process of the knitted fabric samples, followed by a brief description of the G2 plasma treatment machine and treatment parameters used to fade the fabric. The process of measuring data on the fading effect of plasma-treated fabric samples was then described. Finally, the application of the BRNN models and polynomial regression models was presented.

3.1 Fabric samples

There are three types of fabric samples, namely (1) reactive dye-dyed fabric samples (single colour), (2) sulphur-dyed fabric samples (single colour) and (3) reactive dye-dyed fabric samples (two-colour mixed). Details of the fabric samples are described in detail in Chapter 4, Chapter 5, Chapter 6 and Chapter 7, respectively. All three types of fabric samples were 32s/2 100% cotton single pique (Lacoste) knitted fabric with a weight of 220 g/m^2. The material and specifications of the knitted fabric samples are shown in Table 3.1.

Table 3.1. The material and specifications of the knitted fabric samples (Cheung, 2018)

Fabric materials	32s/2 100% cotton
Fabric structure	single pique
Fabric weight	220 g/m^2
Single Lacoste	

3.2 Dyeing

Dyeing was carried out in a dyeing factory in China. The dyeing process of reactive dyes and sulphur dyes is briefly described here.

3.2.1 Dyeing with reactive dyes

According to the dyeing procedure shown in Figure 3.1 and Table 3.2, the process of dyeing with reactive dyes can be divided into four stages.

Table 3.2. The process of dyeing with reactive dyes

Procedure of reactive dyeing	The dyeing process	References
Stage 1	(1) To dye 10 kg of cotton fabric with a 1.5% (by weight of fabric) concentration of reactive dyestuff on an industrial scale winch dyeing machine, 42.5 g/l of sodium chloride was added to the dye bath with the cotton fabric, and the mixture was treated at 30°C for 10 minutes. (2) The reactive dye was then incorporated into the dye bath within 20 minutes. (3) The fabric, salt, and dye were treated in the dye bath for an additional 10 minutes. (4) Soda ash was added to the dye bath at a concentration of 11.5 g/L within 15-30 minutes. (5) The fabric was treated for an additional 10 minutes.	(Cheung, 2018; Kan et al., 2016)
Stage 2	The temperature of the dye bath was increased to 60°C at a rate of 1°C/min within 30 minutes.	
Stage 3	After the temperature reached 60°C, the fabric was kept in the dye bath for 60 minutes.	
Stage 4	(1) The fabric was removed from the dye bath and was rinsed with cold water to remove any undyed dye.	

	(2) Post-treatment was carried out to further remove undyed dyestuff with 1.0% non-ionic detergent. (3) After the detergent treatment, the fabric was rinsed in cold water. The dyed fabric was conditioned at 20±2 °C and 65±2% relative humidity for at least 24 hours before further treatment.	
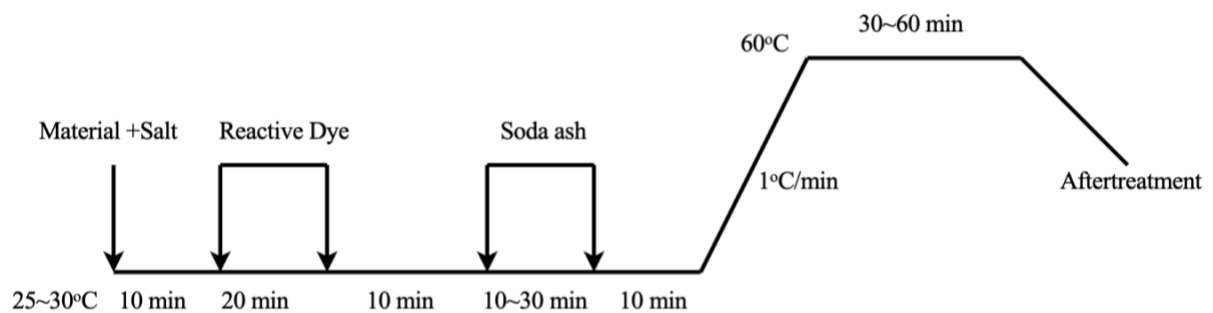
Figure 3.1. Procedure of reactive dyeing (Cheung, 2018; Kan et al., 2016)

3.2.2 Dyeing with sulphur dyes

According to the dyeing procedure shown in Figure 3.2 and Table 3.3, the process of dyeing with sulphur dyes can be divided into four stages.

Table 3.3. The process of dyeing with sulphur dyes

Procedure of sulphur dyeing	The dyeing process	References
Stage 1	(1) Sulphur dyestuff was used to dye knitted cotton fabrics at a ratio of 10:1 liquid-to-goods. Heating the dye bath to 60 °C was required. (2) The fabric was added to the dye bath after 10 minutes. (3) Adding the sulphur dyestuff after 20 minutes was the next step (4) A further 10 minutes were spent maintaining the temperature at 60 °C.	(Kan et al., 2017; Zhong et al., 2018)

Stage 2	A subsequent increase in temperature was carried out at a rate of 1.5 °C per minute until 75 °C is reached.	
Stage 3	(1) Three separate batches of sodium sulphate (20 g/l), sodium sulphate (10 g/l) and sodium sulphate (10 g/l) are added, each at a 5-minute interval. (2) A further 30 minutes were spent maintaining the temperature.	
Stage 4	(1) The process was then followed by oxidation with a mixture of 35% hydrogen peroxide (2% on weight of fabric) and 80% acetic acid (2% on weight of fabric) at 50 °C for 20 minutes at a liquid to goods ratio of 10:1 at a pH of 4-4.5. (2) Following this, the fabric was rinsed with tap water and soaped with detergent at 90 °C for 10 minutes. (3) Prior to further use, the samples were then dried in air and conditioned (relative humidity: 65 ± 2 %; temperature: 20 ± 2 °C) for at least 24 hours.	
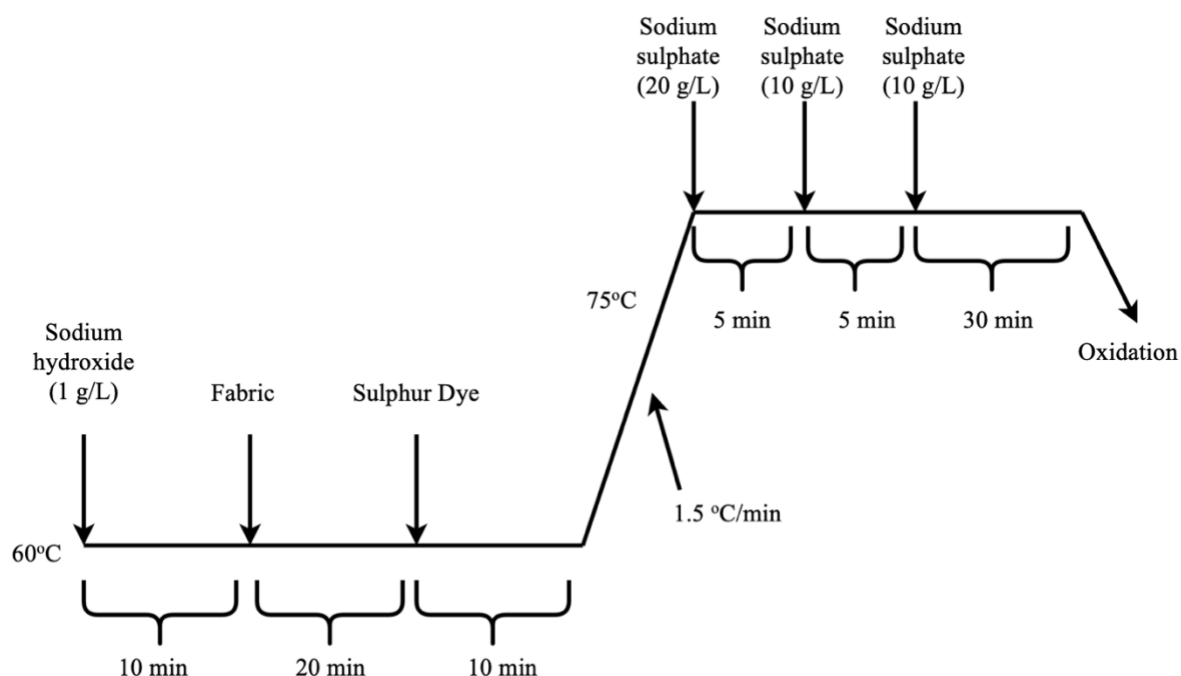
Figure 3.2. Procedure of sulphur dyeing (Kan et al., 2017; Zhong et al., 2018)

3.3 Plasma treatment of faded colours

In the process of plasma treatment, a commercial ozone plasma machine G2 (Standard model, Spain Jeanologia) was used, as shown in Figure 3.3. Compared with the traditional rotary washing machine, G2 equipment has similar space in equipment specifications, and its size is 240 W x 215 D x 205 H (cm). In addition, the inner dimension of the tumbler is 120 x 160 (cm). Therefore, according to the size of the tumbler, it is recommended to have a loading capacity of 50 kg in any case. Table 3.4 shows the technical specifications of G2 equipment.

Figure 3.3. G2 ozone machine (Cheung, 2018)

Table 3.4. Technical specifications of G2 equipment (Cheung, 2018)

Electricity power demand	9 kw per hour
Ozone gas concentration	$0 - 180$ g/Nm^3
Ozone generator power	400 g per hour
Machine loading capacity	50 kg
50 kg convert to garments	80-100 denim jeans or 160 knitted t-shirts
Tumbler measurement	1200×1600 m/m

There is an ozone generator and a pressure swing adsorption (PSA) device inside the G2 equipment, and the operation of the equipment only needs electricity (Cheung, 2018). Its

working principle is that through the PSA process, the peripheral air is extracted to increase the pressure (Cheung, 2018). In addition, the function of an oxygen filter inside is to provide enough pure oxygen gas for the ozone generator (Cheung, 2018). This is because the pure oxygen gas will pass through the high-voltage current and the ozone generator, thus making the oxygen molecules charge from O_2 to O_3 (Cheung, 2018; Nobbs, 1985). Under normal conditions, the percentage of oxygen in the periphery air is only about 22-23% (Cheung, 2018; Jee et al., 2005).

It can be found from Table 3.4 that in the G2 Standard Model, the ozone generator can produce 400 grams of ozone per hour when the pure oxygen supply is sufficient (Cheung, 2018). Therefore, in order to generate enough ozone, it is necessary to provide a stable and sufficient pure oxygen supply for the ozone generator (Cheung, 2018). This means that it needs to have a device to strengthen the supply of pure oxygen, so that the ozone generator can continuously produce ozone, which is the function of PSA device, as shown in Figure 3.4 (Cheung, 2018). This device uses Pressure Swing Adsorption (PSA), a technology that is well suited to the separation and purification of mixed gases (Cheung, 2018; Sircar, 2002; Voss, 2005). After the fading process, the remaining ozone plasma gas can be extracted through a chamber with six metal tubes (Berkner & Marshall, 1965; Cheung, 2018). Due to the fact that the temperature of the metal tube is 280˚C, so, when the ozone plasma gas passes through the tube, the ozone plasma molecules will be decomposed at a higher temperature before exhaust (Berkner & Marshall, 1965; Cheung, 2018).
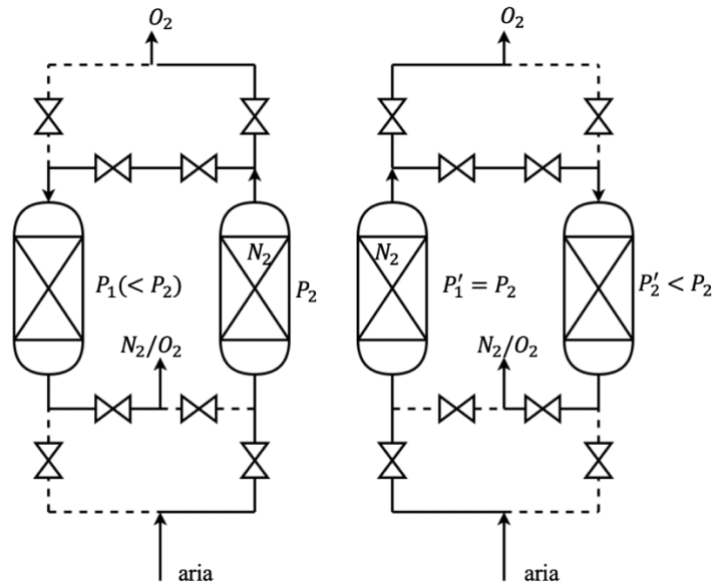
Figure 3.4. The working principle of PSA device (Cheung, 2018; Sircar, 2002; Voss, 2005)

Besides, a total of three plasma treatment process parameters were used, which are the air concentration, the water content of the dyed fabric and the treatment time. The plasma treatment parameters are summarised in Table 3.5. Plasma treatment of the three types of cotton fabrics is described in detail in the methodology in the following chapters respectively. The arrangement for the fading of cotton fabric samples by plasma treatment will be shown in the Appendix.

Table 3.5. Plasma treatment parameters applied to fabric samples

Air (Oxygen) concentration (%)	10, 30, 50, 70
Water Content (%)	35, 45
Treatment time (minutes)	10, 20, 30

In the investigation of the process of plasma treatment on textiles, a series of experimental groups were established to deeply comprehend this procedure. Plasma treatment parameters encompassed air (oxygen) concentration (at 10%, 30%, 50%, and 70% respectively), water content (at 35% and 45% respectively), and treatment time (at 10, 20, and 30 minutes

respectively). The selection of these parameters was neither arbitrary nor capricious, but rather grounded on a profound understanding of the associated reaction mechanisms.

Initially, the oxygen concentration range was chosen, a decision dictated by the pivotal role oxygen performs in plasma treatment. Although the major atmospheric constituents are nitrogen (at 78%) and oxygen (at 21%), only the role of oxygen was considered herein. In the research on the ozone-induced fading mechanism of cotton fibres through plasma (Section 2.3), the presence of oxygen molecules in the atmosphere played an essential function. During the entire plasma treatment process, high-energy electrons were generated due to electron collisions. These electrons interacted with oxygen molecules, producing oxygen atoms ($O \cdot$) and ozone (O_3) (Zhang et al., 2008). In addition, these high-energy electrons reacted with water molecules in the atmosphere, yielding a variety of radicals, including potent oxidizer hydroxyl radicals ($\cdot OH$), which were the main factors causing the fading of cotton fibres (Kan et al., 2016). Hence, despite nitrogen being the major constituent of the atmosphere, the role of oxygen was more crucial in this process. However, this does not imply that nitrogen played no part in this process; its role in this specific reaction mechanism was relatively minor and might be overlooked.

Subsequently, the moisture content in cotton fabrics was regulated to 35% and 45%. This selection was based on the mechanism of ozone-induced fading in cotton fabrics, where hydroxyl radicals (($\cdot OH$), formed from the dissolution of ozone in water, were the key factors influencing the discolouration of cotton fabrics (Kan et al., 2016). Regarding the variable of humidity content, a humidity of 35% seemed to present superior fading effects compared to 45% (Kan et al., 2016). The decreased fading effect could be due to the dilution of bleaching

agents generated during the plasma-induced ozone treatment process by higher moisture content in cotton fabrics (Kan et al., 2016).

As for treatment duration, although 30 minutes might seem extended for textile treatment, it was necessary to explore various plasma operation parameters to understand how fading occurs on single or mixed-dyed cotton fabrics. Different colours fade at various rates, e.g., yellow fades slower than blue (Atav et al., 2022). Furthermore, the three plasma treatment operation parameters are interdependent. Based on the other two plasma treatment operation parameters, such as providing lower oxygen concentrations and higher moisture contents, it might be necessary to extend the plasma treatment time for fading (Kan et al., 2016). In the study by Ibrahim et al. (2010), it was found that when treating linen fabrics with atmospheric pressure plasma and various gases, the carboxyl content of the treated substrate increased significantly when the plasma treatment time was extended from 15 minutes to 30 or 45 minutes. Hence, to encompass the full range of acceptable plasma operation parameters, the treatment time was set to include 30 minutes.

3.4 Colour measurement arrangement

The fabric samples were conditioned at 65±2% relative humidity and 20±2°C for at least 24 hours before colour measurement. In order to get accurate colour measurement data for each type of samples, experiments were carried out using a Macbeth Colour-Eye 7000A (CE-7000A) spectrophotometer. Colour measurement conditions of Macbeth Colour-Eye 7000A were set under the specular, including large aperture value, 10° observer angle and illuminant D65.

As part of the experiments, several fabric samples of each type and four uniformly coloured areas of each fabric sample were tested to improve the accuracy of the colour measurements (Figure 3.5). These data were averaged to produce the final colour measurement.
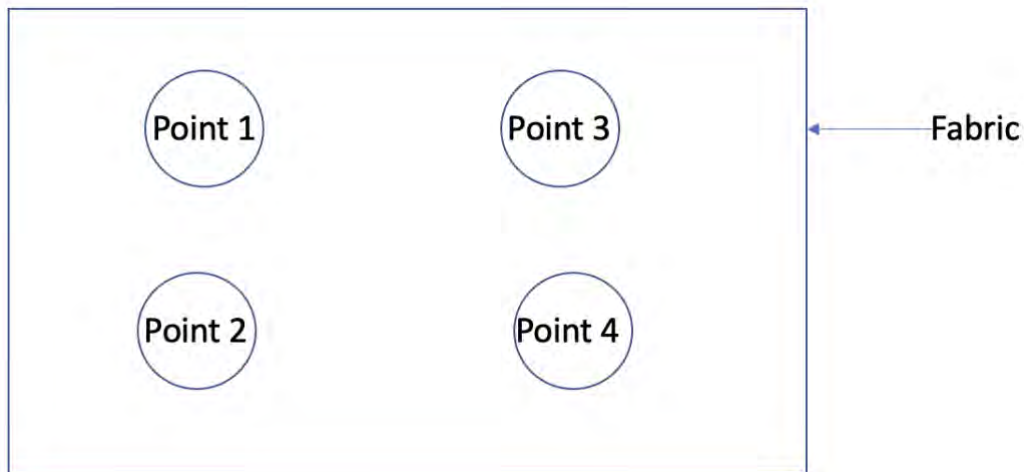
Figure 3.5. Point positions on fabric for colour measurement

3.5 Modelling, simulation and prediction

Bayesian Regularised Neural Network (BRNN) models were used to explore the relationship between the plasma treatment process parameters and the colour measurement data of cotton fabrics after fading. Both a modular approach and a K-fold cross-validation approach were used. The K-fold cross-validation approach facilitates minimising the potential for overfitting problems with small data sets (Farooq et al., 2021; Jung & Hu, 2015; Yadav & Shukla, 2016). The modular approach facilitates the understanding of the relationship between each output value and the plasma treatment parameters, thereby simultaneously reducing training time (Choudhury et al., 2015). The construction of the BRNN model input and output values and related details are discussed in Chapter 4, Chapter 5 and Chapter 6.

In addition, polynomial regression models were used to investigate the relationship between the single-colour fading effect and the two-colour mixed fading effect of plasma-treated cotton fabrics. Three different fitting methods were used in the polynomial regression models, namely (1) least squares (LS), (2) least absolute residual (LAR), and (3) Bisquare weighting (Bisquare) (MathWorks, 2022a). The construction of the polynomial regression model input and output values and related details are discussed in Chapter 7.

The accuracy of the BRNN model and the polynomial regression model will be assessed by a combination of metrics, including mean absolute error (MAE), root mean square error (RMSE), mean absolute percentage error (MAPE) and coefficient of determination (R^2).

3.6 Summary

This chapter was divided into five sections, the first of which was an introduction to the materials and specifications of knitted fabric samples. There are three types: (1) reactive dye-dyed fabric samples (single colour), (2) sulphur-dyed fabric samples (single colour) and (3) reactive dye-dyed fabric samples (two-colour mix). The second part briefly described the dyeing process for knitted fabric samples, including the dyeing process for reactive dyes and the dyeing process for sulphur dyes. The third part described the plasma equipment and treatment parameters used for fabric fading. This includes (1) the technical specifications and operating principles of the G2 plasma treatment machine and (2) the three plasma treatment process parameters of air concentration, moisture content of the dyed fabric and treatment time. The fourth part described the process of measuring data on the fading effect of plasma-treated fabric samples. The fifth part described the application of the BRNN models and the polynomial regression models. A modular approach and a K-fold cross-validation method were used in the BRNN models. Three different fitting methods, (1) least squares (LS), (2) least

absolute residual (LAR), and (3) Bisquare weighting (Bisquare), were used in the polynomial regression models. Detailed applications will be presented, data analysed and discussed in the following Chapter 4, Chapter 5, Chapter 6 and Chapter 7. Specifically, in Chapter 4, the study will focus on examining the correlation between various plasma treatment parameters and the fading effect of cotton fabrics dyed monochromatically with reactive dyes. In Chapter 5, the research will be directed towards examining the relationship between different plasma treatment parameters and the fading effect of cotton fabrics dyed monochromatically with sulphur dyes. Additionally, since fashionable clothing may involve different colour combinations, in Chapter 6, the study will delve into the relationship between different plasma treatment parameters and the fading effect of two-colour cotton fabrics mixed-dyed with reactive dyes. Furthermore, as two-colour dyes are produced by mixing monochromatic dyes in equal concentrations, Chapter 7 will further explore the method of predicting the colour properties of mixed fading effects of two-colour plasma-treated cotton fabrics from known monochromatic fading effects of plasma-treated cotton fabrics.

Chapter 4 Prediction problems regarding the Plasma Treatment fading effect of Reactive Dye dyed cotton fabrics with single colour by means of BRNN

4.1 Introduction

Faded visual effects are a trend in fashion and clothing, which are popular with young people, in products such as faded blue jeans (Hung et al., 2011). Moreover, increasing the fading effect can increase the purchase intention of customers, so that the final products produced by garment enterprises can realize value-addition and increase the profits of enterprises (Samanta et al., 2017).

The fading effects can be achieved through traditional fading technologies, such as stone washing, sand washing, enzyme washing, etc. (Kan et al., 2010). However, there are problems and limitations of traditional fading technology: (i) the surface fading effect is inconsistent (Kan et al., 2010); (ii) it is not friendly to the environment (Venkatraman & Liauw, 2019); and (iii) it is difficult to mass produce garments to meet the huge demand for fading effects in the jeans market (Kan et al., 2010). In addition, the quality of the cotton fabric, such as wear resistance, is reduced after treatment with traditional fading techniques (Samanta et al., 2017).

Therefore, alternative fading techniques have been developed, one of which is plasma treatment (Venkatraman & Liauw, 2019). In the investigation carried out by Ibrahim et al. (2010), it was demonstrated that upon the application of atmospheric pressure plasma with a range of gases on hemp-containing fabrics, the following was observed: (1) The extension of the plasma treatment duration from 15 minutes to 30 or 45 minutes resulted in a substantial elevation of the carboxyl content in the treated specimens. (2) The treatment of textiles with oxygen or air plasma significantly elevated their hydrophilicity and facilitated subsequent

bleaching processes (Ibrahim et al., 2010). Furthermore, it was noted that reactive dyes exhibited varying rates of fading for different colours (Atav et al., 2022). Besides, it is not only a completely dry non-aqueous technology but also an environment-friendly process that can produce fading effects under low health risk conditions (Venkatraman & Liauw, 2019). Additionally, plasma treatment has the capability to alter the surface of fashionable attire, thereby endowing it with new functional characteristics in addition to its existing colour properties (Ibrahim et al., 2022).

Among the various plasma treatment methods, plasma-induced ozone treatment requires little energy for its application and does not necessitate the use of water or chemicals (Srikrishnan & Jyoshitaa, 2022). In the textile colour fading process, the fading effect is achieved by controlling the plasma treatment parameters. The principle is to break the interaction and combination between dye molecules and dye fibres by ionizing gas, or by etching the surface molecules of textiles (Samanta et al., 2017). By investing some effort in process optimization, maximum efficiency, uniformity, and reproducibility of the plasma surface treatment process can be guaranteed when the same operating parameters are used for plasma treatment (Kan et al., 2016; Peran & Ercegović Ražić, 2020). As a result, plasma surface treatment can become a reproducible technique and the fading effect can be regulated through the control of plasma treatment process parameters and the critical treatment environment for plasma generation (Peran & Ercegović Ražić, 2020). Therefore, with the aid of plasma processing technology, the limitations and issues of conventional fading technologies, such as the inability to produce standard colour fading effects, loss of quality, and the inability to achieve the same fading effect in different batches of products, can be overcome in certain situations (Cheung et al., 2013; Ondogan et al., 2005).

However, the interaction between plasma and fabric surfaces can be complicated by various factors such as plasma treatment parameters, chemical composition of plasma gas, and fabric properties, which have hindered the widespread use of plasma treatment in the textile industry (Jelil, 2015; Zille et al., 2015). The study by Kan et al. (2016) identified air concentration, treatment time, and moisture content of the fabric as the key factors that impact the fading of cotton fabrics through plasma treatment. These factors exert a significant influence on the fading of cotton fabrics as they might impact the production and reaction of hydroxyl radicals, the primary agents of oxidation that cause fading (Kan et al., 2016). Increased air concentration leads to the production of more hydroxyl radicals due to the presence of more oxygen molecules. Longer treatment time increases the duration of contact between plasma active substance and dye in the fabric. Lower moisture content reduces the dilution of bleach by water. These factors contribute to greater oxidation and thus, more fading (Kan et al., 2016). Thus, plasma treatment demands meticulous control of treatment parameters to achieve desired fading effects. The challenge in its industrial application lies in determining the optimal treatment parameters swiftly and accurately, which necessitates multiple trials and observations.

One of the most prevalent forms of intelligent techniques is the neural network model, which boasts a remarkable degree of accuracy and predictive power when compared to conventional statistical models. Furthermore, the neural network model possesses the capacity to model complex nonlinear multidimensional functional relationships, demonstrating proficiency in learning and approximating from limited experimental data (Coit et al., 1998). Its ability to generalize well to multiple nonlinear variables with unknown interactions eliminates the need to presume the nature of the relationship beforehand (Coit et al., 1998). Additionally, neural network models frequently surpass statistical models in modelling complex datasets. For

instance, the creation of a formidable simulation model does not require a comprehensive understanding of the chemical or physical properties of the process (Gadekar & Ahammed, 2019). Therefore, by combining plasma treatment with intelligent techniques, such as using Bayesian Regulated Neural Network (BRNN), sustainable growth in cotton production and processing industry can be achieved (Samanta et al., 2017). BRNN is a neural network model improved by Bayesian Regularization method. The neural network model can help good approximation of effects from less experimental data without assuming the relationship in advance. It can also optimize common overfitting problems by considering network structure and fitting degree, and improve the generalization of performance of the neural network model (Abd Jelil et al., 2013; Coit et al., 1998; Doan & Liong, 2004; Gadekar & Ahammed, 2019). This is because the overfitting problem often occurs when there is less data in the training set of the neural network model used for training, and in the dyeing industry, it is not easy to collect a large number of dyeing samples (Hemingray & Westland, 2016; Jawahar et al., 2015). Therefore, using BRNN can improve the efficiency of plasma treatment in most cases (Abd Jelil et al., 2013; Doan & Liong, 2004).

Extant literature has a few studies on combining intelligent techniques, such as BRNN, with plasma treatment to predict the fading effect on cotton materials. However, research has been focused on four aspects: (i) to apply the improved neural network model to predict the impact of plasma treatment on surface wettability of fabrics (Abd Jelil et al., 2013); (ii) to apply the generalized regression neural network to predict the removal of dyes in aqueous solution (Mitrović et al., 2020); (iii) to predict the colour intensity (K/S) of dyed wool fabrics by the adaptive neural network fuzzy inference system (Haji & Payvandy, 2020); and (iv) to predict the dyeing properties of wool by the feedforward neural network models after air-vacuum

plasma treatment, achieving regression values of approximately 0.95 (Omerogullari Basyigit et al., 2023).

Therefore, a study to combine BRNN with plasma treatment is promising. On the one hand, the trained BRNN can be applied to predict the colour change of cotton materials after plasma treatment, so as to reduce the number of repeated attempts and save time and cost of adjusting plasma treatment parameters in a conventional way. On the other hand, it can speed up the intelligent and digital development of the cotton processing industry, provide a reference for manufacturers using plasma to treat cotton fabrics for fading effects, accelerate the scale of application of this environmentally friendly technology and help it become a practical industrial application.

4.2 Methodology

The methodology of this work consists of two parts: (i) preparing textile samples; and (ii) studying the effect of different plasma parameters on samples treated with reactive dyes in terms of the corresponding CIEL*a*b* values and K/S values.

4.2.1 Fabric samples and dyeing

Fabric samples (30cm x 40cm) were dyed in a dyeing factory in China with commercial reactive dyes of three primary colours of red (Levafix Red CA, labelled "RR"), blue (Levafix Blue CA, labelled "RB") and yellow (Levafix Yellow CA, labelled "RY") and the dye concentrations were 0.5%, 1.5% and 2.5%. The fabric is 32s/2 cotton single (Lacoste) knitted fabric (weight: 220 g/m^2). The dyes display remarkable resistance to fading in lighter shades and demonstrate exceptional lightfastness and resistance to sweat in the colour range, possessing a high level of reproducibility and even-dyeing properties (Cheung, 2018).

4.2.2 Plasma treatment for colour fading

In the process of plasma treatment for colour fading, a commercial ozone plasma machine G2 (Standard model, Spain Jeanologia) was used. In comparison to traditional methods, the G2 plasma machine conserves 62% of energy (kW/h), reduces water consumption by 67%, and cuts down the usage of chemicals by 85%, all while decreasing production time by a substantial 85% (Kan et al., 2016). The G2 leverages electric currents to ionize oxygen molecules in incoming air, producing a mixture of reactive oxygen to fade textiles (Kan et al., 2016). The residual ozone plasma is then converted into purified air before being expelled back into the atmosphere (Kan et al., 2016).

The plasma treatment was conducted in a garment processing factory in China; the parameters are summarised in Table 3.5. The operating principle and technical specifications of the G2 plasma machine are outlined in Section 2.4 and Section 3.3. Under different combinations of plasma treatment parameters, 72 fabric samples were used for colour measurements in each type of dye, giving a total of 216 fabric samples for the three dyes. This is because there are a total of 24 combinations of plasma treatment parameters ($4 \times 3 \times 2 = 24$), and the fabric samples are dyed at three different dye concentrations ($24 \times 3 = 72$), and the types of dyes are also three ($72 \times 3 = 216$). The 216 fabric samples obtained by these three dyes were labelled RR1-RR72 (for red colour), RB1-RB72 (for blue colour) and RY1-RY72 (for yellow colour).

4.2.3 Colour measurement arrangement

The fabric samples were conditioned at 65±2% relative humidity and 20±2°C for at least 24 hours before colour measurement. The fabrics were divided into three types, reactive dye-dyed – Red (RR), reactive dye-dyed – Blue (RB) and reactive dye-dyed Yellow (RY). In order to

get accurate colour measurement data for each type of samples, experiments were carried out using a Macbeth Colour-Eye 7000A (CE-7000A) spectrophotometer and the colour was measured in the form of specific CIE L*a* b* and K/S values. Colour measurement conditions of Macbeth Colour-Eye 7000A were set under the specular, including large aperture value, 10º observer angle and illuminant D65. In addition, the colour measuring instrument was calibrated by loading a black trap and a white trap. In the experiments, in order to make the colour measurements for each fabric sample more accurate, four uniformly coloured points of each fabric sample were selected for testing and the final colour measurement is the average of these four points (as shown in Figure 3.5).

4.2.4 Using BRNN to model, simulate and predict

CIE L*a*b* and K/S values corresponding to the 216 cotton samples were measured. After preliminary data processing, BRNN was used to explore the relationship between plasma treatment process parameters and CIE L*a*b* values and K/S values corresponding to the 216 cotton samples. They are divided into three types, namely RR, RY and RB. Among them, 192 groups of data were used in the modelling and simulation of BRNN, and the remaining 24 groups of data selected by stratified sampling are used to test the generalizability of BRNN. The data sets are divided as shown in the following Table 4.1. Moreover, a modular strategy was employed to reduce the intricacy of the neural network (Choudhury et al., 2015). Specifically, a colour coordinate or K/S value was meticulously selected as the input prior to plasma treatment, and a corresponding colour coordinate or K/S value was meticulously selected as the output post-plasma treatment. This approach was adopted to directly anticipate the colour measurements of the reactive dye-dyed cotton fabric that has undergone fading by the BRNN models.

Table 4.1. Division of the data sets for the reactive dye-dyed fabric samples

Datasets for training and validation (192)	Unseen datasets of BRNN for testing (24)
RR2-RR10, RR12-RR20, RR22-RR30, RR32-RR40, RR42-RR50, RR52-RR60, RR62-RR70, RR72	RR1, RR11, RR21, RR31, RR41, RR51, RR61, RR71
RB2-RB10, RB12-RB20, RB22-RB30, RB32-RB40, RB42-RR50, RB52-RB60, RB62-RB70, RB72	RB1, RB11, RB21, RB31, RB41, RB51, RB61, RB71
RY2-RY10, RY12-RY20, RY22-RY30, RY32-RY40, RY42-RY50, RY52-RY60, RY62-RY70, RY72	RY1, RY11, RY21, RY31, RY41, RY51, RY61, RY71

For regression analysis of small data sets, it is preferred to build a small three-layer neural network, and establish neural network models for each value to be explored. In addition, in order to avoid the possible overfitting problem of small data sets, Bayesian Regularization Algorithm is selected to optimize the neural network (Abd Jelil et al., 2013; Doan & Liong, 2004). Although Bayesian Regularization Algorithm needs more computing time, it can effectively improve generalizability of neural network models (Abd Jelil et al., 2013; Doan & Liong, 2004). In addition, validation of the trained neural network is carried out through 10-fold cross validation (Farooq et al., 2021). In 10-fold cross validation, the data is divided into 10 subsets, each of which has about 19 groups of data. In each training, one subset is used for validation and the other nine subsets are used for training. Such training is carried out 10 times. According to the number of input and output layers, in each training, the number of hidden layers of neurons is in the range of 3-12, and the optimal number of hidden layers is selected for each training. When the network is trained 10 times and reaches the performance goal in different rounds of training, the final network selected is evaluated by taking the average value of 10 runs. Therefore, we have created four similar neural networks, and the input and output values are shown in the following Figure 4.1.
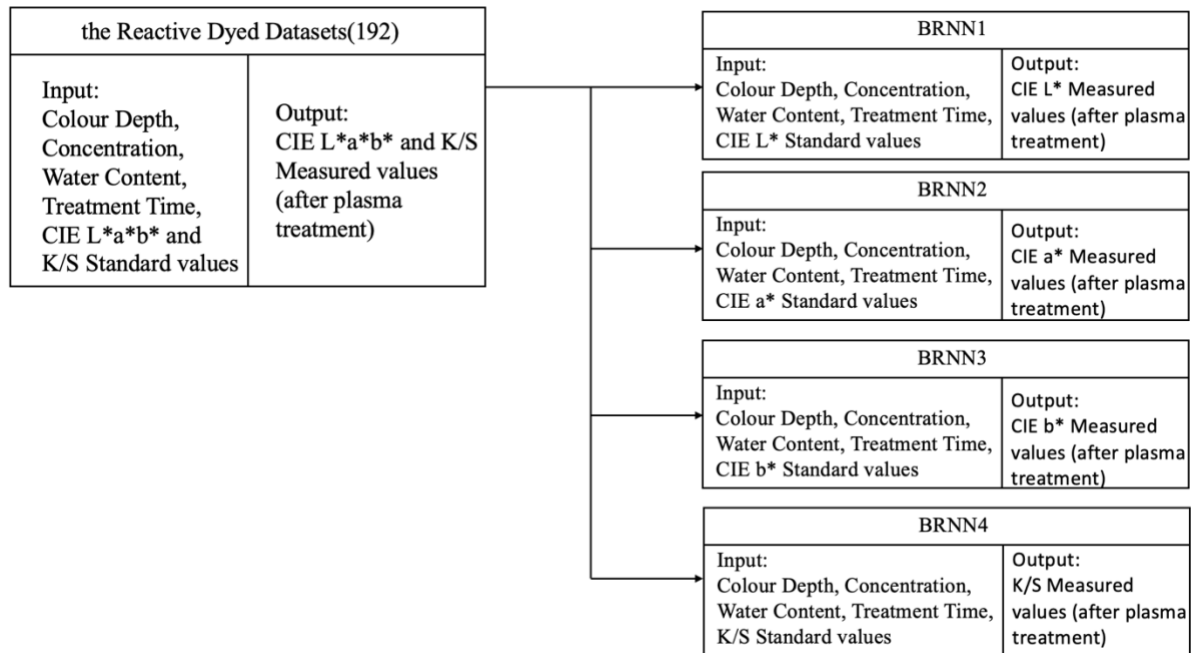
Figure 4.1. BRNN1-BRNN4 models with their inputs and outputs from the reactive dye-dyed Datasets

As shown in Figure 4.1, initial values (standard values) of colour depth, air (oxygen) concentration, water content, treatment time, CIE L*a*b* and K/S corresponding to the samples are selected as the inputs to the BRNN, and the measured CIE L*a*b* and K/S values corresponding to the faded cotton material after plasma treatment are used as the outputs. In addition, the input and output data are normalized to have zero mean and unity standard deviation before training, and the effects of outliers and extreme values are effectively avoided by normalization (Farooq et al., 2021). The topology of the BRNN neural network is shown in Figure 4.2.
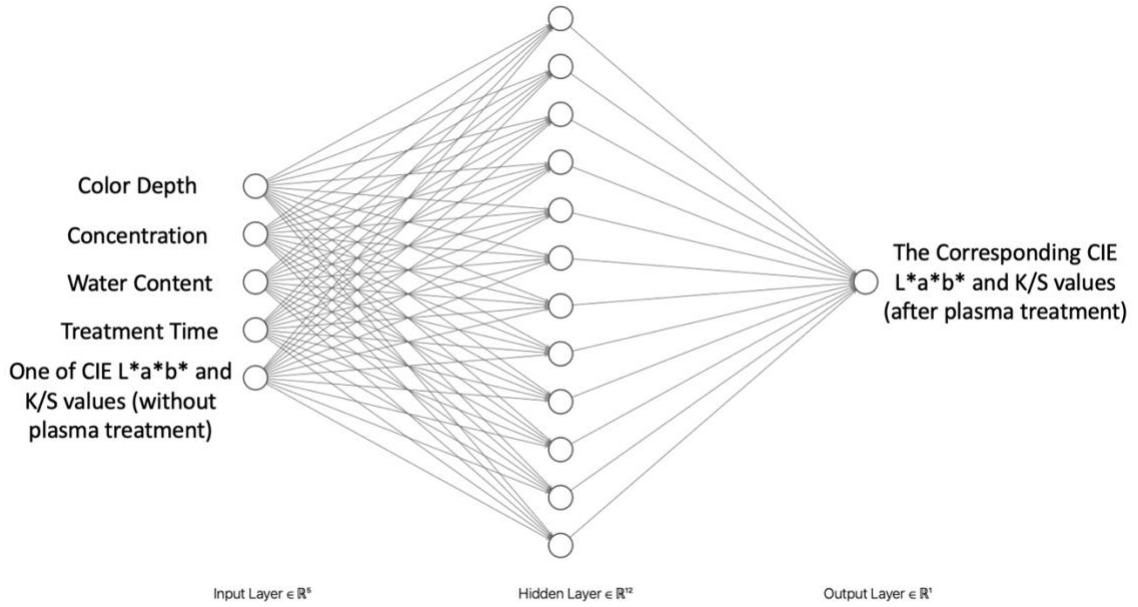
Figure 4.2. The topology of BRNN models

The final BRNN models obtained after 10-fold cross-validation are saved and then predicted for the unseen 24 data sets to further test the utility and generalizability of the BRNN models (Figure 4.3).
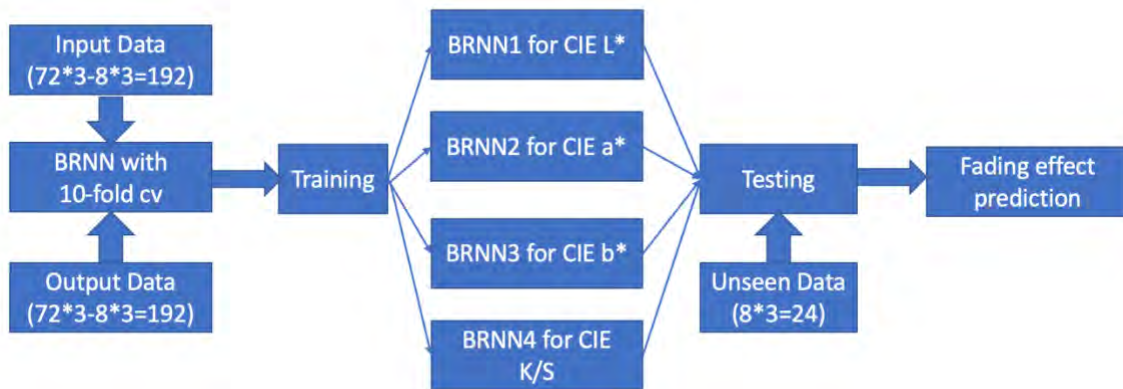
Figure 4.3 Flow chart of fading effect prediction using BRNN models

4.2.5 Verification of the accuracy of BRNN

Mean absolute error (MAE), root mean square error (RMSE) and mean absolute percentage error (MAPE) are used to assess accuracy of BRNN models, and they are also the common metrics used for assessment of accuracy of neural network models and performance of the models in different ways (Abiodun et al., 2019; Hodson, 2022; Ostertagova & Ostertag, 2012). For a sample y_i with n measurements (y_i, $i = 1, 2, \ldots, n$), and n corresponding BRNN model predictions $\hat{y}_i$ ($i = 1, 2, \ldots, n$), MAE, RMSE and MAPE are shown in Equations (4.1), (4.2) and (4.3), respectively (Abiodun et al., 2019; Hodson, 2022; Ostertagova & Ostertag, 2012).

$$MAE = \frac{1}{n} \sum_{i=1}^{n} |y_i - \hat{y}_i| \tag{4.1}$$

$$RMSE = \sqrt{\frac{1}{n} \sum_{i=1}^{n} (y_i - \hat{y}_i)^2} \tag{4.2}$$

$$MAPE = \frac{1}{n} \sum_{i=1}^{n} \left| \frac{\hat{y}_i - y_i}{y_i} \right| \times 100\% \tag{4.3}$$

Among them, MAE is the metric used to measure overall accuracy (Ostertagova & Ostertag, 2012). If the predicted and actual values are well-fitted, MAE is close to zero, which indicates that the BRNN model is highly accurate. If the fit is poor, the MAE is large, which indicates that the BRNN model's accuracy needs to be improved. RMSE is also a measure of overall accuracy; it is the square root of the MSE, with large errors given extra weight, and the severity of the prediction error is the same as the predicted or actual value's dimension (Ostertagova &

Ostertag, 2012). MAPE, on the other hand, measures relative performance. If the calculated value is less than 10%, it is considered a highly accurate prediction, and if it is between 10% and 20%, it is considered a good prediction. If it is between 20% and 50%, it is an acceptable prediction. If it exceeds 50%, the prediction is inaccurate (Ostertagova & Ostertag, 2012).

4.3 Results and discussion

The four trained BRNN models' performances are shown in Table 4.2. It can be seen that the mean absolute errors (MAE) of BRNN1-BRNN4 are 0.6407, 0.8457, 1.2046 and 7.4566, respectively, and the root mean square errors (RMSE) are 0.8507, 1.1621, 1.6398 and 9.7202, respectively, and the mean absolute percentage errors (MAPE) are 1.1426%, 5.3407%, 18.0368% and 14.4288%, respectively. These results are within the acceptable range for CIE L*a*b* values, and the prediction errors are slightly larger for K/S values. The prediction errors may be influenced by the structure of the cotton fabric, which affects reflectance of the dyed sample at a particular wavelength and thus the K/S values (Tang et al., 2018). In terms of the coefficient of determination (R^2), values are 0.9956, 0.9976, 0.9980, and 0.9687 respectively, whereas for CIE L*a*b* values, coefficients of determination are all very close to 1, indicating that the model fits well and that the actual and predicted values are very close to each other. For K/S values, the model fits well, but there is some deviation.

Table 4.2. The four trained BRNN models' performances

	BRNN1: CIE L* values	BRNN2: CIE a* values	BRNN3: CIE b* values	BRNN4: K/S values
MAE	0.6407	0.8457	1.2046	7.4566
RMSE	0.8507	1.1621	1.6398	9.7202
MAPE	1.1426%	5.3407%	18.0368%	14.4288%
Coefficient of determination (R^2)	0.9956	0.9976	0.9980	0.9687

To further verify the practicality and generalizability, the four trained BRNN models are tested on 24 datasets not involved in training and validation, and the results predicted are compared with the actual values, as shown in Figure 4.4 to Figure 4.7. For Figure 4.4 to Figure 4.6, the predicted and actual values are very close to each other, and the fitted trends are basically the same, which indicates that the model provides a good prediction of CIE L*a*b* values of the unseen dataset. For Figure 4.7, the predicted and actual values have the same trend, and the predicted results are slightly different from the actual values. The difference between predicted and actual values is shown in Table 4.3, and the formulas for calculating the difference and the mean of the absolute values of ΔCIE L*a*b* are shown in Equations (4.4) and (4.5). It can be seen that the MAE of ΔCIE L* is 0.53, MAE of ΔCIE a* is 0.96, MAE of ΔCIE b* is 0.97, and MAE of ΔK/S is 7.25. As K/S values are determined by measuring the reflectance spectrum of the dyed fabric, they reflect the concentration of dye on the cotton fabric (Özkan et al., 2018; Tang et al., 2018). The source of its error is then likely to come from the measurement stage and is influenced by the structure, texture, evenness of dyeing and levelness of the knitted fabric (Özkan et al., 2018). For example, yarn structure and fabric porosity of cotton knitwear can have a significant effect on K/S values (Özkan et al., 2018). This suggests that there may already be some error in K/S values at the time of measurement, leading to more significant errors at the time of prediction.

In general, BRNN models have good generalizability and practicality and can effectively predict CIE L*, CIE a*, CIE b* and K/S values of the unseen dataset when the input model is unknown, and the average error in predicting CIE L*, CIE a*, CIE b* values is less than 1, while there is a slight error in predicting K/S values, but the error is mostly within the acceptable range.

$$\Delta\ CIE\ L^*, \Delta\ CIE\ a^*, \Delta\ CIEb^*\ or\ \Delta K/S\ values \qquad (4.4)$$

$$= Predicted\ values - Actual\ values$$

$$The\ MAE\ of\ \Delta\ CIE\ L^*, \Delta\ CIE\ a^*, \Delta\ CIEb^*\ or\ \Delta K/S\ values \qquad (4.5)$$

$$= \frac{\sum_{i=1}^{n}|\Delta\ CIE\ L^*, \Delta\ CIE\ a^*, \Delta\ CIEb^*\ or\ K/S\ values|}{n}$$
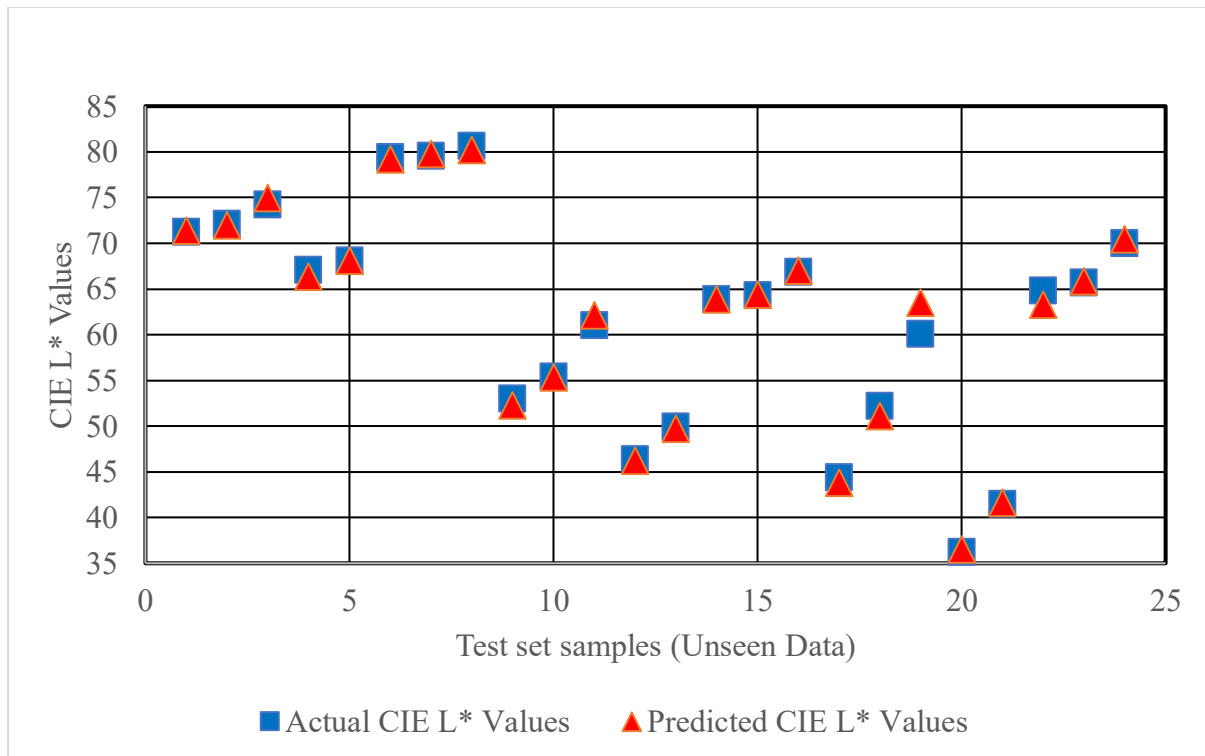
Figure 4.4. The predicted and actual CIE L* values in the reactive dye-dyed unseen data set
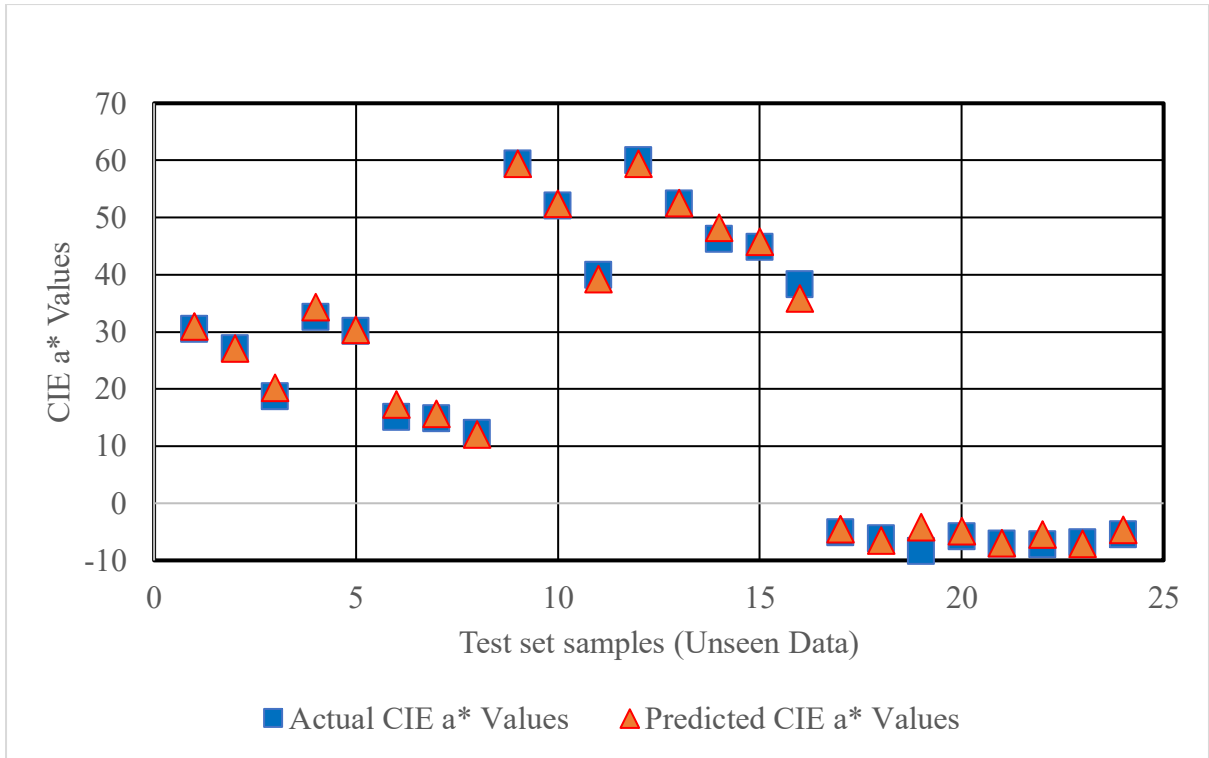
Figure 4.5. The predicted and actual CIE a* values in the reactive dye-dyed unseen data set
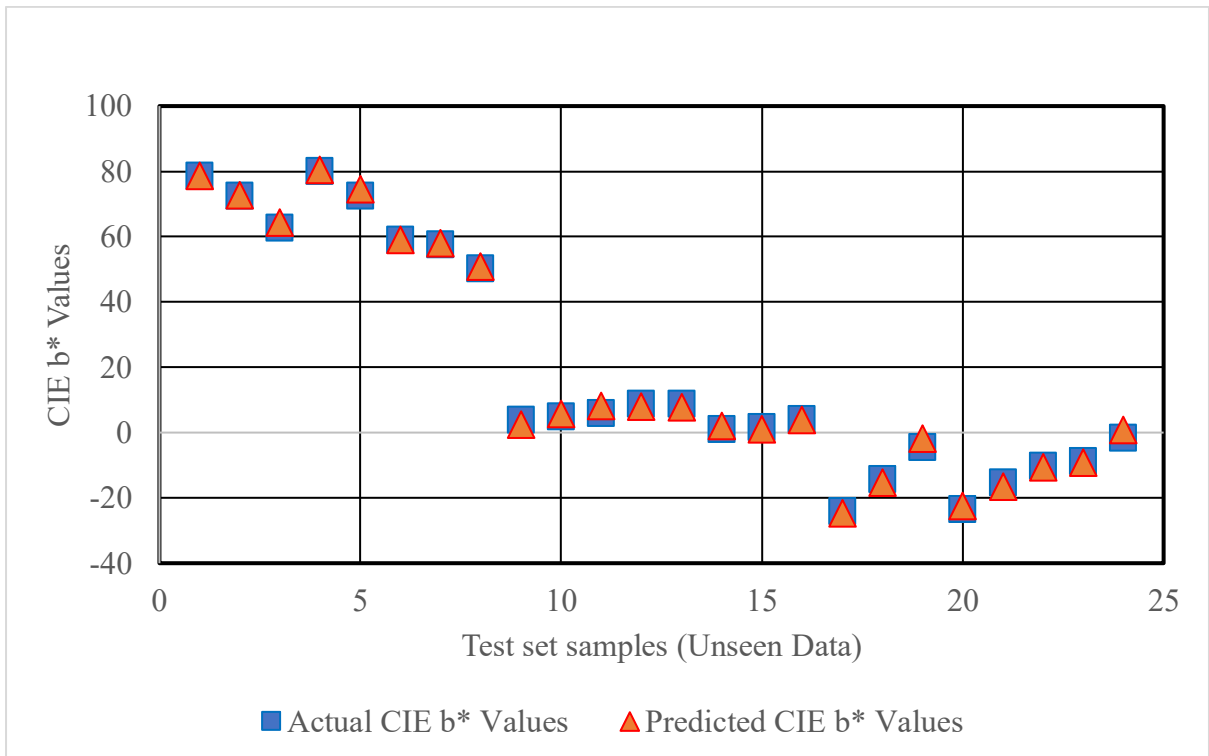
Figure 4.6. The predicted and actual CIE b* values in the reactive dye-dyed unseen data set
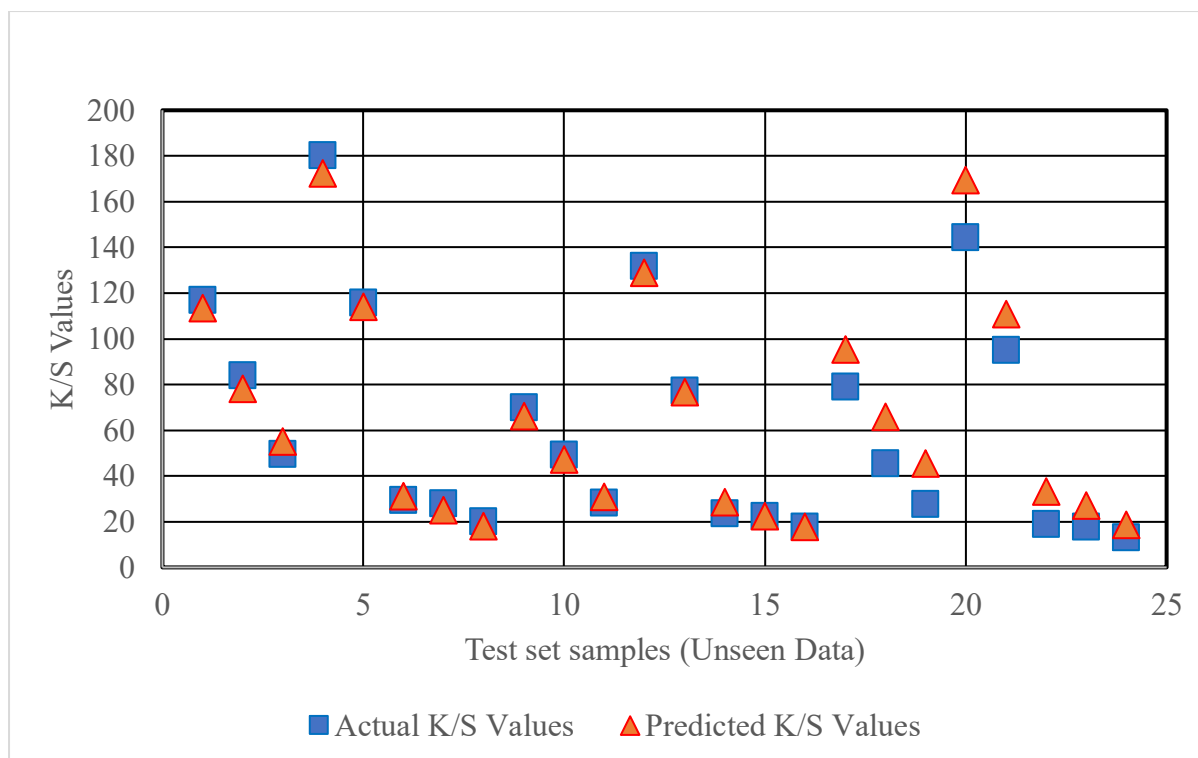
Figure 4.7. The predicted and actual K/S values in the reactive dye-dyed unseen data set

Table 4.3. The colour difference between predicted and actual CIE L*a*b* values and K/S values in the reactive dye-dyed unseen data set

No.	ΔCIE L* values	ΔCIE a* values	ΔCIE b* values	Δ K/S values
RR1	-0.71	0.07	-1.50	-3.88
RR11	-0.06	0.30	0.97	-2.12
RR21	1.05	-0.61	2.26	2.83
RR31	-0.15	-0.52	-0.75	-2.90
RR41	-0.25	0.11	-0.87	-0.59
RR51	-0.01	2.02	1.06	5.22
RR61	0.11	0.90	-0.58	-0.08
RR71	0.13	-2.39	-0.11	-0.04
RB1	-0.60	0.60	-0.57	16.50
RB11	-1.10	-0.29	-1.04	20.59
RB21	3.42	4.27	2.64	17.64
RB31	0.28	0.85	1.03	25.04
RB41	0.14	0.15	-1.22	15.88

RB51	-1.50	1.73	-0.24	14.42
RB61	0.13	-0.32	-0.44	9.39
RB71	0.47	0.83	2.60	5.54
RY1	0.13	0.39	-0.05	-3.54
RY11	-0.17	-0.03	0.24	-6.04
RY21	0.72	1.45	1.58	5.55
RY31	-0.74	1.83	0.44	-7.83
RY41	0.00	0.20	2.11	-1.74
RY51	-0.29	2.24	0.01	1.79
RY61	0.25	0.76	0.28	-2.96
RY71	-0.38	-0.19	0.58	-1.79
MAE	0.53	0.96	0.97	7.25

To further validate the usefulness of the trained BRNN models, differences between predicted and actual CIE L*a*b* values for the unknown dataset were measured. Currently, the CMC formula is widely used in the textile industry, where a colour difference of 1.0 units is evaluated as the accepted tolerance limit (Farooq et al., 2021). In addition, the CIE94 colour distance formula is an improvement based on the CMC formula, which adds observation conditions as a sample representation and observation basis, and it can well predict the subjective colour difference when viewed under reference conditions (Griffin & Sepehri, 2002; Heggie et al., 1996). Furthermore, by using a new data set, the CIE2000 formula was proposed, which is now more consistent with vision, as it also considers other dependencies of chromaticity on hue (Sharma et al., 2005). Thus, the colour difference between CIE L*a*b* predicted values and the actual colour is measured by these three-colour difference formulas and the actual and predicted colours are depicted by CIE L*a*b* values (Table 4.4). In Table 4.4, it can be seen that the values with the superscript "*" are beyond the tolerance limit, and they are RB21, RB51 and RB71, respectively. Among the 24 sets of data, 2 sets of data in the CMC colour difference formula resulted in the difference between predicted and actual colours being outside the

tolerance limits and the passing rate is 91.67% (22/24×100%=91.67%). 3 sets of data in the CIE94 and CIE2000 colour difference formula resulted in colour differences exceeding tolerance limits and the passing rate is 87.50% (21/24=0.875). This also implies that between 87.50% and 91.67% of predicted colours were within the acceptable or imperceptible range. The colour differences between the actual and predicted values for the reactive dye-dyed unseen data are shown in Table 4.5 and Figure 4.8.

Table 4.4. Colour difference between predicted and actual values and colour depiction figure for the reactive dye-dyed unknown data sets

No.	ΔE(CIE94)	ΔE (CMC) (1: 1)	ΔE (CIE 2000) (1:1:1)	Colour depiction figure	
				Actual colour	Predicted colour
RR1	0.89	0.99	0.99		
RR11	0.56	0.54	0.5		
RR21	1.58	1.69	1.64		
RR31	0.4	0.43	0.39		
RR41	0.52	0.53	0.52		
RR51	0.88	1.00	0.84		
RR61	0.47	0.51	0.44		
RR71	0.85	1.06	0.91		
RB1	0.64	1.07	0.76		
RB11	0.83	1.25	1.26		
RB21	3.86*	5.16*	5.61*		
RB31	0.72	1.04	0.93		
RB41	0.77	1.31	0.75		
RB51	1.61	3.01*	2.19*		
RB61	0.36	0.44	0.41		

RB71	2.48*	3.45*	2.53*	
RY1	0.19	0.32	0.24	
RY11	0.11	0.17	0.15	
RY21	0.76	1.15	0.93	
RY31	0.81	1.41	1.07	
RY41	0.52	0.84	0.57	
RY51	1.18	1.79	1.43	
RY61	0.4	0.6	0.49	
RY71	0.3	0.44	0.37	
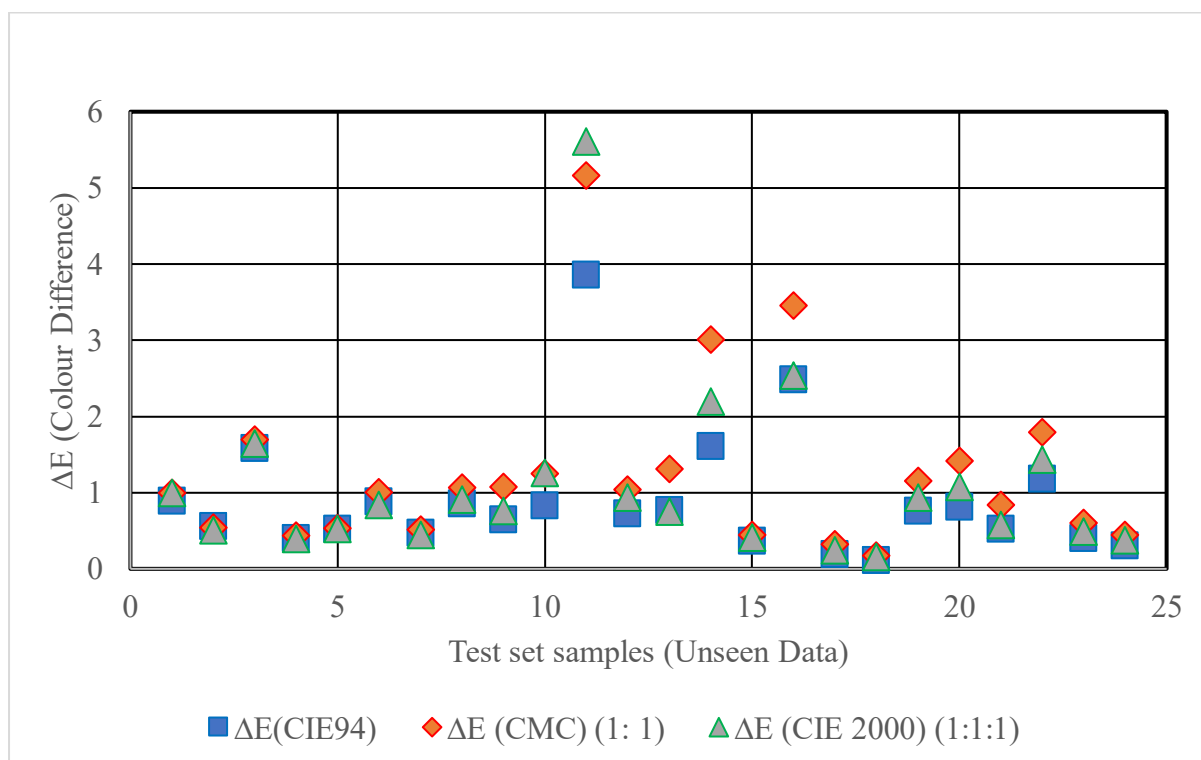
Figure 4.8. Colour Difference between the actual value and predicted value on the reactive dye-dyed unknown data sets

Table 4.5. The summary of the colour differences measured by different formulas for the reactive dye-dyed unknown data sets

Colour difference formula	Average colour difference	Minimum colour difference	Maximum colour difference	Passing Rate
ΔE(CIE94)	0.90	0.11	3.86	87.50%
ΔE (CMC) (1: 1)	1.26	0.17	5.16	91.67%
ΔE (CIE 2000) (1:1:1)	1.08	0.15	5.61	87.50%
Note: The number of the reactive dye-dyed unknown data sets is 24, the tolerance setting is 2.				

In general, BRNN with 10-fold cross-validation can fit the training dataset well and generalised well to the unseen dataset, and the colour differences between predicted values and the actual colours are mostly within the acceptable range. It demonstrated the reproducibility and scalability of the BRNN models, rather than simply fitting a pre-existing data set. These models are also capable of effectively predicting the fading effect of various combinations of plasma treatment parameters on cotton fabrics dyed with reactive dyes, such as varying combinations of plasma treatment parameters with air concentrations ranging from 11% to 69%, cotton fabrics with moisture contents ranging from 36 to 44%, and treatment time ranging from 11 to 29 minutes.

For the prediction error, there may be several sources. First, it is easy to have a certain amount of deviation in the colour measurement process. The second is related to the fabric characteristics, such as the evenness of dyeing, levelness of the fabric, and the structure and surface texture of the cotton fabric (Özkan et al., 2018; Tang et al., 2018). The third is influenced by the small size of the samples; although 10-fold cross-validation does improve the model's ability to predict small data sets to a large extent, it still produces minor errors during changes in the training set (Fushiki, 2011; Rodriguez et al., 2009). The fourth point

pertains to the presence of prediction errors in the dataset of fading samples of reactive dyes in blue colours, such as RB21, RB51, and RB71. This might be due to the fact that different colours of reactive dyes require varying fading times (Atav et al., 2022). Blue might fade faster than red and yellow when exposed to plasma-induced ozone (Atav et al., 2022). For blue, which is prone to fading, it is suggested to limit the ozone treatment time to 5 minutes if only using ozone (Atav et al., 2022). As the fading time ranges from 10 to 30 minutes, the blue colour might have already faded, while the yellow and red colours are still undergoing the fading process. When the neural network is simulating the fading patterns of these three colours simultaneously, since blue fades faster, this might result in a prediction error in the neural network's simulation of its fading pattern.

Thus, the BRNN model has the aptitude to precisely predict the colour measurement data of yellow and red reactive dye-dyed cotton fabrics after plasma fading treatment, but it presents a slight degree of error in predicting the colour measurement data of blue reactive dye-dyed cotton fabrics after plasma fading treatment. The validated and trained BRNN model was successful in reducing the number of trials required to attain a particular colour change in reactive dye-dyed cotton fabrics following plasma treatment, thereby conserving time and costs. The incorporation of AI methods with plasma fading treatment technology has the potential to facilitate the development of intelligent and digitized cotton processing, offering manufacturers a tool to anticipate variations in fade effects and the ability to upscale its use within the industry as an ecologically sustainable technology.

4.4 Conclusion

The use of plasma treatment of cotton fabrics dyed with reactive dyes can achieve fading effects and is an environmentally friendly process. This article has shown that by combining plasma

treatment with BRNN with 10-fold cross-validation, it is possible to effectively predict how different plasma treatment parameters correspond to fading effects, thus reducing the number of invalid attempts and uncertainties. Through the utilization of a modular approach, four BRNN models were constructed to separately predict CIE L*, CIE a*, CIE b*, and K/S values, thereby reducing the complexity of the models and increasing their generalizability to unfamiliar datasets. The BRNN model, which alone predicts one of the CIE L*, CIE a*, CIE b* and K/S values, is trained and can make effective predictions on an unknown dataset. By integrating the four trained networks, a prediction system can be formed to predict how particular sets of plasma treatment parameters produce particular fading effects and colours. Meanwhile, the MAE of the BRNN models for the CIE L*, CIE a*, CIE b* and K/S values are 0.6407, 0.8457, 1.2046 and 7.4566 respectively, and the RMSE are 0.8507, 1.1621, 1.6398 and 9.7202 respectively. MAPE are 1.1426%, 5.3407%, 18.0368% and 14.4288%, the fitted coefficients of determination R^2 are 0.9956, 0.9976, 0.9980, and 0.9687, respectively, and the ΔCIE L*, ΔCIE a*, ΔCIE b* values and ΔK/S values for the 24 unseen data sets are 0.53, 0.96, 0.97 and 7.25 respectively. Besides, the system predicts a small colour difference between the actual colour and the predicted colour, and the percentage of predicted colours within the acceptable range is approximately 87.5% - 91.67%, which means that most of the predictions are acceptable or have imperceptible colour differences. Specifically, the prediction of faded cotton fabric samples after dyeing with red and yellow reactive dyes was accurate, while the prediction of faded cotton fabric samples after dyeing with blue reactive dyes had some errors. Moreover, this means that the developed prediction system based on BRNN with 10-fold cross-validation can be a useful tool to help the dyer to adjust the parameter settings of the plasma machine and the selected recipe before treating the cotton fabric with plasma, thus reducing the cost and the time of trying and contributing to the efficiency. In future research, attempts will be made to enhance the precision of the BRNN model in predicting the fading of cotton

fabric samples dyed with blue reactive dyes. Additionally, the BRNN model will be employed to generate and forecast various combinations of plasma treatment parameters in order to establish the optimal fading colour effect. Further utilization of artificial intelligence methods for inverse prediction of the correlation between fading effect and plasma treatment parameter combinations will also be explored, thereby promoting the advancement of intelligence and digitization in the area of garment fading.

4.5 Disclosure statement

This Chapter has been published in *The Journal of the Textile Institute*.

Chapter 5 Predicting the effect of plasma treatment on the fading of Sulphur-Dyed cotton fabric using BRNN

5.1 Introduction

Fading effectively improves the visual appearance of fabrics and has become a trend in fashionable clothing (Kan et al., 2017; Kan & Song, 2016). For example, cotton apparel products such as faded blue jeans are popular with young people as they provide them with a stylish casual look (Kan et al., 2017; Samanta et al., 2017). In addition, adding the fading effect is a great way for garment manufacturers to increase the value of their final product, as it increases the customer's desire to purchase and therefore the profitability of the business (Samanta et al., 2017).

However, it is possible to achieve the desired fading effect in certain areas of the fabric through traditional chemical or mechanical processes such as sanding, sandblasting, brushing, and pre-washing (Kan & Song, 2016; Liu et al., 2019; Samanta et al., 2017), the traditional processes are restrained by certain challenges and problems. First, it is difficult to establish repeatable and standardised designs and the fading effect of the product tends to be inconsistent (Samanta et al., 2017). Second, large amounts of water are consumed in the production process and highly contaminated effluent is generated due to the chemical products that need to be used in the fading process (Samanta et al., 2017). Third, it is time-consuming and difficult to meet the huge demand for fading results in the jeans market (Kan et al., 2010; Samanta et al., 2017).

Thus, the reliance of traditional fading processes on repetitive trials makes them time-consuming and inefficient and they tend to produce large amounts of wastewater during production (Hossain, Hossain, Choudhury, et al., 2016). This has led to the gradual development of efficient and environmentally friendly fading technologies. Dry treatment and

virtually water-free treatment are becoming a major trend in order to achieve zero emissions (Paul, 2015). Plasma treatment is one such treatment method (Venkatraman & Liauw, 2019). Not only is plasma treatment a completely dry and non-aqueous treatment process, but it is also an effective surface modification treatment for textile materials that can produce fading effects under low health risk conditions and without affecting the bulk properties of the cotton fabric product (Kan et al., 2017; Venkatraman & Liauw, 2019). Moreover, plasma treatment has the ability to modify the surface of fashionable garments, thereby imbuing them with fresh functional attributes alongside changing their original colour properties (Ibrahim et al., 2022). Therefore, the limitations and problems of conventional fading techniques, such as the inability to produce uniform fading effects, loss of quality and difficulty in producing the same fading effect in different batches, can be solved in some cases with the aid of plasma treatment technology (Cheung et al., 2013; Ondogan et al., 2005).

Plasma, as an ionising gas consisting of ions, electrons, excited molecules and energetic photons, can be used to alter textile fibre surfaces in dry state (Samanta et al., 2017). In the textile fading process, faster fading can be achieved by adjusting the settings of the plasma treatment parameters (Liu et al., 2019), which are based on the principle of breaking the interaction and bonding between dye molecules and the fibres by means of the ionising gas, or by etching the surface molecules of the textile fibres (Samanta et al., 2017). The ozone plasma gas that remains in the plasma device at the end of the fading process is also broken down into oxygen due to its unstable and self-decomposing nature (Liu et al., 2019). Through devoting some time to process optimization, the attainment of maximum efficiency, consistency, and reproducibility of the plasma surface treatment procedure can be assured when identical operational parameters are employed for plasma treatment (Kan et al., 2017; Peran & Ercegović Ražić, 2020). Consequently, plasma surface treatment has the potential to become a

reproducible method, and the fading colour effect can be regulated by managing the plasma treatment process parameters and the crucial treatment environment for plasma generation (Peran & Ercegović Ražić, 2020). The plasma treatment process, therefore, has the potential to replace the less environmentally friendly conventional processes (Samanta et al., 2017). However, there are a number of factors that affect the fading effects, the key among them being the water content, treatment time and air concentration (Hossain, Hossain, Choudhury, et al., 2016). As they interact with each other and are non-linear (Hossain, Hossain, Choudhury, et al., 2016), this makes plasma treatment technology still a work-in-progress. According to the study of Kan et al. (2017), the extent of fading of cotton fabrics dyed with sulphur can be regulated by adjusting the process parameters. For example, longer treatment durations and greater air concentrations can considerably enhance the fading effect (Kan et al., 2017). Besides, a lower level of moisture content in the cotton fabric produced better-fading results than a higher level of moisture content (Kan et al., 2017). The dilemma is that obtaining a specific fading effect requires several attempts and observations, as it is difficult to know the right plasma treatment parameters quickly and accurately.

The neural network model is one of the most prevalent forms of intelligent techniques, exhibiting a remarkable degree of accuracy and predictive power in contrast to conventional statistical models. Furthermore, the neural network model showcases its capability of modelling complex nonlinear multidimensional functional relationships, demonstrating excellence in learning and approximating with limited experimental data (Coit et al., 1998). Its ability to generalize well to various nonlinear variables with unknown interactions obviates the need to assume the relationship's nature beforehand (Coit et al., 1998). Moreover, neural network models often surpass statistical models in the modelling of complex datasets. For example, creating an impressive simulation model does not necessitate an exhaustive

comprehension of the chemical or physical characteristics of the process (Gadekar & Ahammed, 2019). Sustainable growth in the cotton production and processing industry can therefore be facilitated by combining plasma processing with intelligent techniques such as the use of Bayesian Regulated Neural Networks (BRNN) (Samanta et al., 2017). BRNN is a neural network model improved by Bayesian regularisation methods, which has effective and accurate predictive power in the non-linear domain (Hossain et al., 2017), allowing good approximations of effects to be obtained from less experimental data, without the need to assume relationships in advance. It can also improve generalisability of neural network models by taking into account the network structure to optimise common overfitting problems (Abd Jelil et al., 2013; Coit et al., 1998; Doan & Liong, 2004; Gadekar & Ahammed, 2019). This is due to the fact that overfitting problems often occur when the data in the training set of the neural network model is small, as it is not simple to acquire a big number of dyeing samples in the textile sector (Hemingray & Westland, 2016; Jawahar et al., 2015). Therefore, the prediction of fading effects of plasma treatment can be facilitated by BRNN (Abd Jelil et al., 2013; Doan & Liong, 2004).

There are a few studies in the existing literature on use of intelligent techniques for predicting outcome of plasma treatment. However, the current studies have focused on four main areas: (i) predicting the effect of plasma treatment on surface wettability of fabrics through improved neural network models (Abd Jelil et al., 2013); (ii) predicting the removal of dyes in aqueous solutions through generalised regression neural networks (Mitrović et al., 2020); (iii) applying adaptive neural network fuzzy inference systems to predict the colour intensity (K/S) of dyed wool fabrics (Haji & Payvandy, 2020); and (iv) employing feedforward neural network models to predict the dyeing properties of wool after air-vacuum plasma treatment, resulting in regression values of approximately 0.95 (Omerogullari Basyigit et al., 2023).

Therefore, the main objective of this study was to construct a BRNN model for predicting the fading effect of plasma treatment of sulphur-dyed cotton fabrics. Firstly, sulphur dyes, a dye category accounting for approximately 30% of global textile dye consumption, are used to dye 14% of apparel products, which may be subjected to fading-related treatments (Kan et al., 2017). Secondly, using the trained and validated BRNN to predict the colour change of sulphur-dyed cotton fabrics after plasma treatment can effectively reduce the number of repeated attempts. This can reduce time and cost compared to traditional ways of adjusting plasma treatment parameters. Additionally, it can accelerate the growth of use of intelligent and digital techniques in the cotton processing sector, offer manufacturers a reference for using plasma treatment to fade cotton fabrics, hasten the scaling up of this environmentally friendly technology, and support it in becoming a useful industrial application.

5.2 Methodology

5.2.1 Fabric samples and dyeing

Fabric samples (30cm x 40cm) were dyed at a dyeing factory in China with commercial sulphur dyes in primary colours of red (Diresul Red RDT-BG liq, labelled "SR"), blue (Diresul Blue RDT-2G liq 150, labelled "SB") and yellow (Diresul Yellow RDT-E liq, labelled "SY") at 0.5%, 1.5% and 2.5% dye concentrations. The fabric was a 32s/2 cotton single (Lacoste) knitted fabric with a weight of $220g/m^2$.

5.2.2 Plasma treatment of faded colours

A commercial ozone plasma machine G2 (standard model, Spain Jeanologia) was used for plasma treatment. The plasma treatment of cotton fabrics was carried out at a garment processing plant in China and parameters used are summarised in Table 3.5. Section 2.4 and

Section 3.3 delineate the operational principle and technical characteristics of the G2 plasma apparatus. A total of three process parameters were used: the air concentration, the water content of the dyed fabric and the treatment time. With different combinations of plasma treatment parameters, 72 fabric samples were used for colour measurements for each type of dye and a total of 216 fabric samples for the three different colours of sulphide dyes. There were 24 combinations of plasma treatment parameters (4×3×2=24), and fabric samples were dyed at three different dye concentrations (24×3=72) and three types of dyes (72×3=216). The 216 fabric samples obtained through these three dyes were labelled SR1-SR72 (for red colour), SB1-SB72 (for blue colour) and SY1-SY72 (for yellow colour).

5.2.3 Colour measurement arrangements

The dried and decoloured fabric samples were conditioned at 65±2% relative humidity and 20±2°C for at least 24 hours prior to colour measurement. The fabrics were divided into three types: sulphur dye-red (SR), sulphur dyed-blue (SB) and sulphur dyed-yellow (SY). Macbeth Colour-Eye 7000A (CE-7000A) spectrophotometer was used to obtain accurate colour measurements for each type of sample, with colours measured as specific CIE L*a* b* and K/S values. Colour measurement conditions for the Macbeth Colour-Eye 7000A were set under a specular that included a large aperture value, a 10° viewing angle and illuminant D65. In the experiments, four fabric samples of each kind of fabric sample and four uniformly coloured areas of each fabric sample were selected for testing in order to make the colour measurements for each fabric sample more accurate and the final colour measurement was the average of these data (as shown in Figure 3.5).

5.2.4 Modelling, simulation and prediction using BRNN

The CIE L*a*b* and K/S values for 216 sulphur-dyed cotton fabric samples were measured. Then, the relationship between plasma treatment process parameters and the CIE L*a*b* and K/S values corresponding to the 216 cotton samples was explored using BRNN after preliminary data processing. They were divided into three types, labelled SR, SB and SY. 192 of these data sets were used for modelling and simulation of BRNN. The remaining 24 data sets, selected by stratified sampling, were used to test the generalisability of BRNN. These data sets were divided as shown in Table 5.1.

Table 5.1. Division of the data sets for the sulphur dyed fabric samples

Datasets for training and validation (192)	Unseen datasets of BRNN for testing (24)
SR1, SR3-SR11, SR13-SR21, SR23-SR31, SR33-SR41, SR43-SR51, SR53-SR61, SR63-SR71	SR2, SR12, SR22, SR32, SR42, SR52, SR62, SR72
SB1, SB3-SB11, SB13-SB21, SB23-SB31, SB33-SB41, SB43-SB51, SB53-SB61, SB63-SB71	SB2, SB12, SB22, SB32, SB42, SB52, SB62, SB72
SY1, SY3-SY11, SY13-SY21, SY23-SY31, SY33-SY41, SY43-SY51, SY53-SY61, SY63-SY71	SY2, SY12, SY22, SY32, SY42, SY52, SY62, SY72

For regression analysis of small data sets, a small three-layer neural network was built and a Bayesian Regularisation Algorithm was chosen to optimise the neural network to avoid possible overfitting problems with small data sets (Coit et al., 1998; Doan & Liong, 2004). Even though Bayesian Regularisation Algorithm needs more processing time, it substantially enhances the neural network model's generalisability. (Abd Jelil et al., 2013; Doan & Liong, 2004). Furthermore, validation of the trained neural network is performed by 10-fold cross-validation (Farooq et al., 2021). In 10-fold cross-validation, the data were separated into 10 subsets, each containing around 19 data sets, and then cross-validated. One subset is used for

validation and the other nine subsets are used for training in each training session. Such training was performed 10 times. Depending on the number of input and output layers, the number of hidden layers of neurons in each training session ranged between 3 and 12, with the optimal number of hidden layers being determined by each training session. The final selected network was evaluated by taking the average of the 10 runs after the network had been trained 10 times and had reached the performance target in different rounds of training. In addition to using Bayesian regularisation algorithms and cross-validation to enhance the performance of the designed neural network, a modular approach was used to reduce the complexity of the model (Choudhury et al., 2015). For prediction of the four output values, the designed BRNN model was divided into four modules. The modular approach allows the user to better understand the relationship between each output value and the plasma processing parameters, while effectively reducing the training time. Therefore, four similar neural network modules were created with the input and output values as shown in Figure 5.1.

As shown in Figure 5.1, inputs to the BRNN model selected were: colour depth corresponding to the sample, air (oxygen) concentration, water content, treatment time, and initial values of CIE L*a*b* and K/S (standard values). Outputs selected were: measured CIE L*a*b* and K/S values corresponding to the faded cotton material after plasma treatment. In the construction of the BRNN model, MATLAB (version R2021a) software was used, and the maximum number of training epochs (iterations) was set to 1000 so that the network would have enough time and iterations to converge to the minimum error. Transfer functions for the hidden and output layers were set to MATLAB's built-in 'logsig' and 'purelin' functions respectively. Meanwhile, the learning rate was set to 0.01 and the training termination error was set to 10^{-6}. Besides, the input and output data were normalised to have a mean of zero and a standard deviation of one before training. By normalising the data, effects of outliers and extreme values

were effectively avoided and the predictive performance of the BRNN was further improved during training due to the reduction of computational errors related to parameter size (Choudhury et al., 2015; Farooq et al., 2021). The topology of the BRNN system is shown in Figure 5.2.
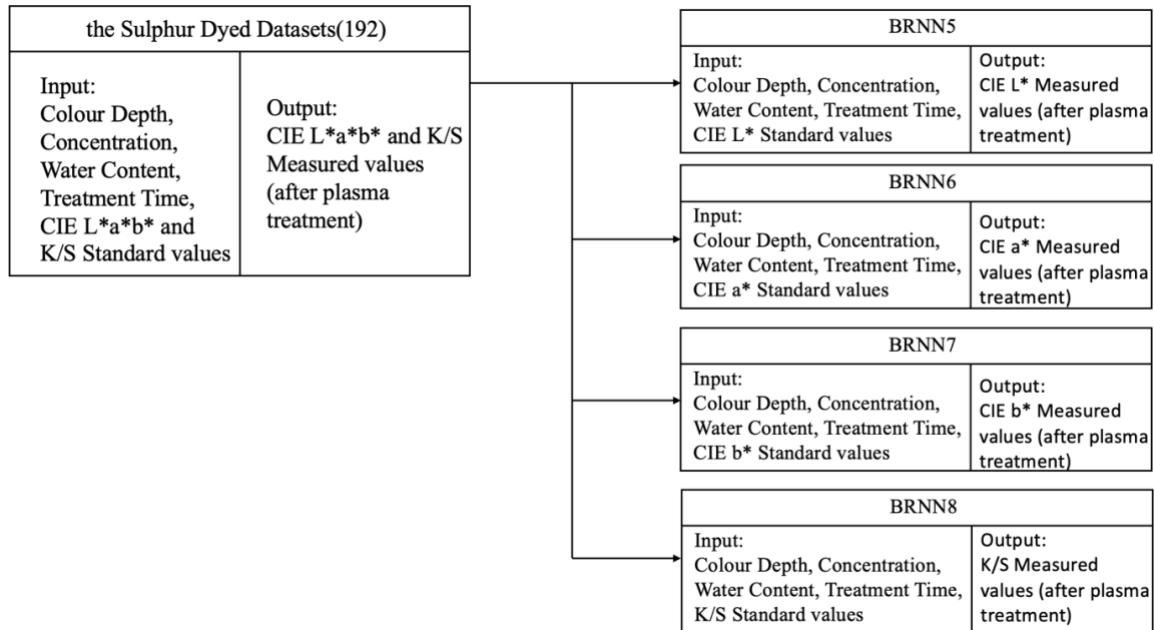
Figure 5.1. The inputs and outputs of four BRNN models
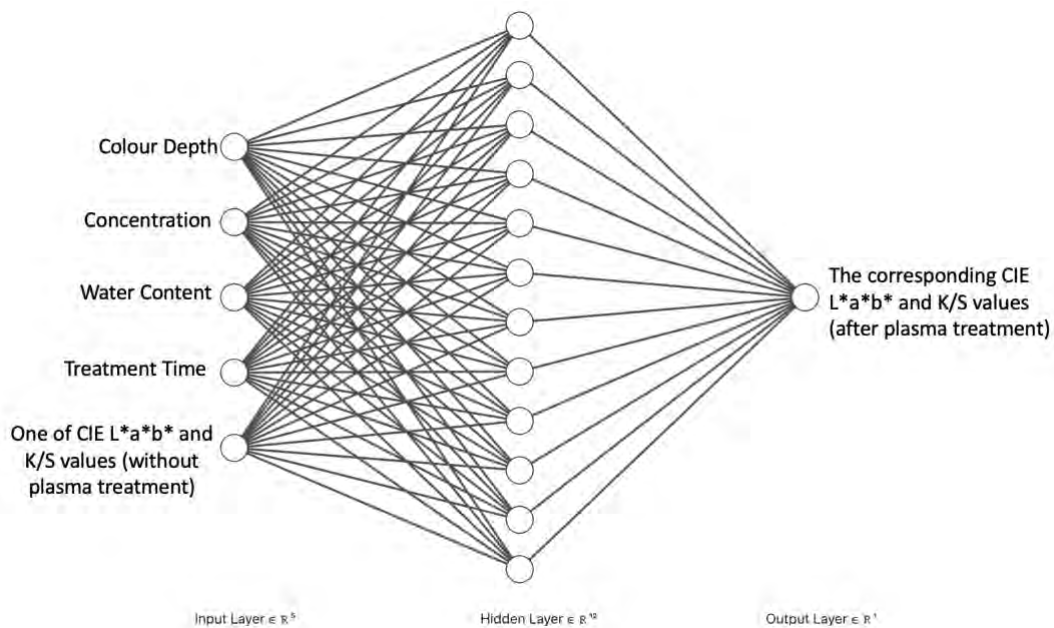
Figure 5.2. The topology of BRNN models
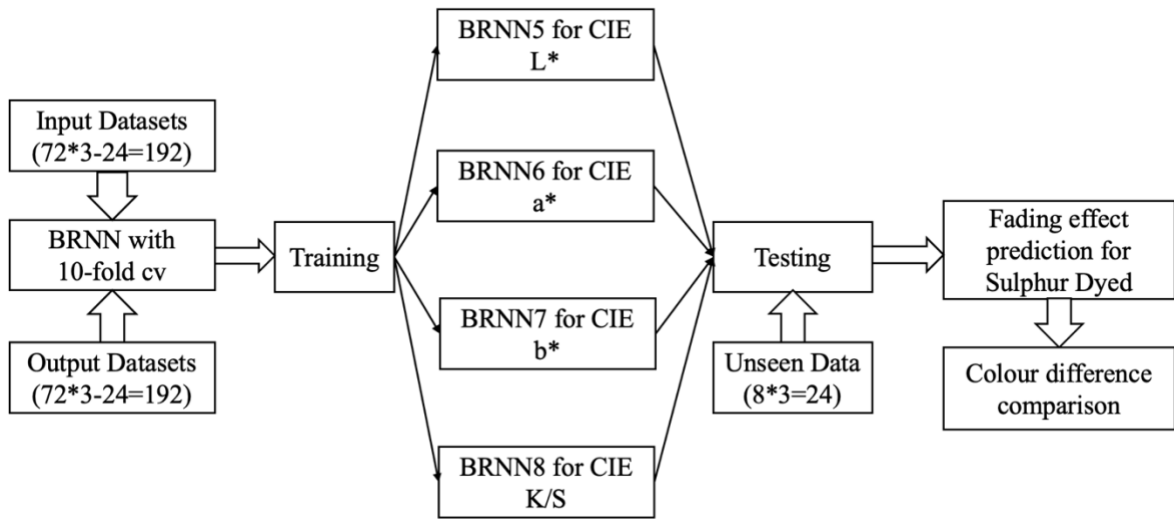
Figure 5.3. Flow chart of fading effect prediction using BRNN models

The final BRNN model created after 10-fold cross-validation was retained and then used to predict an unseen dataset of 24 to assess the applicability and generalizability of the BRNN model (Figure 5.3).

5.2.5 Verification of the accuracy of BRNN

Mean absolute error (MAE) and root mean square error (RMSE), as common metrics for assessing the accuracy of neural network models and model performance, are used to evaluate the accuracy of BRNN models (Abiodun et al., 2019; Chai & Draxler, 2014; Ostertagova & Ostertag, 2012). MAE and RMSE are presented in Equations (5.1), (5.2) for a sample y_i with n measurements (y_i, $i = 1, 2, \ldots, n$), and n matching BRNN model predictions $\hat{y}_i$ ($i = 1, 2, \ldots, n$) (Abiodun et al., 2019; Chai & Draxler, 2014; Ostertagova & Ostertag, 2012).

$$MAE = \frac{1}{n}\sum_{i=1}^{n}|y_i - \hat{y}_i|$$

(5.1)

$$RMSE = \sqrt{\frac{1}{n}\sum_{i=1}^{n}(y_i - \hat{y}_i)^2} \qquad (5.2)$$

Where MAE is the metric used to measure the overall accuracy (Ostertagova & Ostertag, 2012). If the predicted and actual values closely match, the MAE is near zero, indicating that the BRNN model is very precise. If the fit is poor, MAE is big, this indicates that the BRNN model's accuracy must be enhanced. RMSE, the square root of MSE, is another measure of total accuracy, which gives extra weight to large errors, with the severity of the prediction error being the same as the dimensionality of the predicted or actual values (Ostertagova & Ostertag, 2012).

In addition, the coefficient of determination R^2 was also used as a measure of generalisability of the BRNN model (Choudhury et al., 2015). If the R^2 value is closer to 1, then it means that the correlation between the predicted and actual values is better, indicating that the trained network is more capable of generalising to unseen data, which may indicate better performance of the constructed BRNN model.

In general, when assessing model performance, it is often necessary to combine various metrics (Chai & Draxler, 2014), such as MAE, RMSE and the coefficient of determination R^2. For example, MAE is suitable for describing uniformly distributed errors and is not suitable for reflecting some large errors (Chai & Draxler, 2014). RMSE is more suitable for describing normally distributed errors and is sensitive to outliers (Chai & Draxler, 2014). The coefficient of determination R^2 reflects how well the model fits but gives no information about the residuals of the model. Thus, a single indicator usually emphasises one aspect of the error

characteristics, whereas a combined indicator evaluation system is more suitable for assessing the overall performance of the model (Chai & Draxler, 2014).

5.3 Results and discussion

The performance of the four well-trained BRNN modules is shown in Table 5.2. It can be seen that the mean absolute errors (MAE) of BRNN5-BRNN8 are 0.9150, 0.6836, 0.8833 and 1.0216, respectively, and the root mean square errors (RMSE) are 1.3166, 0.9035, 1.1572 and 1.6768, respectively, both within acceptable ranges of CIE L*a*b* and K/S values. In terms of the coefficient of determination (R^2), the values were 0.9819, 0.9906, 0.9908 and 0.9649 respectively, while for CIE L*a*b* values, the coefficients of determination were highly close to 1, indicating that the model fitted well and the actual and predicted values matched closely. For K/S values, the model fits well, but with some deviations.

Table 5.2. The performances of the trained BRNN5-BRNN8 models

	BRNN5: CIE L* values	BRNN6: CIE a* values	BRNN7: CIE b* values	BRNN8: K/S values
MAE	0.9150	0.6836	0.8833	1.0216
RMSE	1.3166	0.9035	1.1572	1.6768
Coefficient of determination (R^2)	0.9819	0.9906	0.9908	0.9649

Four trained BRNN modules were tested on 24 datasets not involved in training and validation to further validate the utility and generalisability, and the predicted results were compared with the actual values (Figure 5.4 to Figure 5.7). It can be seen that predicted and actual values match closely match and the fit trends are generally consistent, with the predictions differing slightly from the actual values, indicating that the model provides good predictions of CIE L*, CIE a*, CIE b* or K/S values for the unseen dataset. The differences between the predicted

and actual values are shown in Table 5.3, and the formulae for the differences and MAE of ΔCIE L*, ΔCIE a*, ΔCIE b* or ΔK/S are given in Equations (5.3) and (5.4). It can be seen that the MAE of ΔCIE L* is 0.72, the MAE of ΔCIE a* is 0.36, the MAE of ΔCIE b* is 0.77, and the MAE of ΔK/S is 0.82.

$$\Delta\ CIE\ L^*, \Delta\ CIE\ a^*, \Delta\ CIE\ b^*\ or\ \Delta K/S\ values \tag{5.3}$$
$$= Predicted\ values - Actual\ values$$

$$The\ MAE\ of\ \Delta\ CIE\ L^*, \Delta\ CIE\ a^*, \Delta\ CIE\ b^*\ or\ \Delta K/S \tag{5.4}$$
$$= \frac{\sum_{i=1}^{n} |\Delta\ CIE\ L^*, \Delta\ CIE\ a^*, \Delta\ CIE\ b^*\ or\ \Delta K/S\ values|}{n}$$
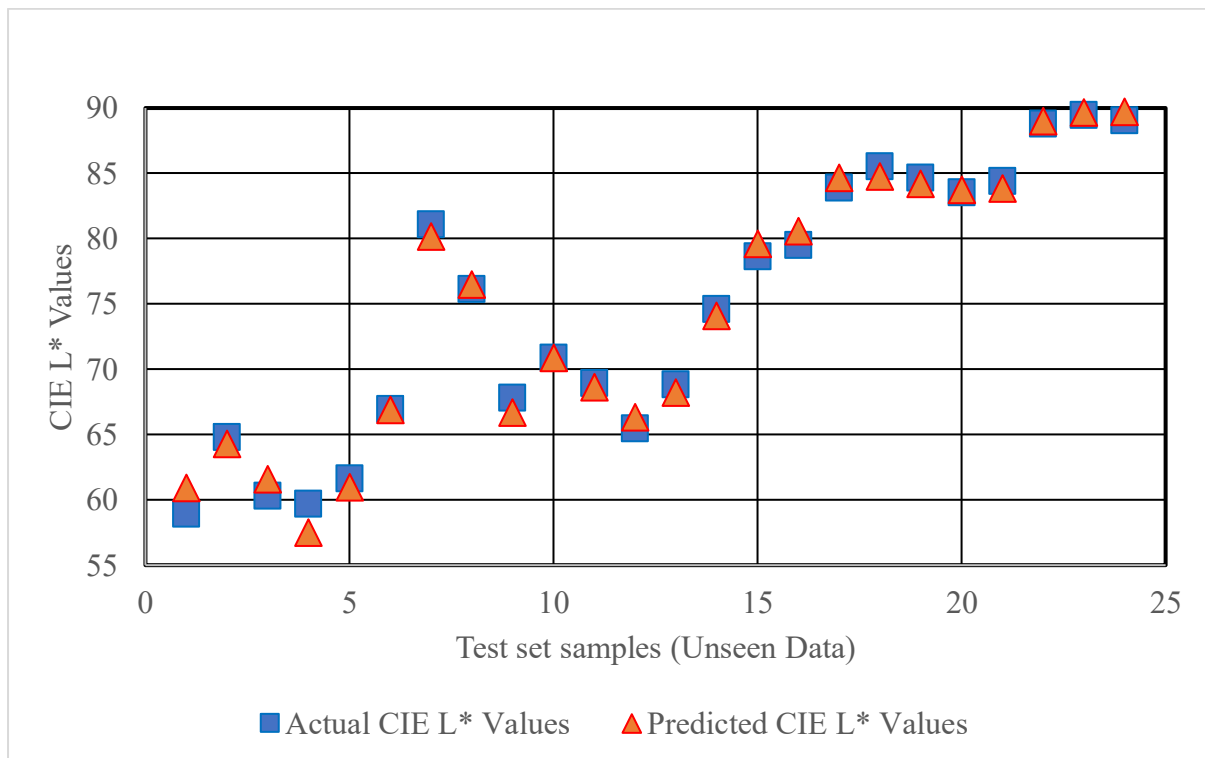
Figure 5.4. The predicted and actual CIE L* values in the sulphur dyed unseen data set
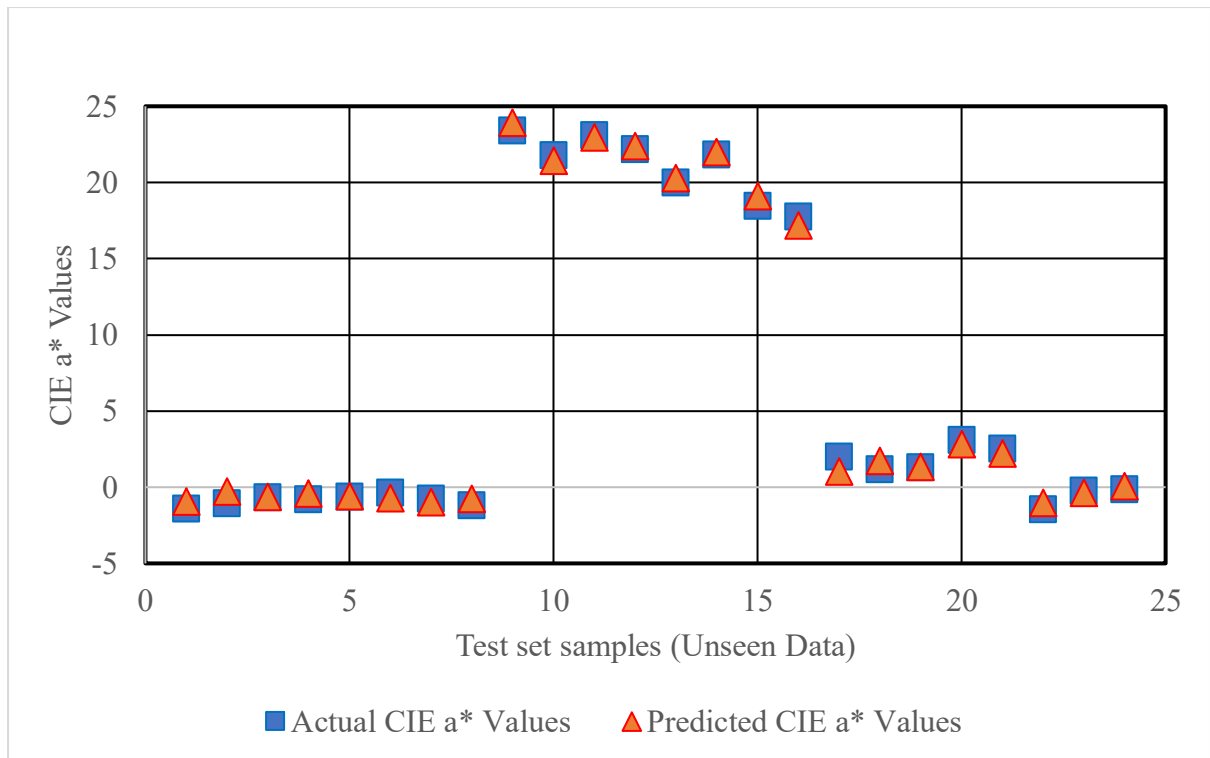
Figure 5.5. The predicted and actual CIE a* values in the sulphur dyed unseen data set
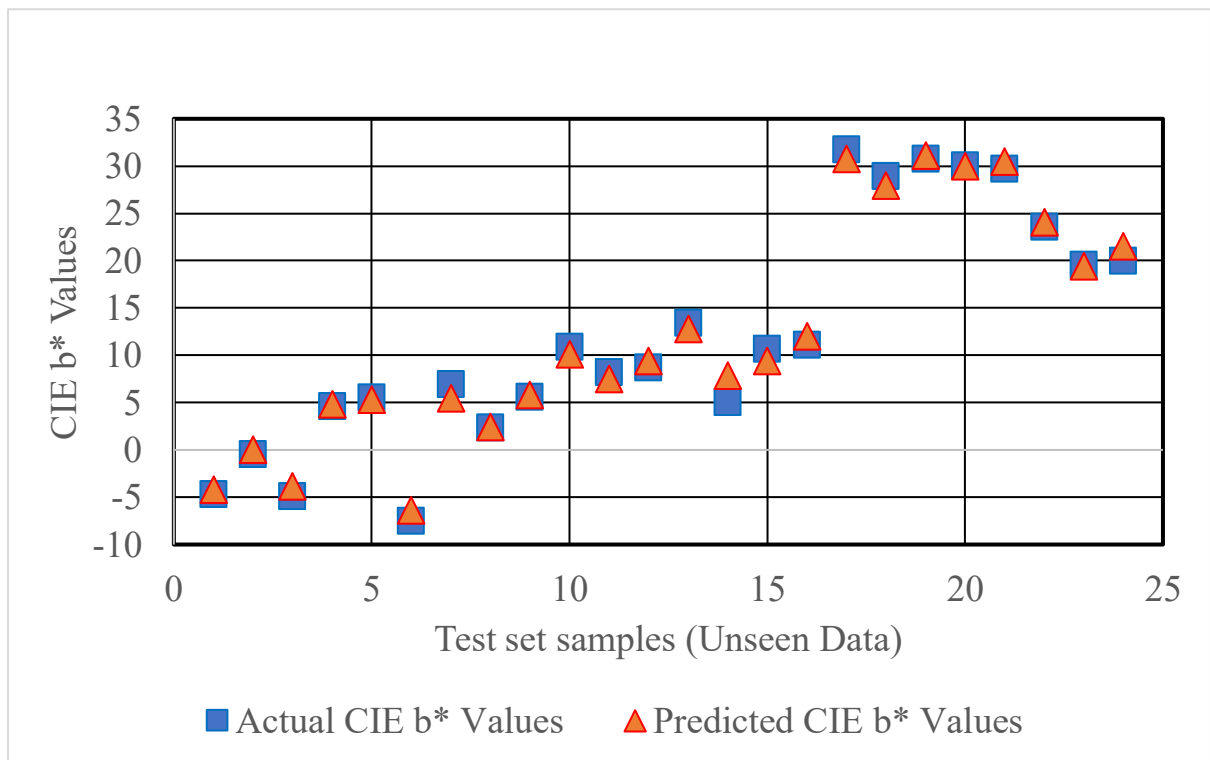
Figure 5.6. The predicted and actual CIE b* values in the sulphur dyed unseen data set
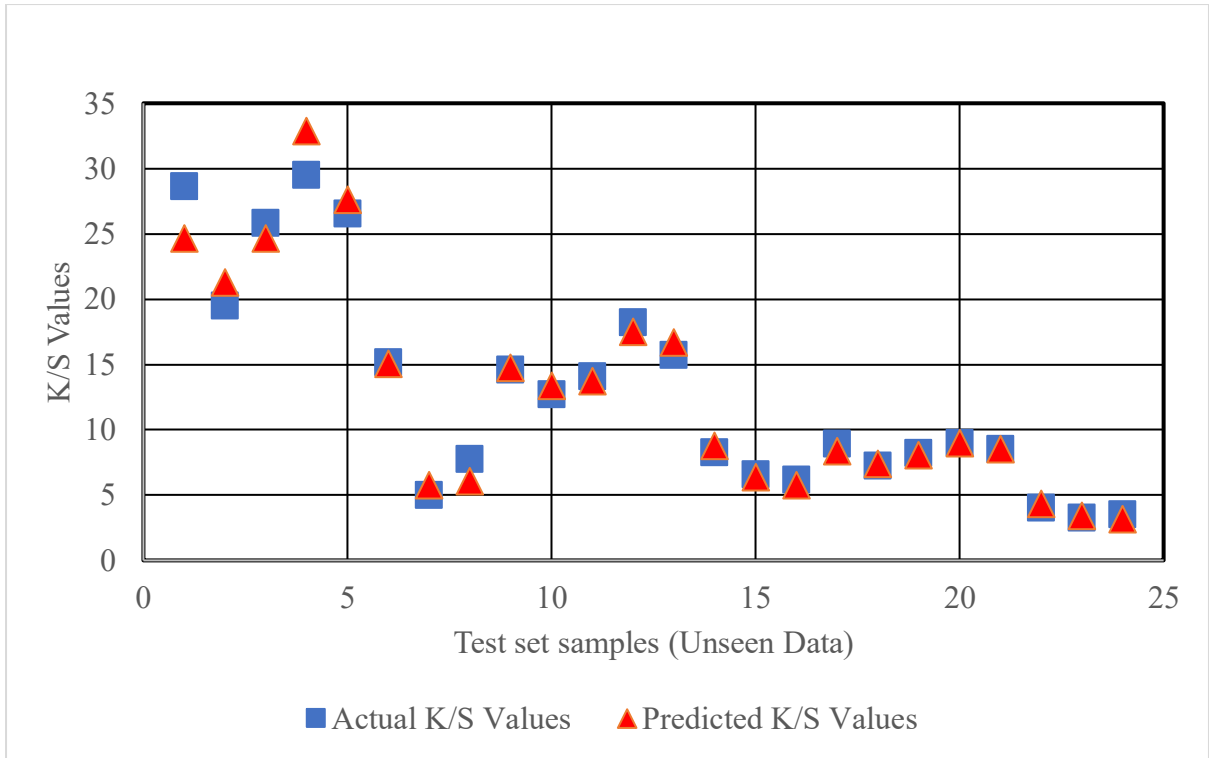
Figure 5.7. The predicted and actual K/S values in the sulphur dyed unseen data set

Table 5.3. The difference between predicted and actual CIE L*a*b* values or K/S values in the sulphur dyed unseen data set

No.	ΔCIE L* values	ΔCIE a* values	ΔCIE b* values	Δ K/S values
SR2	-1.13	0.52	0.20	0.21
SR12	-0.05	-0.38	-0.74	0.67
SR22	-0.31	-0.14	-0.71	-0.32
SR32	0.87	0.21	0.77	-0.73
SR42	-0.58	0.31	-0.57	0.99
SR52	-0.52	0.19	2.84	0.53
SR62	0.98	0.65	-1.24	-0.22
SR72	1.05	-0.59	0.90	-0.39
SB2	2.01	0.45	0.46	-4.01
SB12	-0.52	0.76	0.49	1.80
SB22	1.25	0.04	1.00	-1.15
SB32	-2.17	0.42	0.20	3.40
SB42	-0.65	0.06	-0.24	1.06
SB52	-0.09	-0.34	1.16	-0.08
SB62	-0.93	-0.20	-1.48	0.79
SB72	0.33	0.40	0.12	-1.68
SY2	0.74	-0.98	-0.96	-0.57
SY12	-0.81	0.59	-1.03	0.13
SY22	-0.47	0.02	0.39	-0.14
SY32	0.22	-0.28	-0.08	0.00
SY42	-0.55	-0.30	0.78	0.00
SY52	0.23	0.44	0.52	0.35
SY62	0.19	-0.16	-0.13	0.11
SY72	0.66	0.23	1.50	-0.34
MAE	0.72	0.36	0.77	0.82

The prediction errors are probably influenced by the structure of the cotton fabric, which affects reflectance of the dyed sample at a particular wavelength and thus the K/S values (Tang et al., 2018). The K/S value reflects the concentration of the dye on the cotton fabric and is

determined by measuring the reflection spectrum of the dyed fabric (Özkan et al., 2018). Errors can occur during the measurement phase due to influence of the structure, texture, dye uniformity and flatness of the knitted fabric (Özkan et al., 2018; Tang et al., 2018). For instance, K/S value of cotton knitwear may be significantly impacted by the yarn structure and fabric porosity (Özkan et al., 2018). This implies that there could already be some mistakes in measurements of K/S values, which would cause comparable problems in the prediction.

In summary, the BRNN model can effectively predict CIE L*a*b* and K/S values for unseen datasets when the input model is unknown, with good generalisability and practicality. There is a slight error in predicted CIE L*a*b* values or K/S values, but the average error is less than 1 and the errors are mostly within acceptable limits.

In addition, colour differences between predicted and actual CIE L*a*b* values for the unknown dataset were measured to further validate the usefulness of the trained BRNN model. A colour variation of 1.0 units is considered to be an acceptable tolerance level when using the CMC formula, which is now commonly employed in the textile industry (Farooq et al., 2021). Besides, the CIE94 colour difference formula, which is an improvement on the CMC formula (Melgosa, 2000), adds observation conditions as a sample representation and observation basis, and can be a good predictor of subjective colour differences when viewed under reference conditions (Griffin & Sepehri, 2002; Heggie et al., 1996). Moreover, the CIE2000 formula, when using a new data set, makes its results more consistent with the vision, as it also takes into account other dependencies of chromaticity on hue (Sharma et al., 2005). Therefore, these three-colour difference formulas can be used to measure the colour difference between CIE L*a*b* predicted values and the actual colours, which are depicted by the CIE L*a*b* values (Table 5.4). For the colour difference range, the observer finds it challenging to distinguish

between colours when the ΔE is between 0 and 1, and an experienced observer can distinguish the difference when the ΔE is between 1 and 2 (Minaker et al., 2021). An inexperienced observer may see the difference when the ΔE is more than 2 (Minaker et al., 2021). Thus, the tolerance value for ΔE set at 2 is acceptable.

As can be seen from Table 5.4, values with the superscript "*" (SR52 and SB32) are outside the tolerance limits. Out of the 24 sets of data, one set of data in each colour difference formula yielded a colour difference between the predicted and actual colours outside the tolerance limits, and the remaining 23 sets of data had acceptable colour difference values. This also implies that the proportion of differences between predicted and actual colours found to be within acceptable (or imperceptibly higher) range is approximately 95.83% (23/24 = 0.9583). The colour differences between the actual and predicted values for the unseen data are shown in Figure 5.8 and Table 5.5.

Table 5.4. Colour difference between predicted and actual values and colour depiction figure for the sulphur dyed unknown data sets

No.	ΔE(CIE94)	ΔE (CMC) (1: 1)	ΔE (CIE 2000) (1:1:1)	colour depiction figure	
				Actual colour	Predicted colour
SR2	0.62	0.95	0.95		
SR12	0.48	0.58	0.49		
SR22	0.52	0.62	0.53		
SR32	0.68	0.93	0.87		
SR42	0.56	0.78	0.68		
SR52	2.10*	2.37*	1.96		
SR62	1.18	1.57	1.29		

SR72	0.98	1.35	1.14		
SB2	1.15	1.87	1.91		
SB12	0.90	1.34	1.26		
SB22	1.02	1.50	1.37		
SB32	1.17	1.92	2.05*		
SB42	0.38	0.60	0.60		
SB52	0.92	1.24	1.01		
SB62	1.23	1.64	1.37		
SB72	0.44	0.60	0.63		
SY2	0.84	1.14	1.00		
SY12	0.74	0.99	0.88		
SY22	0.29	0.39	0.36		
SY32	0.22	0.32	0.27		
SY42	0.48	0.65	0.57		
SY52	0.43	0.56	0.52		
SY62	0.17	0.24	0.23		
SY72	0.85	1.06	0.92		
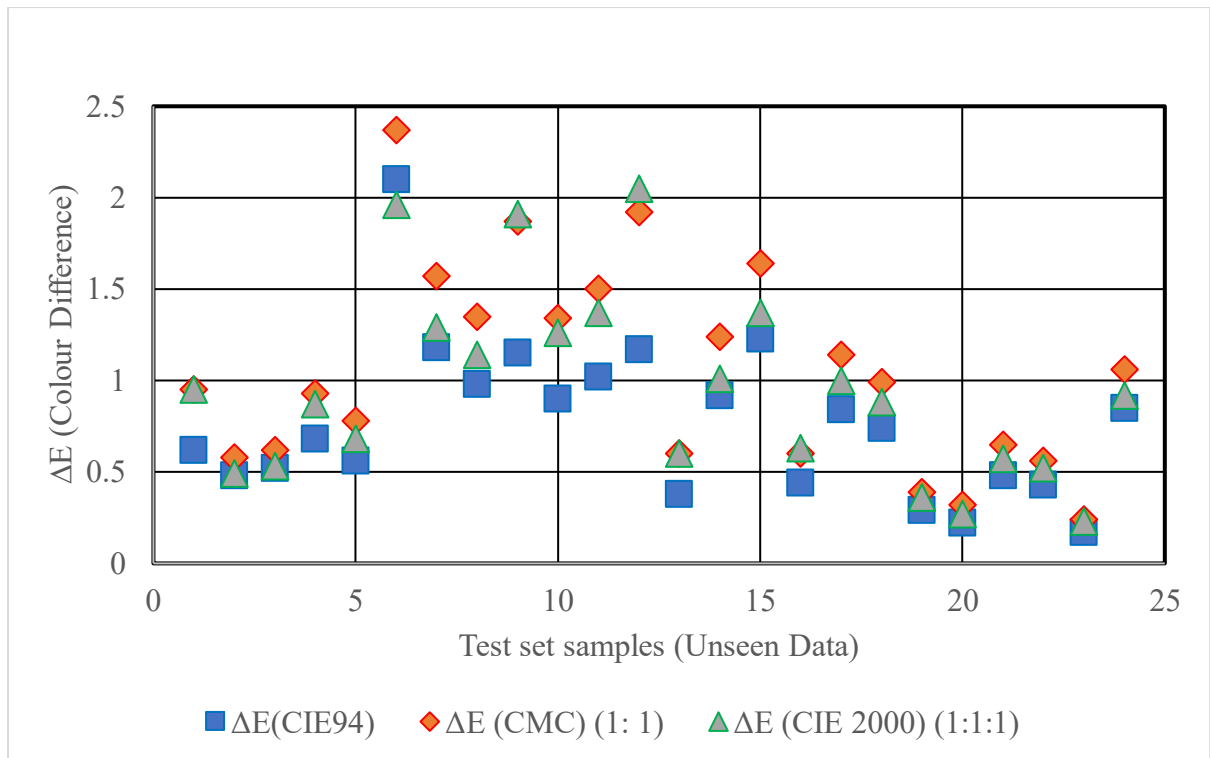
Figure 5.8. Colour Difference between the actual value and predicted value on the sulphur dyed unknown data sets

Table 5.5. The summary of the colour differences measured by different formulas for the sulphur dyed unknown data sets

Colour difference formula	Average colour difference	Maximum colour difference	Passing Rate
ΔE(CIE94)	0.76	2.1	95.83%
ΔE (CMC) (1: 1)	1.05	2.37	95.83%
ΔE (CIE 2000) (1:1:1)	0.95	2.05	95.83%
Note: The number of the unseen Data is 24, the tolerance setting is 2.			

Overall, the 10-fold cross-validated BRNN adapted well to the training dataset, generalised well to unseen datasets, and maintained most of the colour differences between predicted and actual colours within acceptable bounds. The BRNN models showcased their capacity for reproducibility and scalability, rather than solely fitting an already-existing dataset. Additionally, these models exhibit proficiency in precisely predicting the fading impact of

diverse combinations of plasma treatment parameters on cotton fabrics dyed with reactive dyes. Such combinations include a variety of plasma treatment parameters with air concentrations spanning from 10% to 70%, cotton fabrics with moisture contents fluctuating from 35 to 45%, and treatment duration ranging from 10 to 30 minutes. There are several reasons why prediction errors occur: (i) There is a tendency for some small bias to occur during the colour measurement phase; (ii) It is related to fabric characteristics such as evenness of dyeing, levelness of the fabric, structure and surface texture of the cotton fabric (Özkan et al., 2018; Tang et al., 2018); and (iii) It is influenced by the limited small sample size. Even though 10-fold cross-validation does improve the predictive power of the model for small data sets to a large extent, it still produces minor errors during variation of the training set (Fushiki, 2011; Rodriguez et al., 2009). This is because there is a random splitting mechanism in k-fold cross-validation that makes the resulting average accuracy not a constant (Wong, 2015).

Therefore, the BRNN model possesses the capacity to precisely predict the colour measurements of yellow, red, and blue sulphur-dyed cotton fabrics following plasma fading treatment with fewer errors. The trained and validated BRNN models provide manufacturers with a usable tool to effectively reduced the number of experiments necessary to achieve a particular colour change in sulphur-dyed cotton fabrics after plasma treatment, leading to time and cost savings. Integrating artificial intelligence technology with plasma fading treatment technology can contribute to the intelligent and digitalized processing of cotton and holds the potential to be popularized and employed as an ecologically sustainable technology in the industry.

5.4 Conclusions

As an environmentally friendly process, plasma treatment of sulphur-dyed cotton fabrics facilitates the fading effects. This research shows that by combining plasma treatment with a BRNN model using 10-fold cross-validation, the correspondence between different plasma treatment parameters and fading effects can be effectively predicted, thus minimising invalid attempts and uncertainties. By building four BRNN models to predict CIE L*, CIE a*, CIE b* and K/S values separately through a modular approach, the complexity of the models is reduced and good generalisation to unknown data sets is achieved. By integrating the four trained networks, a system that predicts how a particular set of plasma processing parameters will produce a particular fading effect and colour can be formed. Meanwhile, the MAE of the BRNN model for CIE L*, CIE a*, CIE b* and K/S values were 0.9150, 0.6836, 0.8833 and 1.0216 respectively, with RMSEs of 1.3166, 0.9035, 1.1572 and 1.6768. The fitted coefficients of determination R^2 were 0.9819, 0.9906, 0.9908 and 0.9649, and the MAE values of ΔCIE L*, ΔCIE a*, ΔCIE b* values and ΔK/S values for the 24 unseen datasets (test set) were 0.72, 0.36, 0.77 and 0.82, respectively. In addition, the difference between the actual and predicted colours was small, with the proportion of predicted colours being within the acceptable range, around 95.83%, which implies that most of the predictions are accurate or have little and imperceptible colour variation. Furthermore, this indicates that the BRNN prediction system with 10-fold cross validation can be a useful tool to assist dyers in adjusting the parameter settings of the plasma machine and the chosen recipe prior to plasma treatment of cotton fabrics, minimising trial-and-error and making the process more efficient. In future research, the BRNN model will be utilized to generate and forecast diverse combinations of plasma treatment parameters to ascertain the ideal fading effect, thereby facilitating intelligent and digital advancements in the realm of garment fading. Furthermore, artificial intelligence methods will be used to further

reverse predict the correlation between the fading effect of sulphur dyeing and the plasma treatment parameter combinations.

5.5 Disclosure statement

This Chapter has been submitted to the Journal, which is *Fashion and Textiles*, and it is replying to comments.

Chapter 6 Analysing the effects of plasma treatment process parameters on fading of cotton fabrics dyed with Two-colour mix dyes using BRNNs

6.1 Introduction

A prevailing trend in fashionable clothing involves the fading of textiles to enhance their visual appeal, traditionally achieved through chemical or mechanical processes. However, these methods present challenges concerning (1) measurement precision, (2) environmental harm, and (3) difficulty in meeting high production demands (Ibrahim & Eid, 2020; Liu et al., 2019; Samanta et al., 2017). Plasma treatment emerges as a sustainable alternative, achieving zero emissions and improved hydrophilicity of treated textiles (Ibrahim et al., 2010; Paul, 2015). It can also generate fading effects and modify surface characteristics on cotton textiles without impacting their bulk properties (Atav et al., 2022; Ibrahim et al., 2022; Kan et al., 2017). Moreover, plasma-induced ozone treatment presents high efficiency in terms of energy use, obviating the need for water or chemicals (Srikrishnan & Jyoshitaa, 2022). The process of fading cotton textiles exposed to plasma-induced ozone can be represented by twelve equations, as shown in Section 2.3. When operating parameters for plasma treatment are kept constant, investing some effort in process optimization ensures maximum performance, uniformity, and repeatability of the plasma surface treatment process, thus achieving control over the fading effect (Peran & Ercegović Ražić, 2020).

However, the interaction of plasma with the fabric surface is complicated by a number of factors, such as plasma treatment operating parameters, chemical composition of the plasma gas and fabric properties, which has resulted in plasma treatment still not being widely used in the textile industry (Jelil, 2015; Zille et al., 2015). Among the parameters, air concentration, treatment time and water content in the fabric are the main factors that affect the fading effect

(Kan et al., 2016). The role of these three main factors is described below. (1) Under the influence of plasma treatment, more hydroxyl radicals can be generated as the air concentration increases (i.e., there are more oxygen molecules) (Kan et al., 2016). Thus, in the presence of dyes in the fabric, more hydroxyl radicals can cause greater oxidation, which results in a higher degree of fading (Kan et al., 2016). (2) The longer the treatment time, the longer the contact time between the plasma active substance and the dye in the fabric (Kan et al., 2016). Thus, dyes are more likely to be oxidized, resulting in fading (Kan et al., 2016). (3) In terms of water content in the fabric, a lower water content (e.g. 35%) can have a better fading effect than a higher water content (e.g. 45%) (Kan et al., 2016). The reduced fading effect may be attributed to the dilution of the bleach during plasma-induced ozone treatment as a result of the higher water content in the fabric (Kan et al., 2016). Since it is difficult to know the right plasma treatment parameters quickly and accurately, achieving a specific fading effect requires several attempts and observations to ensure the best possible treatment.

When it comes to modelling complicated data sets, neural network models are often superior to statistical models (Gadekar & Ahammed, 2019). It is not necessary, for example, to have a detailed understanding of the chemical or physical characteristics of a process in order to model complex nonlinear multidimensional functional relationships (Gadekar & Ahammed, 2019). Therefore, cotton processing needs to be made more sustainable by integrating plasma processing with intelligent techniques such as Bayesian Regulated Neural Networks (BRNN) (Samanta et al., 2017) since that can help predict fading effects generated by treatment with different sets of operating parameters and thereby reduce the number of trials and errors. Studies of plasma treatment using intelligent techniques have been few. In the presently available studies, the primary research areas that have been investigated include: (1) the utilization of Feedforward neural network models to predict the dyeing properties of wool

fabrics after air-vacuum plasma treatment, resulting in regression values of approximately 0.95 (Omerogullari Basyigit et al., 2023); (2) the use of generalized regression neural networks to forecast dye removal in aqueous solutions (Mitrović et al., 2020); and (3) the development of adaptive neural network fuzzy inference systems to predict dye intensity (K/S) in dyed wool fabrics (Haji & Payvandy, 2020).

The current bottleneck in plasma treatment is that the interaction between the plasma and the fabric surface is still unclear and it is difficult to choose the right plasma treatment conditions (Jelil, 2015). As garments may contain different colour combinations, this study aimed to develop a BRNN system that can accurately predict the fading effect of plasma treatment on two-colour mixed-dyed cotton fabrics with reactive dyes. Meanwhile, four metrics were used to evaluate the model accuracy and its performance in a comprehensive manner, which are mean absolute error (MAE), root mean square error (RMSE), mean absolute percentage error (MAPE), and coefficient of determination (R^2).

6.2 Methodology

6.2.1 Fabric samples and dyeing

Cotton single-knitted fabric (Lacoste: 32s/2) with a weight of 220g/m^2 was dyed by mixing two reactive dyes of three primary colours, red (Levafix Red CA), blue (Levafix Blue CA) and yellow (Levafix Yellow CA) at a dyeing plant in China. The dyes were supplied by DyStar, China and were used as received for dyeing without purification. Di-chloro quinoxaline is the structure of the Levafix series (Shaffer et al., 2012), as shown in Figure 6.1. This type of dye exhibits good lightfastness in lighter shades and excellent perspiration and lightfastness in the colour range and has a high degree of reproducibility and level-dyeing properties (Cheung, 2018).
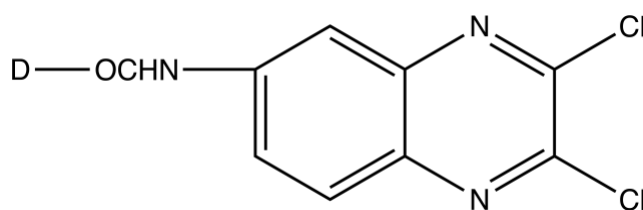
Figure 6.1. The dye structure about Di-chloro quinoxaline (Shaffer et al. 2012)

Three mixed secondary colours of green (RG), nacarat (RN) and violet (RV) were used for dyeing to different depths of 0.5%, 1.5% and 3%. The dyed fabric samples were of size approximately 30 cm x 40 cm. Of these, green is made by combining equal concentrations of blue and yellow. Nacarat (a shade of pale red-orange) at 0.5% concentration is made by combining dyes of equal concentrations of red and yellow, and violet is made by combining equal concentrations of red and blue dyes. For example, in this study, a 0.5% concentration of violet is a combination of a 0.5% concentration of red with a 0.5% concentration of blue, and so on. The process of dyeing cotton fabrics with dyestuff was described in Section 3.2.

6.2.2 Plasma treatment of faded colours

For the plasma treatment used for fading, a commercial ozone plasma machine G2 (standard model, Spain Jeanologia) was used. In comparison to conventional processes, the G2 plasma machine saves 62% of energy (kW/h), 67% of water, 85% of chemicals, and reduces the amount of time required for production by 85% (Kan et al., 2016). Using electric currents to ionize oxygen molecules within the incoming air, the G2 creates a mixture of reactive oxygen to fade textiles (Kan et al., 2016). Before being returned to the atmosphere, residual plasma ozone undergoes a transformation into purified air (Kan et al., 2016). Table 3 demonstrates how the G2 plasma machine works.

Table 6.1 summarizes the plasma treatment parameters used at a garment processing factory in China for cotton fabrics. Three parameters were used in the process, air concentration, dyed fabric water content and treatment time. Though 30 minutes is a long time for textile treatment, different plasma operating parameters need to be investigated to determine how fading occurs on two-colour mixed dyed cotton fabrics. Different colours fade at different rates. For example, yellow fades more slowly than blue (Atav et al., 2022). Furthermore, the operating parameters of the three plasma treatments are interdependent (Kan et al., 2016). Depending on the operating parameters of the other two plasma treatments, such as providing a lower concentration of air (oxygen) and a higher water content, the treatment time of the plasma used for fading might need to be extended (Ibrahim et al., 2010; Kan et al., 2016). Thus, in order to include the full range of acceptable plasma operating parameters, the treatment time included 30 minutes.

For each type of dye, 54 fabric samples were used for colour measurements, and 162 samples were used for the three different reactive dye colours. There were 18 combinations of plasma treatment parameters ($3\times3\times2=18$), and dyes were applied at three different dye concentrations ($18\times3=54$), and there were three different dyes ($54\times3=162$). These three dyes were used to produce 162 fabric samples labelled RN1-RN54 (for nacarat colour), RG1-RG54 (for green colour) and RV1-RV54 (for violet colour).

Table 6.1. Plasma treatment parameters applied to two-colour mixed dyed fabric samples

Air (Oxygen) concentration (%)	10, 30, 50
Water Content (%)	35, 45
Treatment time (minutes)	10, 20, 30

6.2.3 Colour measurement arrangements

Prior to measuring colour, the fabric samples were conditioned at 65±2% relative humidity and 20±2°C for at least 24 hours. There were three types of fabrics dyed with reactive dyes: two-colour mix dyed-green (RG), two-colour mix dyed-nacarat (RN), and two-colour mix dyed-violet (RV). For each type of sample, precision colour measurement was performed with a Macbeth Colour-Eye 7000A (CE-7000A) spectrophotometer. Colours were measured as specific CIE L*a* b*C*h and K/S values.

The CIE L* value indicates the lightness level of the fabric sample and the CIE a* value indicates the magnitude of red and green, i.e., +a* indicates red and -a* indicates green. In contrast, the degree of yellow and blue of a fabric sample is reflected by the b* value, i.e. +b* values represent yellow and -b* values represent blue (Hunt & Pointer, 2011). For the CIE L*a*b*C*h value, it can be divided into two different expressions, CIE L*a*b* and CIE L*C*h; CIE C* value and CIE h value can be calculated from the CIE a* value and the CIE b* value (Hunt & Pointer, 2011), as shown in Equation (6.1) and Equation (6.2) below.

$$C^* = \sqrt{a^{*2} + b^{*2}} \qquad\qquad (6.1)$$

$$h = arctan\frac{b^*}{a^*} \qquad\qquad (6.2)$$

Besides, in order to calculate the K/S value, Equation (6.3), the Kubelka-Munk dyeing depth equation shown below is used (Brinkworth, 1972). The higher the K/S value obtained by the calculation, the darker the fabric sample's surface colour, which means better dyeing performance (Brinkworth, 1972).

$$K/S = \frac{(1-R)^2}{2*R}$$ (6.3)

An illuminant D65, plus a large aperture value and a 10º observer angle were used to measure colour with the Macbeth colour eye 7000A. The colour-measuring device was also calibrated with black and white traps. As part of the experiments, seven fabric samples of each type and four uniformly coloured areas of each fabric sample were tested to improve the accuracy of the colour measurements (as shown in Figure 3.5). These data were averaged to produce the final colour measurement.

6.2.4 Modelling, simulation and prediction using BRNN

For 162 two-colour mixed dye cotton fabric samples, the CIE L*a*b*C*h and K/S values were measured. After preliminary data processing, the relationship between plasma treatment process parameters and CIE L*a*b*C*h and K/S values was investigated using BRNN. The samples were divided into three types: RG, RN, and RV. 145 of these data sets were used for BRNN modelling and simulation, while the remaining 17 unseen data, selected by stratified sampling, were used for testing the generalizability of the BRNN. Table 6.2 below illustrates how these data sets were divided.

Table 6.2. Division of the data sets for the two-colour mixed dye fabric samples

Datasets for training and validation (145)	Unseen datasets of BRNN for testing (17)
RG1, RG3-RG11, RG13-RG21, RG23-RG31, RG33-RG41, RG43-RG51, RG53, RG54	RG2, RG12, RG22, RG32, RG42, RG52
RN1-RN7, RN9-RN17, RN19-RN27, RN29-RN37, RN39-RN47, RN49-RN54	RN8, RN18, RN28, RN38, RN48
	RV4, RV14, RV24, RV34, RV44, RV54

RV1-RV3, RV5-RV13, RV15-RV23, RV25-RV33, RV35-RV43, RV45-RV53	

In order to perform regression analysis on small data sets, a small three-layer neural network was constructed, and a Bayesian Regularization Algorithm was used to improve the performance of the neural network so as to minimize the possibility of overfitting problems with small data sets (Coit et al., 1998; Doan & Liong, 2004). In spite of the fact that Bayesian Regularization Algorithm requires more processing time, it significantly enhances the generalizability of the neural network model (Abd Jelil et al., 2013; Doan & Liong, 2004). K-fold cross-validation has been widely used in model regression problems (Jung & Hu, 2015) and increasing the value of K improves the accuracy of cross-validation. However, too high a value of K may lead to overtraining the model and consuming a large amount of time, and a K value of 5 or 10 is often taken (Yadav & Shukla, 2016). A 10-fold cross-validation procedure is further used to validate the trained neural network (Farooq et al., 2021). Cross-validation is based on data division, where the majority of the data is used to train the model and the remaining small portion of the data is used to validate the error to measure the predictive performance of the model and to select the best performing model at the end (Yadav & Shukla, 2016; Zhang & Yang, 2015). For each training session, the data sets were divided into ten subsets, one of which is used for validation, and the other nine are used for training. There were ten repetitions of such training. Each training session has between 3 and 12 hidden layers of neurons, depending on the number of input and output layers, with the optimal number of hidden layers being determined by the particular training session. After the selected network has been trained 10 times and has met the performance target in different training rounds, the final value is calculated by taking the average of the 10 runs. In the case of limited datasets, a

modular approach was further used to minimize complexity of the neural network in addition to Bayesian Regularization Algorithms and cross-validation (Choudhury et al., 2015). The designed BRNN model was divided into six modules in order to predict the six output values. Modularization facilitates the understanding of the relationship between each output value and the plasma processing parameters, thereby reducing training time at the same time. With the input and output values shown in Figure 6.2, six similar neural network modules were created.
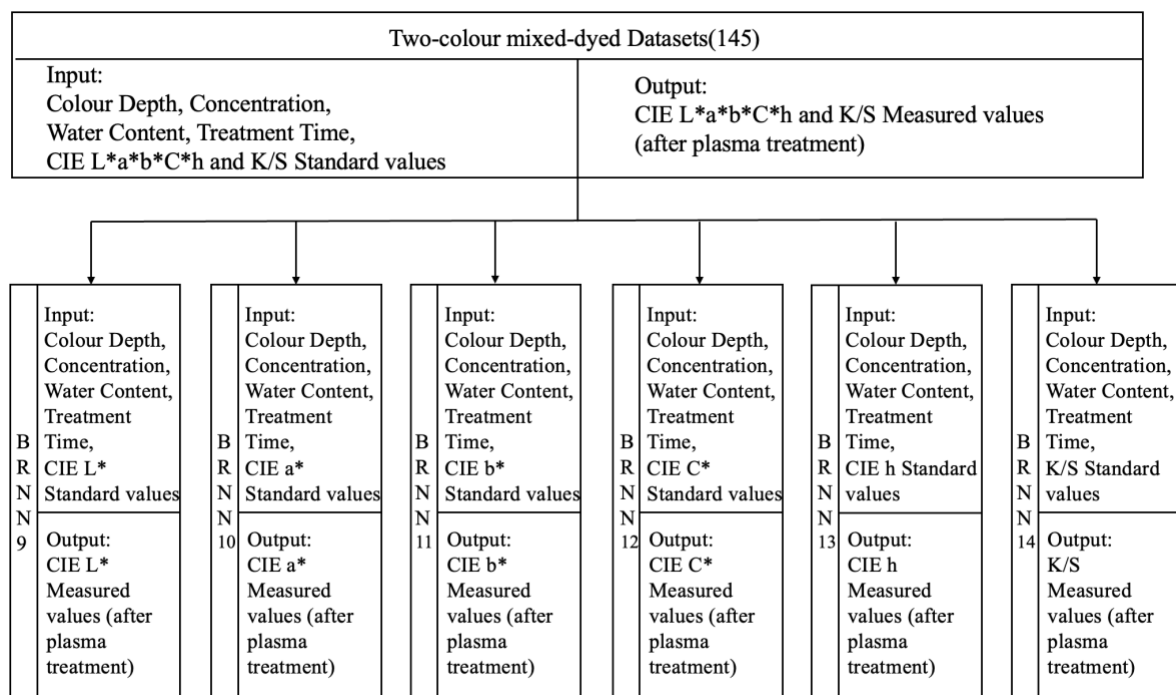
Figure 6.2. BRNN9-BRNN14 models with their inputs and outputs from the two-colour mixed-dyed Datasets

Figure 6.2 illustrates that in the fading prediction system, the input consists of plasma treatment parameters as well as colour measurements of the cotton fabric before fading treatment, while the output comprises colour measurements after fading treatment. The plasma treatment parameters include colour depth, air (oxygen) concentration, water content and treatment time, whereas colour measurements include CIE L*a*b*C*h values and K/S values. MATLAB (version R2021a) software was used to construct the BRNN model, with the maximum number

97

of training epochs (iterations) set to 1000 so that the network would have sufficient time and iterations to minimize the error. For transfer functions of the hidden and output layers, MATLAB's built-in functions 'logsig' and 'purelin' were used respectively. Additionally, a learning rate of 0.01 was also set, as well as a training termination error of 10^{-6}. The input and output data were also normalized before training so as to have a mean of zero and a standard deviation of one. BRNN's predictive performance was further enhanced as normalization of data helped reduce computational errors related to parameter size, thereby avoiding the effects of outliers and extreme values (Choudhury et al., 2015; Farooq et al., 2021). Figure 6.3 illustrates the BRNN model's topology.
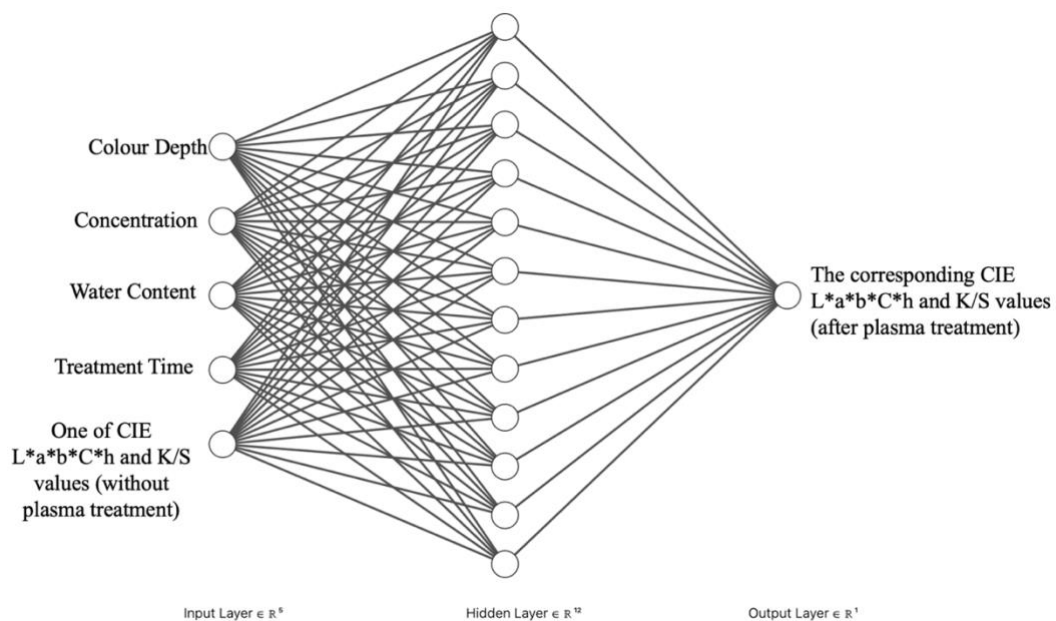
Figure 6.3. The topology of BRNN models

In order to assess applicability and generalizability of the BRNN model, the final BRNN model created after 10-fold cross-validation was used to predict an unseen dataset of 17 (Figure 6.4).
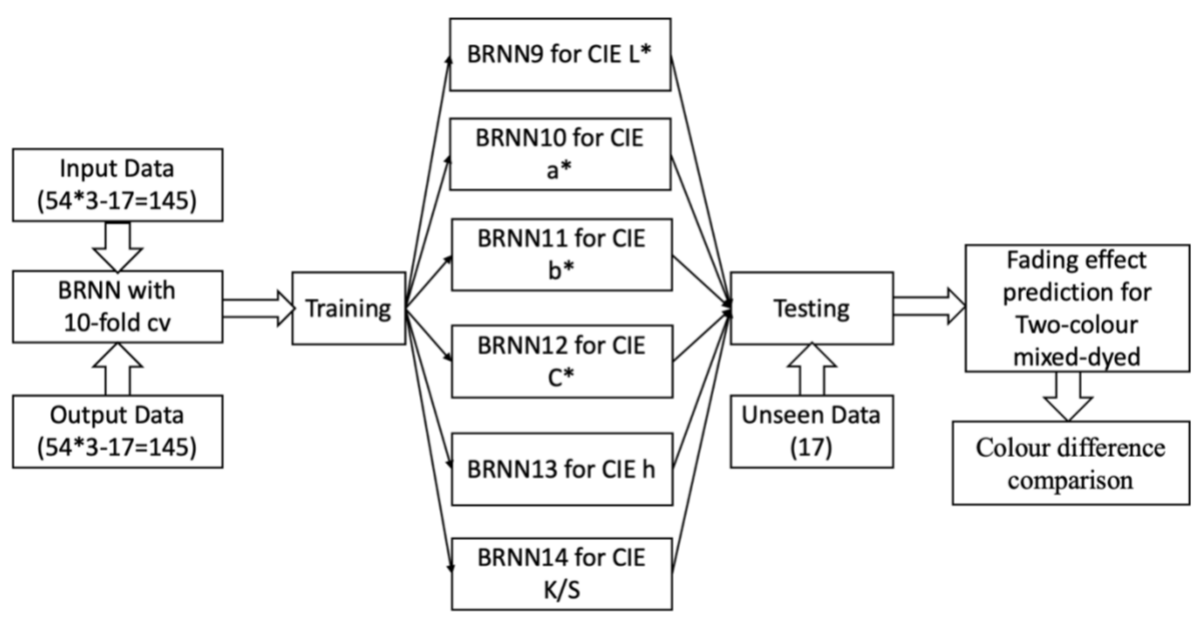
Figure 6.4. A flowchart showing how BRNN models predict fading effects about the two-colour mixed dyed

6.2.5 Verification of the BRNN's accuracy

To assess the accuracy of predictions made by BRNN models, mean absolute errors (MAE), root mean square errors (RMSE), and mean absolute percentage errors (MAPE) are used, which are also indicators of the accuracy of neural network models and their performance (Abiodun et al., 2019; Chai & Draxler, 2014; Ostertagova & Ostertag, 2012). A sample y_i with n measurements (y_i, $i = 1, 2, \dots, n$) is shown in Equations (6.4), (6.5) and (6.6), as are corresponding BRNN model predictions ($\hat{y}_i$, $i = 1, 2, \dots, n$) (Abiodun et al., 2019; Chai & Draxler, 2014; Ostertagova & Ostertag, 2012).

$$MAE = \frac{1}{n} \sum_{i=1}^{n} |y_i - \hat{y}_i|$$

(6.4)

$$RMSE = \sqrt{\frac{1}{n} \sum_{i=1}^{n} (y_i - \hat{y}_i)^2}$$

(6.5)

99

$$MAPE = \frac{1}{n}\sum_{i=1}^{n}\left|\frac{\hat{y}_i - y_i}{y_i}\right| \times 100\%$$

<div align="right">(6.6)</div>

It is among these metrics that MAE is used to measure the accuracy of the prediction system as a whole (Ostertagova & Ostertag, 2012). An accurate BRNN model will have MAE close to zero if the predicted and actual values are well-fitted. The MAE may be large if the fit is poor, indicating that it is necessary to improve the accuracy of the BRNN model. There is also a measure of overall accuracy called the RMSE, which is derived from the square root of the MSE, with larger errors being given extra weight and it is more sensitive to outliers (Chicco et al., 2021). The magnitude of the prediction error is similar to the dimension of the predicted or actual value (Ostertagova & Ostertag, 2012). Alternatively, MAPE focuses on assessing percentage error and is an optional metric calculation when the relative change affects the regression task more than the absolute value, but is not suitable for assessing tasks in which large errors are anticipated (Chicco et al., 2021). It means that MAPE measures relative performance, with a calculated value of less than 10% considered a highly accurate prediction, and a calculated value of between 10% and 20% considered a good prediction. It is considered an acceptable prediction if it falls between 20% and 50%, and if it exceeds 50%, it is considered inaccurate (Ostertagova & Ostertag, 2012).

Another measure of generalizability of the BRNN model was the coefficient of determination R^2 (Choudhury et al., 2015). It may be an indication that the constructed BRNN model is performing better if the value of R^2 is closer to 1, as it implies that the predicted and actual values are more closely correlated, indicating that the trained network can generalize to unseen data better.

To evaluate model performance, various metrics are often combined (Chai & Draxler, 2014), such as MAE, MAPE, RMSE, and coefficient of determination R^2. The MAE is appropriate for describing uniformly distributed errors, whereas it is ineffective for describing some large errors (Chai & Draxler, 2014). It is more appropriate to use RMSE for describing normally distributed errors because it is more sensitive to outliers (Chai & Draxler, 2014). In spite of the fact that the coefficient of determination R^2 can provide insights into how well the model fits, it cannot provide information regarding the residuals. As a result, a single indicator tends to highlight one aspect of error characteristics, while a combined indicator evaluation system is more appropriate for assessing the overall performance of the model (Chai & Draxler, 2014).

6.3 Results and discussion

Table 6.3 summarizes the performance of the six well-trained BRNN modules. According to the results, BRNN9-BRNN14 have mean absolute errors of 0.7056, 0.5766, 0.6077, 0.6283, 3.5861 and 9.8915 respectively, as well as root mean square errors of 0.9476, 0.7212, 0.8257, 0.8228, 7.5433 and 14.1220, respectively, and mean absolute percentage errors (MAPEs) of 1.1451%, 4.0250%, 4.5659%, 2.4275%, 3.1745% and 10.2545%, respectively. As stated earlier, the results fall within the acceptable range for CIE L*a*b*C* values, and the prediction errors are slightly larger for CIE h values and K/S values. There may be an impact on the prediction error due to the structure of the cotton fabric, which may affect reflectance of the dyed sample at a particular wavelength, thereby affecting the K/S value. In terms of the coefficient of determination (R^2), values are 0.9939, 0.9989, 0.9979, 0.9963, 0.9935 and 0.9700 respectively. For CIE L*a*b*C*h values, the values of R^2 are all extremely close to one, which indicates that the model fits well and the actual and predicted values are extremely close, whereas there are some deviations from predicted K/S values.

Table 6.3. Performance of the trained BRNN9-BRNN14 models

	BRNN9: CIE L* values	BRNN10: CIE a* values	BRNN11: CIE b* values	BRNN12: CIE C* values	BRNN13: CIE h values	BRNN14: K/S values
MAE	0.7056	0.5766	0.6077	0.6283	3.5861	9.8915
RMSE	0.9476	0.7212	0.8257	0.8228	7.5433	14.1220
MAPE (%)	1.1451	4.0250	4.5659	2.4275	3.1745	10.2545
R^2	0.9939	0.9989	0.9979	0.9963	0.9935	0.9700

In order to further test the utility and generalizability of trained BRNN modules, six modules were tested on 17 datasets not involved in training and validation, and the predicted values were compared to the actual values (Figure 6.5 to Figure 6.10). As shown in Figure 6.5 to Figure 6.9, the predicted and actual values are very close to each other, and the fitted trends are essentially the same, indicating that the model provides good predictions of CIE L*a*b*C*h values of the unseen dataset. Figure 6.10 depicts a similar trend, with the predicted values being slightly different from the actual results. Table 6.4 presents a comparison of predicted and actual values, and Equations (6.7) and (6.8) provide the formulas for calculating the difference and the MAE of ΔCIE L*a*b*C*h of predicted and actual values. The MAE of ΔCIE L* is 1.00, MAE of ΔCIE a* is 0.30, MAE of ΔCIE b* is 0.82, MAE of ΔCIE C* is 0.50, MAE of ΔCIE h is 4.83, and MAE of ΔK/S is 8.92. Since K/S values are calculated based on the reflectance spectrum of dyed cotton fabric, they indicate the amount of dye present in the dyed fabric (Özkan et al., 2018; Tang et al., 2018). The probable cause of its inaccuracy may be at the measuring stage, which is impacted by the fabric structure, texture, evenness of dyeing, and flatness (Özkan et al., 2018). For instance, K/S values of cotton knitwear can be significantly affected by fibre structure and fabric porosity (Özkan et al., 2018). It is possible that there is already some error in K/S values at the time of measurement, which can cause more significant errors during prediction.

$$\Delta\ CIE\ L^*, \Delta\ CIE\ a^*, \Delta\ CIE\ b^*, \Delta\ CIE\ C^*, \Delta\ CIE\ h\ or\ \Delta K/S\ values \qquad (6.7)$$

$$= Predicted\ values - Actual\ values$$

The MAE of $\Delta\ CIE\ L^*, \Delta\ CIE\ a^*, \Delta\ CIE\ b^*, \Delta\ CIE\ C^*, \Delta\ CIE\ h\ or\ \Delta K/S\ values$

$$= \frac{\sum_{i=1}^{n}|\Delta\ CIE\ L^*, \Delta\ CIE\ a^*, \Delta\ CIE\ b^*, \Delta\ CIE\ C^*, \Delta\ CIE\ h\ or\ \Delta K/S\ values\ values|}{n} \qquad (6.8)$$

Table 6.4. Difference between predicted and actual CIE L*a*b*C*h values or K/S values for the two-colour mixed-dyed unseen data set

No.	ΔCIE L* values	ΔCIE a* values	ΔCIE b* values	ΔCIE C* values	ΔCIE h values	ΔK/S values
RG2	1.44	0.08	0.56	-0.11	3.43	-3.52
RG12	0.38	-0.25	0.17	0.17	-1.57	-4.23
RG22	-1.50	-0.12	-0.78	0.81	9.25	-11.17
RG32	-1.04	-0.30	-0.05	-0.15	-0.41	-3.03
RG42	0.42	-0.05	0.27	-0.58	-0.88	3.72
RG52	0.13	-0.07	-1.29	-0.47	3.23	24.19
RN8	-0.48	-0.08	-0.49	-0.18	-2.16	6.67
RN18	5.26	0.04	4.13	-1.04	4.30	-0.41
RN28	0.29	0.10	0.54	0.24	-0.74	14.02
RN38	-0.05	0.56	-0.08	-0.80	2.86	33.36
RN48	-0.62	-0.28	-0.81	-1.37	-2.73	3.59
RV4	-0.64	0.17	-0.69	0.04	-0.89	2.23
RV14	0.01	1.15	1.55	-0.37	42.83	0.08
RV24	-0.45	-0.36	-0.25	-0.82	-3.25	-1.75
RV34	-2.18	-0.57	0.06	-0.58	0.42	6.13
RV44	0.07	0.32	0.19	0.38	0.30	-28.54
RV54	-2.05	-0.56	-2.03	-0.37	2.79	-4.93
MAE	1.00	0.30	0.82	0.50	4.83	8.92
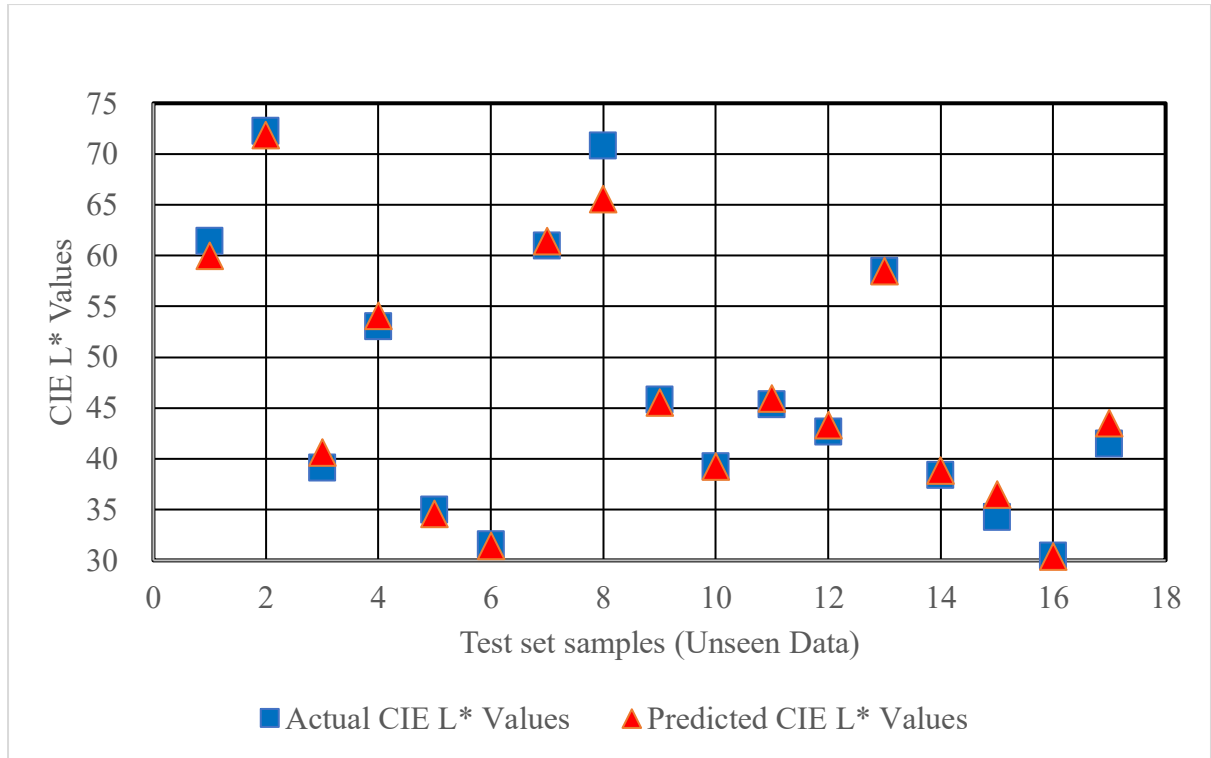
Figure 6.5. The predicted and actual CIE L* values in the two-colour mixed-dyed unseen data set
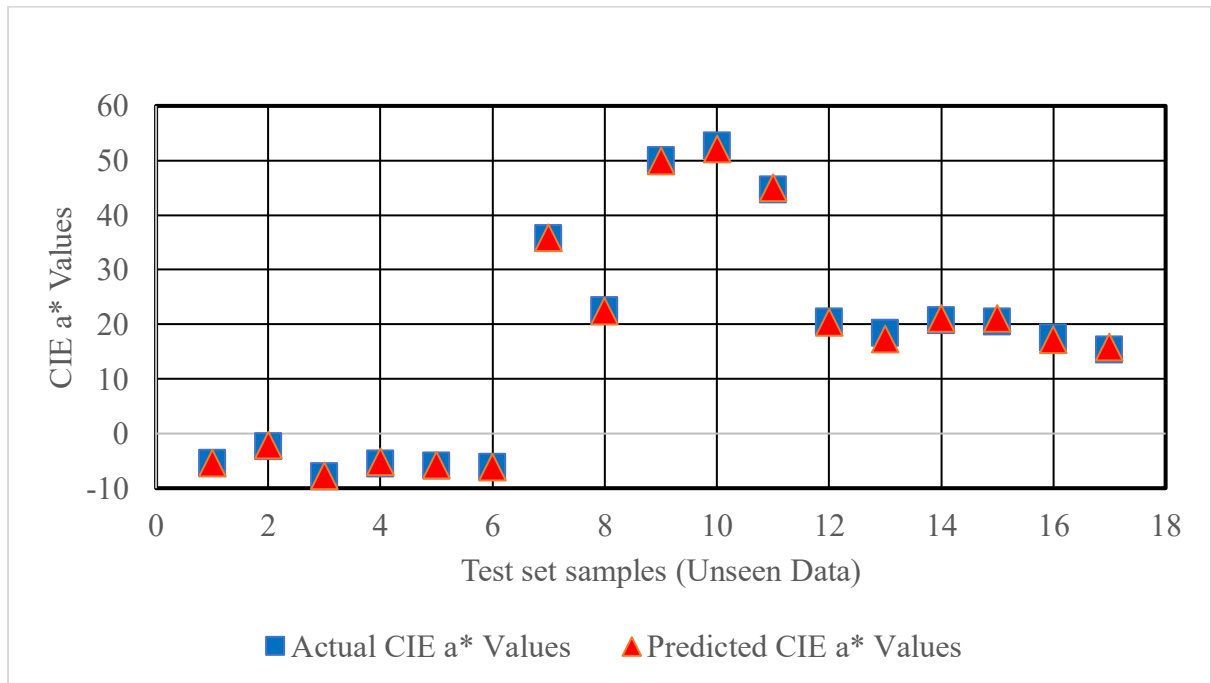
Figure 6.6. The predicted and actual CIE a* values in the two-colour mixed-dyed unseen set
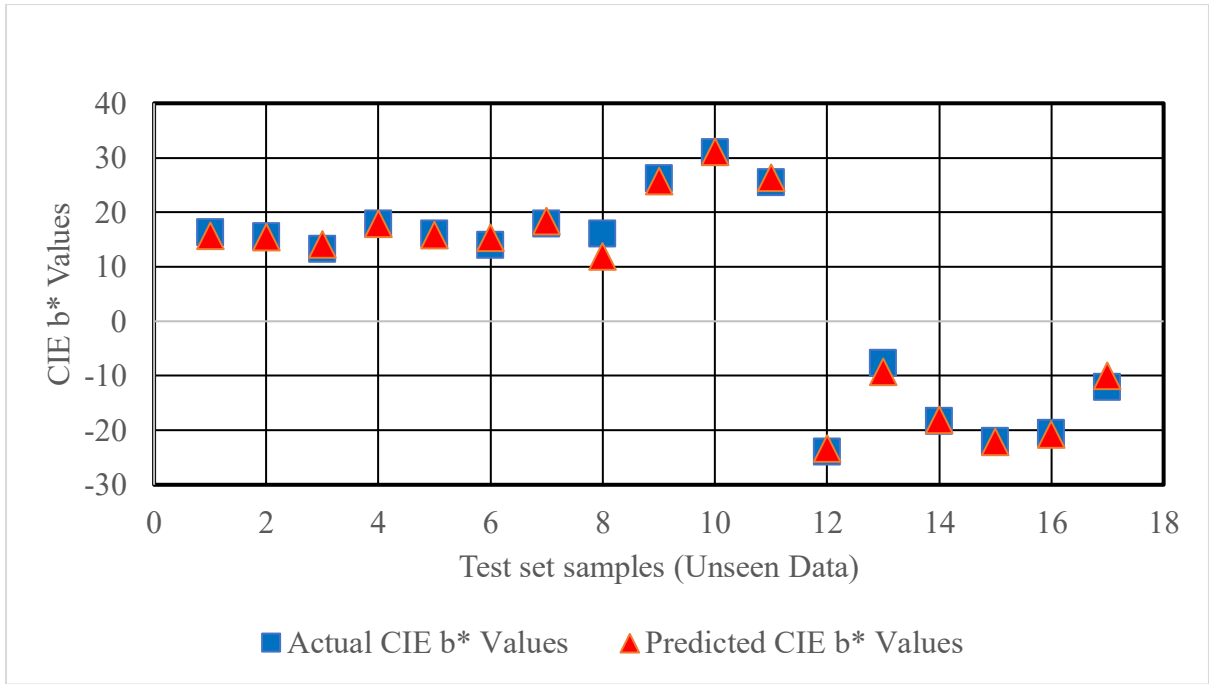
Figure 6.7. The predicted and actual CIE b* values in the two-colour mixed-dyed unseen data set
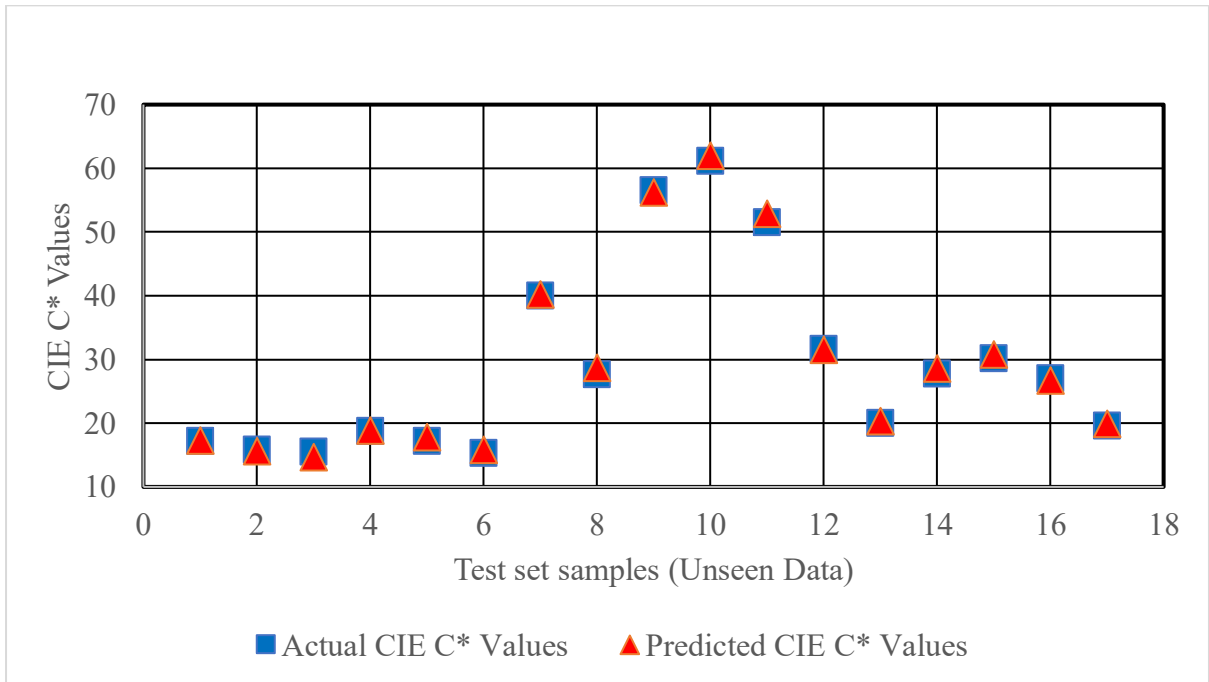
Figure 6.8. The predicted and actual CIE C* values in the two-colour mixed-dyed unseen data set

105
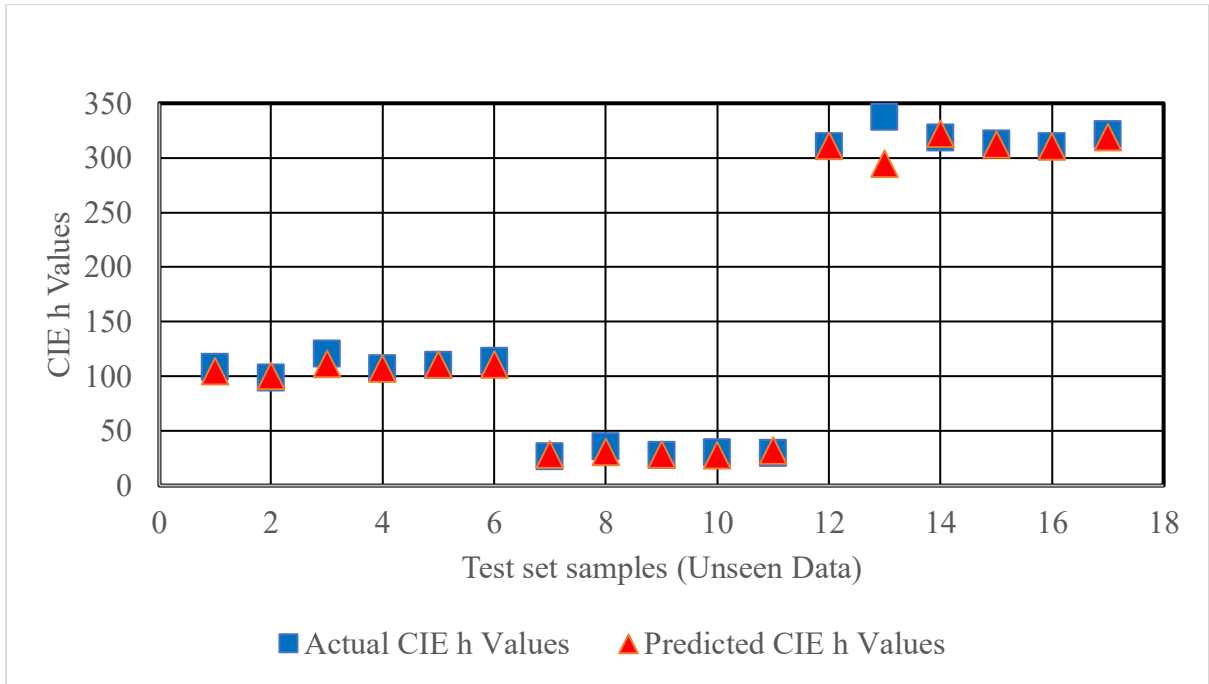
Figure 6.9. The predicted and actual CIE h values in the two-colour mixed-dyed unseen data

set
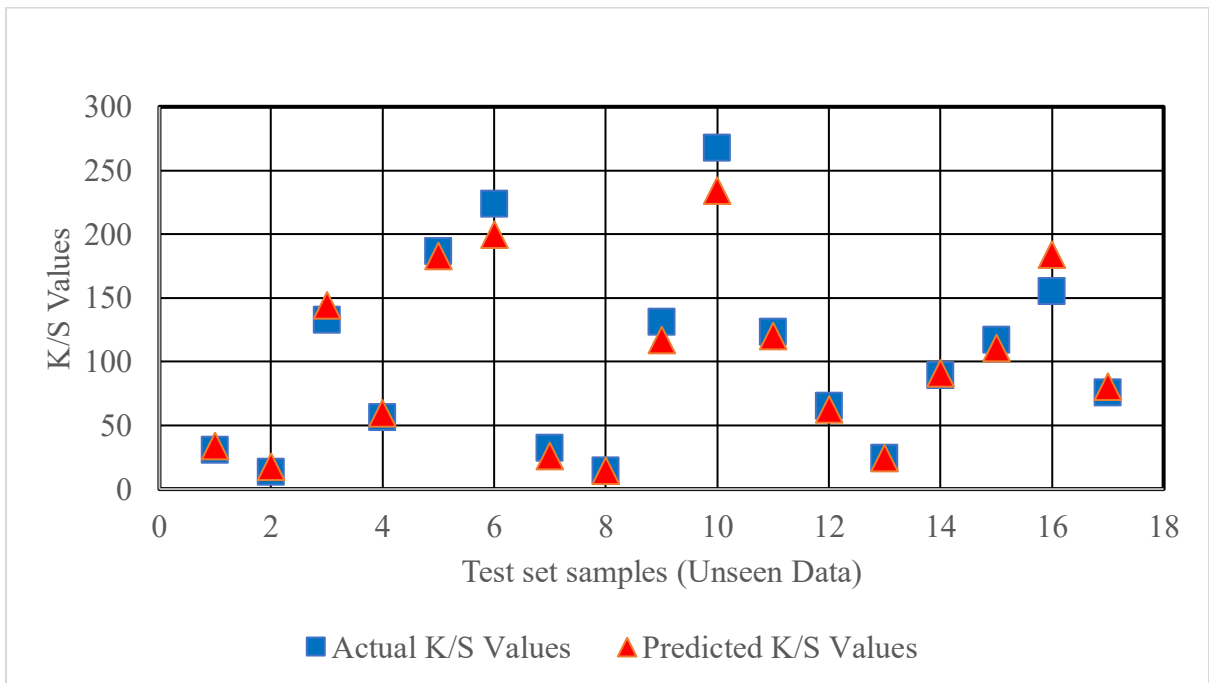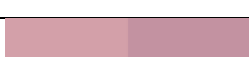
Figure 6.10. The predicted and actual K/S values in the two-colour mixed-dyed unseen data

set

Overall, the BRNN model can reliably predict CIE L*a*b*C*h and K/S values for unseen datasets, with good generalizability and practicality. It is possible to predict the CIE L*a*b*C*h and K/S values accurately within acceptable limits.

Furthermore, validation of effectiveness of the trained BRNN model was carried out by measuring differences between predicted and actual values for the unknown dataset. The CMC formula, which is now commonly used in the textile sector, is considered to have an acceptable tolerance level of 1.0 units for colour variations. Besides, the CIE94 colour difference formula, which improves upon the CMC formula, incorporates observation conditions as a sample representation and observation basis, and provides a good predictor of subjective colour differences when used in conjunction with a reference system. Additionally, the CIE2000 formula more closely resembles vision since it incorporates other dependencies of chromaticity on hue, as well as using a new data set. Thus, it is possible to use these three-colour difference formulas to measure the difference between predicted and actual colour values, and the differences are depicted by the CIE L*a*b* values (Table 6.5). Observers find it difficult to distinguish between colours when the ΔE is between 0 and 1, and experienced observers may identify the difference when the ΔE is between 1 and 2 (Minaker et al., 2021). As the ΔE exceeds 2, an inexperienced observer is able to discern the difference (Minaker et al., 2021). Therefore, the tolerance value of ΔE set at 2 is acceptable.

Table 6.5. Colour difference between predicted and actual values and colour depiction figure for the two-colour mixed-dyed unknown data sets

No.	ΔE(CIE94)	ΔE (CMC) (1: 1)	ΔE (CIE 2000) (1:1:1)	Colour depiction figure	
				Actual colour	Predicted colour
RG2	0.80	1.27	1.31		

RG12	0.29	0.41	0.41	
RG22	0.93	1.72	1.43	
RG32	0.58	0.99	1.07	
RG42	0.26	0.51	0.38	
RG52	0.82	1.00	0.84	
RN8	0.37	0.51	0.50	
RN18	3.76*	5.33*	5.00*	
RN28	0.30	0.41	0.39	
RN38	0.22	0.27	0.24	
RN48	0.49	0.75	0.72	
RV4	0.46	0.73	0.69	
RV14	1.49	1.52	1.35	
RV24	0.38	0.56	0.49	
RV34	1.14	2.51*	1.83	
RV44	0.28	0.29	0.31	
RV54	1.90	2.68*	2.38*	

As shown in Table 6.5, values with superscript "*" are outside the tolerance limits (RN18, RV34 and RV54). As a result, of the 17 sets of data, in the case of 1 set the difference between predicted and actual colour CIE94 was found to be beyond tolerance limits and the passing rate is 94.12% ($16/17 \times 100\% = 94.12\%$). 3 sets of data in the CMC colour difference formula resulted in the difference between predicted and actual colours being outside the tolerance limits and the passing rate is 82.35% ($14/17 \times 100\% = 82.35\%$). 2 sets of data in the CIE2000 colour difference formula resulted in colour differences exceeding tolerance limits and the passing rate is 88.24% ($15/17 \times 100\% = 88.24\%$). For the remaining data, the difference between predicted and actual colours is within acceptable limits. Besides, this implies that between

82.35% and 94.12% of predicted colours were within the acceptable or imperceptible range. Table 6.6 and Figure 6.11 illustrate the colour differences between the actual and predicted values for the unseen data.

Table 6.6. Summary of the colour differences measured by different formulas for the two-colour mixed-dyed unknown data sets

Colour difference formula	Average colour difference	Minimum colour difference	Maximum colour difference	Passing Rate
ΔE (CIE94)	0.85	0.22	3.76	94.12%
ΔE (CMC) (1: 1)	1.26	0.27	5.33	82.35%
ΔE (CIE 2000) (1:1:1)	1.14	0.24	5.00	88.24%
Note: The number of the unseen Data is 17, the tolerance setting is 2.				
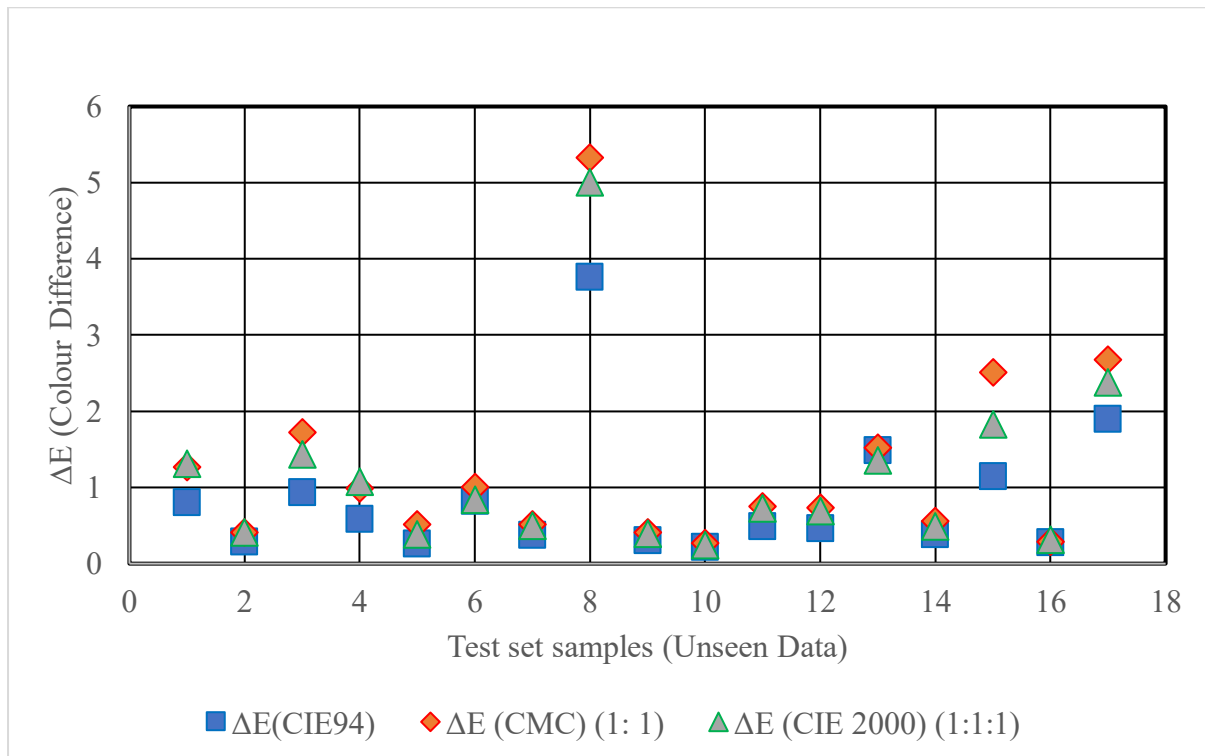
Figure 6.11. Colour Difference between the actual value and predicted value on the two-colour mixed-dyed unknown data sets

109

In general, the 10-fold cross-validated BRNN did well in adapting to the training dataset, generalizing to unseen datasets, and maintaining most of the colour differences between predicted and actual colours within acceptable limits. It indicates the reproducibility and extensibility of BRNN models, rather than just fitting known data sets. The models can effectively predict the fading effect of various combinations of plasma treatment parameters on two-colour mixed dyed cotton fabrics, such as a combination of different plasma treatment parameters with an air concentration of 11%, a cotton fabric with a water content of 36%, a treatment time of 21 minutes, etc.

Errors in prediction can be attributed to several factors. Firstly, the colour measurement phase is prone to some small biases. Secondly, several fabric characteristics are involved with this issue, including the evenness of dyeing, levelness of the fabric, its structure, and its surface texture (Özkan et al., 2018; Tang et al., 2018). Thirdly, the limited sample size has a significant impact on the results. The 10-fold cross-validation technique does improve the predictive power of the model to a great extent for small data sets. However, it still produces minor errors during the variation of the training data (Fushiki, 2011; Rodriguez et al., 2009), because the process of the variation is random. For example, k-fold cross-validation contains a random splitting mechanism in splitting the training data that causes the average accuracy not to be constant.

Therefore, the trained and validated BRNN models can effectively reduce the number of trials required to achieve a specific colour change in reactive dyed cotton fabrics after plasma treatment. It is possible to save time and cost by adjusting the plasma treatment parameters in this manner. In addition, since most fading techniques for fashion garments are applied to garments, the garments may contain different colour combinations. In this study, an artificial

intelligence technique was used to simulate the fading effect of different combinations of plasma operation parameters on two-colour mixed-dye cotton fabrics. Thus, in future work, when the fading effect of plasma operation parameters on garments for different colours can be predicted more intuitively by artificial intelligence techniques, the prediction of fading effect using plasma treatment on garments will be operable. This also facilitates the use of plasma treatment technology to fade fashion garments. Furthermore, this BRNN prediction system provides a useful tool for manufacturers. By utilizing artificial intelligence techniques, manufacturers could simulate the fading effect of cotton fabrics under plasma treatment, which would contribute to the advancement of intelligence and digitization in the field of cotton processing. Meanwhile, by combining artificial intelligence technology with plasma fading treatment technology, this environmentally friendly technology could be scaled up and made useful in industry.

6.4 Conclusions

Plasma treatment of cotton fabrics dyed with two-colour mixed dyes is an environmentally friendly method of fading. The findings of this study demonstrate that using a BRNN model combined with 10-fold cross-validation, it is possible to accurately predict the correlation between different plasma treatment parameters and fading effects, thus minimizing invalid attempts and uncertainties. Through a modular approach, six BRNN models are built to predict CIE L*, CIE a*, CIE b*, CIE C*, CIE h, K/S values separately, reducing the complexity of the models and enhancing their generalizability to unknown data sets. With integration of the six trained networks, a system can be developed to predict how a particular set of plasma processing parameters will result in a particular fading effect and colour. Accordingly, the MAE of the BRNN model for CIE L*, CIE a*, CIE b*, CIE C*, CIE h, K/S values was 0.7056, 0.5766, 0.6077, 0.6283, 3.5861 and 9.8915, respectively, with RMSEs of 0.94761, 0.7212,

0.8257, 0.8228, 7.5433 and 14.1220. A fitting coefficient of determination R^2 was 0.9939, 0.9989, 0.9979, 0.9979, 0.9935 and 0.9700. The MAE of CIE L*, CIE a*, CIE b*, CIE C*, CIE h and K/S values were 1.00, 0.30, 0.82, 0.50, 4.83 and 8.92 for the 17 unseen datasets, respectively. Furthermore, the actual and predicted colours were within the acceptable range of the colour difference, with more than 80% of predicted colours being within the acceptable range, indicating that most predictions are accurate. As a result of this study, dyers may be able to optimize the parameters settings of the plasma machine and the chosen recipe prior to plasma treatment of cotton fabrics using a useful tool, the BRNN prediction system with 10-fold cross validation, reducing trial-and-error and thereby improving the efficiency of the plasma treatment procedure. Moreover, this study can effectively predict the fading effect of different combinations of plasma parameters on two-colour mixed dyed cotton fabrics, avoiding unpredictable fading effects caused by the interaction of different plasma operating parameters. In future research, the BRNN model will be employed to further investigate which combinations of plasma treatment parameters determine the optimal fading colour effect. Additionally, the relationship between the inverse prediction of the two-colour mixed-dyed fading effect and plasma treatment parameter combinations will be further explored using artificial intelligence methods.

6.5 Disclosure statement

This Chapter has been submitted to the *Journal of Natural Fibers* and it is replying to the comments.

Chapter 7 A novel prediction method for predicting multicolour colour measurements datasets from single colour measurements datasets by means of Polynomial Regression model

7.1 Introduction

In Chapter 4, the study confirms that the combination of plasma treatment with BRNN models effectively predicts the correlation between various plasma treatment parameters and the fading effect of cotton fabrics dyed monochromatically with reactive dyestuffs. In Chapter 6, the study further demonstrates the accuracy of this combination in predicting the relationship between different plasma treatment parameters and the fading effect of cotton fabrics dyed with reactive dyestuffs in two colours. The two-colour dyes are created by equal concentrations of monochromatic dyes, such as green from a combination of blue and yellow dyes, nacarat (a light red-orange hue) from a mixture of red and yellow dyes, and violet from a blend of red and blue dyes.

However, the intricacies of the interaction between plasma and fabric surfaces make it uncertain how the fading effect of single-colour dyeing corresponds to the mixed fading effect of two-colour dyeing in plasma-treated cotton fabrics. Further research is necessary to explore methods for predicting the colour properties of the mixed fading effect of two-colour plasma-treated cotton fabrics from the known single-colour fading effect of plasma-treated cotton fabrics.

The polynomial regression model is a commonly employed empirical model for ascertaining functions and is a specific type of multivariate linear regression (Maulud & Abdulazeez, 2020). Besides, the Weierstrass Approximation Theorem points out that any continuous function

defined on a closed interval [a, b] can be uniformly approximated to a degree of precision by a polynomial function (Stone, 1948). The primary benefit of polynomial regression models is that they offer a universal mathematical framework for predicting an observed phenomenon, which renders polynomial regression models suitable for describing any engineering quantity based on a collection of observed data (Marasco et al., 2022). Nevertheless, the existence of outliers in the data might result in less accurate outcomes from polynomial regression models when compared to other AI-based methods (Marasco et al., 2022). Robust regression is required to mitigate the influence of outlier data points on the estimation of model parameters (Marasco et al., 2022).

It is therefore necessary to integrate plasma treatment with machine learning methods, such as the polynomial regression model, in order to make cotton processing more sustainable (Samanta et al., 2017). The relationship between the single-colour fading effect and the two-colour mixed fading effect of plasma-treated cotton fabrics is still unclear. If the relationship between the single-colour fading effect and the two-colour mixed fading effect can be explored clearly by means of the polynomial regression models, it will help to understand the colour characteristics of the two-colour mixed fading effect of plasma-treated cotton fabrics without considering the complex effects of plasma treatment parameters. Due to the difficulty of obtaining a large number of dye samples in the textile field, overfitting problems can be avoided by incorporating robust regression when the training data set for the polynomial regression model is very small.

Few studies have been conducted on plasma treatment using machine learning methods. Related studies encompass the following: (1) A response surface methodology was utilized to optimize the wool dyeing process with natural dyes (Haji et al., 2022). Linear, quadratic, and

cubic models were fitted to the experimental data, with the quadratic polynomial model displaying a superior R^2 fit to the experimental data when compared to the other models (Haji et al., 2022). (2) Machine learning methods, specifically quadratic polynomial regression, were employed to model the colour removal process from industrial wastewater with activated carbon from wheat straw (Agarwal et al., 2023). The colour removal efficiency exceeded 70%, and the R^2 value was 0.945 (Agarwal et al., 2023). (3) The dyeing effectiveness of green natural dyes in lyocell fabrics was optimized through response surface analysis (Ke et al., 2023). The R^2 value of the quadratic polynomial model fitted to the experimental data was 0.9714 (Ke et al., 2023). (4) The process parameters for cotton fabrics dyed with natural dyes were optimized through the quadratic regression model to obtain maximum colour intensity and antibacterial activity (Boominathan et al., 2022).

Plasma treatment is currently hindered by the lack of understanding of how plasma interacts with fabric surfaces and the difficulty of choosing the proper plasma treatment conditions (Jelil, 2015). Therefore, the aim of this study was to develop a polynomial regression model to investigate the relationship between the single-colour fading effect and the two-colour mixed fading effect of plasma-treated cotton fabrics. The colour properties of the two-colour mixed fading effect of plasma-treated cotton fabrics were predicted from the known single-colour fading effect of plasma-treated cotton fabrics. By avoiding complex adjustments of plasma treatment parameters in this way, time and costs can be reduced. Additionally, this can contribute to the development of intelligence and digitalization within the cotton processing industry. This can also help manufacturers to scale up this environmentally friendly technology and make it useful in the manufacturing sector by providing a reference for fading cotton fabrics with plasma.

7.2 Methodology

7.2.1 Fabric samples and dyeing

There were two types of cotton fabrics, one of which was a single-colour reactive dye-dyed cotton fabric and the other was a two-colour mixed-dye cotton fabric. These were described below.

For the first type of cotton fabric, in a dyeing factory in China, fabric samples (30cm $\times$ 40cm) were dyed with commercial reactive dyes of three primary colours of red (Levafix Red CA, labelled "RR"), blue (Levafix Blue CA, labelled "RB") and yellow (Levafix Yellow CA, labelled "RY") and the dye concentrations were 0.5%, 1.5%. The fabric is 32s/2 cotton single (Lacoste) knitted fabric (weight: 220 g/m^2).

For the second type of cotton fabric, cotton single-knitted fabric (Lacoste: 32s/2) with a weight of 220g/m^2 was dyed by mixing two reactive dyes of three primary colours, red (Levafix Red CA), blue (Levafix Blue CA) and yellow (Levafix Yellow CA) at a dyeing plant in China. The dyes were supplied by DyStar, China and were used as received for dyeing without purification. Mixed secondary colours of green (RG), nacarat (RN) and violet (RV) are used for dyeing to different depths of 0.5%, 1.5%. The fabric samples are approximately 30 cm $\times$ 40 cm in size. Among these colours, green was produced by combining equal amounts of blue and yellow. Red and yellow dyes were combined to make nacarat (a bright orange-red colour), and red and blue dyes were combined to make violet. In this study, a 0.5% concentration of violet was composed of 0.5% concentrations of red and 0.5% concentrations of blue.

7.2.2 Plasma treatment of faded colours

An ozone plasma machine G2 (standard model, Spain Jeanologia) was used to treat the fabric for fading. Table 7.1 summarizes the plasma treatment parameters used at a garment processing factory in China for cotton fabrics. A total of three parameters were used in the process: air concentration, dyed fabric water content, and treatment time.

Table 7.1. Plasma treatment parameters applied to fabric samples

Air (Oxygen) concentration (%)	10, 30, 50
Water Content (%)	35, 45
Treatment time (minutes)	10, 20, 30

For each type of dye, 114 samples were used for single-colour reactive dye-dyed cotton fabric and two-colour mixed-dye cotton fabric, respectively. There were 18 combinations of plasma treatment parameters ($3 \times 3 \times 2 = 18$), and dyes were applied at two different dye concentrations ($18 \times 2 + 2 = 38$), and there were three different dyes, including three single-colour dyes and three two-colour mixed dyes($38 \times 3 = 114$). These dyes were used to produce 114 fabric samples for single-colour reactive dye-dyed cotton fabric and two-colour mixed-dye cotton fabric, respectively.

For the single-colour reactive dye-dyed cotton fabric, they were labelled RR1-RR38 (for red colour), RB1-RB38 (for blue colour) and RY1-RY38(for yellow colour). For the two-colour mixed-dye cotton fabric, they were labelled RN1-RN38 (for nacarat colour), RG1-RG38 (for green colour) and RV1-RV38 (for violet colour).

7.2.3 Colour measurement arrangements

To obtain accurate colour measurements, fabric samples were conditioned at 65±2% relative humidity and 20±2°C for a minimum of 24 hours prior to measurement. A Macbeth Colour-Eye 7000A (CE-7000A) spectrophotometer was used to perform precision colour measurements for each type of sample. Colours were measured as specific CIE L*a* b* and K/S values.

Besides, the Macbeth colour eye 7000A was used to measure colour with an illuminant D65, a large aperture value, and a 10° observer angle. Black and white traps were also used to calibrate the colour-measuring device. To improve the accuracy of the colour measurements, four fabric samples of each type and four uniformly coloured areas of each fabric sample were tested (as shown in Figure 3.5). The average of these data was then used to calculate the final colour measurement.

7.2.4 Input and output datasets for Polynomial Regression models

After measuring the colour measurements of the cotton fabrics and initial data processing, a polynomial regression model was used to explore the relationship between the single-colour fading effect and the two-colour mixed fading effect of the plasma-treated cotton fabrics. This is shown in Equation 7.1.

$$\sum_{i=1}^{4} zData_i = \sum_{i=1}^{4} f(xData_i, yData_i)$$

(7.1)

Where $xData_i$ ($i = 1, 2, 3, 4$) and $yData_i$ ($i = 1, 2, 3, 4$) represented the post-fade colour measurement data for cotton fabrics dyed with single-colour reactive dyes, which were the

input datasets for the polynomial regression models. $zData_i$ $(i = 1, 2, 3, 4)$ represented the corresponding post-fade colour measurement data for cotton fabrics dyed with two-colour mixed dyes, which were the output datasets for the polynomial regression models. Specifically, the CIE L* value of RN was determined by some relationship between the CIE L* value of RR and the CIE L* value of RY (RN = RR + RY, i.e., nacarat = red + yellow). The CIE L* value of RG was determined by some relationship between the CIE L* value of RB and the CIE L* value of RY (RG = RB + RY, i.e., green = blue + yellow). The CIE L* value of RV was determined by some relationship between the CIE L* value of RR and the CIE L* value of RB (RV = RR + RB, i.e., violet = red + blue). The rest of the CIE a*, CIE b* and K/S values were also based on the above rule. This was shown in the Table 7.2 below.

Table 7.2. Division of the data sets for the polynomial regression models

$xData_i$ $(i = 1, 2, 3, 4)$	$yData_i$ $(i = 1, 2, 3, 4)$	$zData_i$ $(i = 1, 2, 3, 4)$
$xData_{01}$: CIE L* (RR1-RR38) CIE L* (RB1-RB38) CIE L* (RR1-RR38)	$yData_{01}$: CIE L* (RY1-RY38) CIE L* (RY1-RY38) CIE L* (RB1-RB38)	$zData_{01}$: CIE L* (RN1-RN38) CIE L* (RG1-RG38) CIE L* (RV1-RV38)
$xData_{02}$: CIE a* (RR1-RR38) CIE a* (RB1-RB38) CIE a* (RR1-RR38)	$yData_{02}$: CIE a* (RY1-RY38) CIE a* (RY1-RY38) CIE a* (RB1-RB38)	$zData_{02}$: CIE a* (RN1-RN38) CIE a* (RG1-RG38) CIE a* (RV1-RV38)
$xData_{03}$: CIE b* (RR1-RR38) CIE b* (RB1-RB38) CIE b* (RR1-RR38)	$yData_{03}$: CIE b* (RY1-RY38) CIE b* (RY1-RY38) CIE b* (RB1-RB38)	$zData_{03}$: CIE b* (RN1-RN38) CIE b* (RG1-RG38) CIE b* (RV1-RV38)
$xData_{04}$: K/S (RR1-RR38) K/S (RB1-RB38) K/S (RR1-RR38)	$yData_{04}$: K/S (RY1-RY38) K/S (RY1-RY38) K/S (RB1-RB38)	$zData_{04}$: K/S (RN1-RN38) K/S (RG1-RG38) K/S (RV1-RV38)

7.2.5 Structure of the Polynomial Regression model

For convenience in expressing the structure of the polynomial regression model, $xData$ was simplified to x, $yData$ was simplified to y, and $zData$ was simplified to z. If m is the degree of x and n is the degree of y, the total degree of the polynomial is the maximum of m and n (MathWorks, 2022b). An example of a model name would be $poly23$ with an x degree of 2 and a y degree of 3. Table 7.3 showed the model terms in the following format (MathWorks, 2022b). A polynomial regression model could not have a degree greater than the maximum of m and n. Therefore, terms such as xy^3 and x^2y^2 were excluded since their sum degrees exceeded 3, i.e., both cases had a total degree of 4 (MathWorks, 2022b).

The polynomial regression models mentioned in this study had a total degree of no more than 5. Thus, there were a total of 25 polynomial regression models with the model names $poly11$-$poly55$, i.e., $\sum_{m=1}^{5}\sum_{n=1}^{5} polymn$. The specific Equations (7.2—7.26) were shown in Table 7.4.

Table 7.3. The format of $poly23$ model terms

Degree of Term	0	1	2	3
0	1	y	y^2	y^3
1	x	xy	xy^2	N/A
2	x^2	x^2y	N/A	N/A

Table 7.4. The specific Equations for a total of 25 polynomial regression models

Model names	The specific Equations	No.
$poly11$	$f(x,y) = p_{00} + p_{10}x + p_{01}y$	(7.2)
$poly12$	$f(x,y) = p_{00} + p_{10}x + p_{01}y + p_{11}xy + p_{02}y^2$	(7.3)
$poly13$	$f(x,y) = p_{00} + p_{10}x + p_{01}y + p_{11}xy + p_{02}y^2 + p_{12}xy^2 + p_{03}y^3$	(7.4)

$poly14$	$f(x,y) = p_{00} + p_{10}x + p_{01}y + p_{11}xy + p_{02}y^2 + p_{12}xy^2 + p_{03}y^3$ $+ p_{13}xy^3 + p_{04}y^4$	(7.5)
$poly15$	$f(x,y) = p_{00} + p_{10}x + p_{01}y + p_{11}xy + p_{02}y^2 + p_{12}xy^2 + p_{03}y^3$ $+ p_{13}xy^3 + p_{04}y^4 + p_{14}xy^4 + p_{05}y^5$	(7.6)
$poly21$	$f(x,y) = p_{00} + p_{10}x + p_{01}y + p_{20}x^2 + p_{11}xy$	(7.7)
$poly22$	$f(x,y) = p_{00} + p_{10}x + p_{01}y + p_{20}x^2 + p_{11}xy + p_{02}y^2$	(7.8)
$poly23$	$f(x,y) = p_{00} + p_{10}x + p_{01}y + p_{20}x^2 + p_{11}xy + p_{02}y^2 + p_{21}x^2y$ $+ p_{12}xy^2 + p_{03}y^3$	(7.9)
$poly24$	$f(x,y) = p_{00} + p_{10}x + p_{01}y + p_{20}x^2 + p_{11}xy + p_{02}y^2 + p_{21}x^2y$ $+ p_{12}xy^2 + p_{03}y^3 + p_{22}x^2y^2 + p_{13}xy^3 + p_{04}y^4$	(7.10)
$poly25$	$f(x,y) = p_{00} + p_{10}x + p_{01}y + p_{20}x^2 + p_{11}xy + p_{02}y^2 + p_{21}x^2y$ $+ p_{12}xy^2 + p_{03}y^3 + p_{22}x^2y^2 + p_{13}xy^3 + p_{04}y^4$ $+ p_{23}x^2y^3 + p_{14}xy^4 + p_{05}y^5$	(7.11)
$poly31$	$f(x,y) = p_{00} + p_{10}x + p_{01}y + p_{20}x^2 + p_{11}xy + p_{30}x^3 + p_{21}x^2y$	(7.12)
$poly32$	$f(x,y) = p_{00} + p_{10}x + p_{01}y + p_{20}x^2 + p_{11}xy + p_{02}y^2 + p_{30}x^3$ $+ p_{21}x^2y + p_{12}xy^2$	(7.13)
$poly33$	$f(x,y) = p_{00} + p_{10}x + p_{01}y + p_{20}x^2 + p_{11}xy + p_{02}y^2 + p_{30}x^3$ $+ p_{21}x^2y + p_{12}xy^2 + p_{03}y^3$	(7.14)
$poly34$	$f(x,y) = p_{00} + p_{10}x + p_{01}y + p_{20}x^2 + p_{11}xy + p_{02}y^2 + p_{30}x^3$ $+ p_{21}x^2y + p_{12}xy^2 + p_{03}y^3 + p_{31}x^3y + p_{22}x^2y^2$ $+ p_{13}xy^3 + p_{04}y^4$	(7.15)
$poly35$	$f(x,y) = p_{00} + p_{10}x + p_{01}y + p_{20}x^2 + p_{11}xy + p_{02}y^2 + p_{30}x^3$ $+ p_{21}x^2y + p_{12}xy^2 + p_{03}y^3 + p_{31}x^3y + p_{22}x^2y^2$ $+ p_{13}xy^3 + p_{04}y^4 + p_{32}x^3y^2 + p_{23}x^2y^3 + p_{14}xy^4$ $+ p_{05}y^5$	(7.16)
$poly41$	$f(x,y) = p_{00} + p_{10}x + p_{01}y + p_{20}x^2 + p_{11}xy + p_{30}x^3 + p_{21}x^2y$ $+ p_{40}x^4 + p_{31}x^3y$	(7.17)
$poly42$	$f(x,y) = p_{00} + p_{10}x + p_{01}y + p_{20}x^2 + p_{11}xy + p_{02}y^2 + p_{30}x^3$ $+ p_{21}x^2y + p_{12}xy^2 + p_{40}x^4 + p_{31}x^3y + p_{22}x^2y^2$	(7.18)
$poly43$	$f(x,y) = p_{00} + p_{10}x + p_{01}y + p_{20}x^2 + p_{11}xy + p_{02}y^2 + p_{30}x^3$ $+ p_{21}x^2y + p_{12}xy^2 + p_{03}y^3 + p_{40}x^4 + p_{31}x^3y$ $+ p_{22}x^2y^2 + p_{13}xy^3$	(7.19)

$poly44$	$$\begin{aligned} f(x,y) = \ & p_{00} + p_{10}x + p_{01}y + p_{20}x^2 + p_{11}xy + p_{02}y^2 + p_{30}x^3 \\ & + p_{21}x^2y + p_{12}xy^2 + p_{03}y^3 + p_{40}x^4 + p_{31}x^3y \\ & + p_{22}x^2y^2 + p_{13}xy^3 + p_{04}y^4 \end{aligned}$$	(7.20)
$poly45$	$$\begin{aligned} f(x,y) = \ & p_{00} + p_{10}x + p_{01}y + p_{20}x^2 + p_{11}xy + p_{02}y^2 + p_{30}x^3 \\ & + p_{21}x^2y + p_{12}xy^2 + p_{03}y^3 + p_{40}x^4 + p_{31}x^3y \\ & + p_{22}x^2y^2 + p_{13}xy^3 + p_{04}y^4 + p_{41}x^4y + p_{32}x^3y^2 \\ & + p_{23}x^2y^3 + p_{14}xy^4 + p_{05}y^5 \end{aligned}$$	(7.21)
$poly51$	$$\begin{aligned} f(x,y) = \ & p_{00} + p_{10}x + p_{01}y + p_{20}x^2 + p_{11}xy + p_{30}x^3 + p_{21}x^2y \\ & + p_{40}x^4 + p_{31}x^3y + p_{50}x^5 + p_{41}x^4y \end{aligned}$$	(7.22)
$poly52$	$$\begin{aligned} f(x,y) = \ & p_{00} + p_{10}x + p_{01}y + p_{20}x^2 + p_{11}xy + p_{02}y^2 + p_{30}x^3 \\ & + p_{21}x^2y + p_{12}xy^2 + p_{40}x^4 + p_{31}x^3y + p_{22}x^2y^2 \\ & + p_{50}x^5 + p_{41}x^4y + p_{32}x^3y^2 \end{aligned}$$	(7.23)
$poly53$	$$\begin{aligned} f(x,y) = \ & p_{00} + p_{10}x + p_{01}y + p_{20}x^2 + p_{11}xy + p_{02}y^2 + p_{30}x^3 \\ & + p_{21}x^2y + p_{12}xy^2 + p_{03}y^3 + p_{40}x^4 + p_{31}x^3y \\ & + p_{22}x^2y^2 + p_{13}xy^3 + p_{50}x^5 + p_{41}x^4y + p_{32}x^3y^2 \\ & + p_{23}x^2y^3 \end{aligned}$$	(7.24)
$poly54$	$$\begin{aligned} f(x,y) = \ & p_{00} + p_{10}x + p_{01}y + p_{20}x^2 + p_{11}xy + p_{02}y^2 + p_{30}x^3 \\ & + p_{21}x^2y + p_{12}xy^2 + p_{03}y^3 + p_{40}x^4 + p_{31}x^3y \\ & + p_{22}x^2y^2 + p_{13}xy^3 + p_{04}y^4 + p_{50}x^5 + p_{41}x^4y \\ & + p_{32}x^3y^2 + p_{23}x^2y^3 + p_{14}xy^4 \end{aligned}$$	(7.25)
$poly55$	$$\begin{aligned} f(x,y) = \ & p_{00} + p_{10}x + p_{01}y + p_{20}x^2 + p_{11}xy + p_{02}y^2 + p_{30}x^3 \\ & + p_{21}x^2y + p_{12}xy^2 + p_{03}y^3 + p_{40}x^4 + p_{31}x^3y \\ & + p_{22}x^2y^2 + p_{13}xy^3 + p_{04}y^4 + p_{50}x^5 + p_{41}x^4y \\ & + p_{32}x^3y^2 + p_{23}x^2y^3 + p_{14}xy^4 + p_{05}y^5 \end{aligned}$$	(7.26)

7.2.6 Modelling and simulation using Polynomial Regression models

In MATLAB (version R2021a) software, three different fitting methods were used for each of the 25 polynomial regression Models, namely (1) Least Squares (LS), (2) Least Absolute Residual (LAR), and (3) Bisquare Weights (Bisquare). In the polynomial regression model, the coefficients were estimated based on the fitting process. These three fitting methods and the 25

polynomial regression models were also available in MATLAB's Curve Fitting Toolbox (version R2021a) (MathWorks, 2022a).

The LS fitting process minimises the sum of squares of residuals for a linear model, defined as an equation with linear coefficients (MathWorks, 2022a). Every linear term in the model requires an additional normal equation for higher degrees of polynomiality (MathWorks, 2022a). LS fit, however, has the main disadvantage of being sensitive to outliers, because residual squaring amplifies the effect of extreme data points, outliers have an important impact on fit (MathWorks, 2022a).

As a result, there are two other robust regression methods that are proposed, which are LAR and Bisquare. When using the LAR method, the curve is chosen that minimizes the absolute value of the residuals, not the squared difference (MathWorks, 2022a). In this way, extreme values will not have as much of an impact on the fit as they would otherwise. For the Bisquare, this method minimises the weighted sum of squares in which the weight given to each data point is based on its distance from the fitted line (MathWorks, 2022a). A higher weight is assigned to points near the line and a lower weight is assigned to points that are further away from the line (MathWorks, 2022a). Besides, in addition to finding a curve that accommodates most of the data, Bisquare may also minimise the effect of outliers by using the usual least squares method (MathWorks, 2022a).

The polynomial regression models obtained by fitting in different ways will also vary. The accuracy of the model will be assessed by a combination of metrics, including mean absolute errors (MAE), root mean square errors (RMSE) and coefficient of determination (R^2).

123

7.2.7 Verification of the Polynomial Regression models' accuracy

As a common method for assessing machine learning models' accuracy and model performance, mean absolute errors (MAE) and root mean square errors (RMSE) were used to evaluate polynomial regression models' accuracy (Abiodun et al., 2019; Chai & Draxler, 2014; Ostertagova & Ostertag, 2012). For a sample y_i with n measurements (y_i, $i = 1, 2, \ldots, n$), and n matching polynomial regression models' predictions $\hat{y}_i$ ($i = 1, 2, \ldots, n$), MAE and RMSE are presented in Equations (7.27), (7.28) (Abiodun et al., 2019; Chai & Draxler, 2014; Ostertagova & Ostertag, 2012).

$$MAE = \frac{1}{n}\sum_{i=1}^{n}|y_i - \hat{y}_i| \qquad (7.27)$$

$$RMSE = \sqrt{\frac{1}{n}\sum_{i=1}^{n}(y_i - \hat{y}_i)^2} \qquad (7.28)$$

MAE is a metric that measures overall accuracy (Ostertagova & Ostertag, 2012). A MAE near zero indicates that the polynomial regression models are very accurate if the predicted and actual values are closely aligned. MAE is large if the fit is poor, indicating that the accuracy of the polynomial regression models needs to be improved. RMSE, the square root of MSE, represents another measure of total accuracy, which gives extra weight to large errors, with the severity of the prediction error being the same as the dimensions of the actual or predicted values (Ostertagova & Ostertag, 2012).

As an additional measure of generalisability, the coefficient of determination R^2 was also used (Choudhury et al., 2015). It is possible that a higher R^2 value indicates a better correlation

between the predicted and actual values, which may indicate that the constructed polynomial regression models may be more able to generalize to unknown data.

The performance of a model can often be evaluated using a combination of metrics (Chai & Draxler, 2014), including MAE, RMSE, and R^2. The MAE method is suitable for describing uniformly distributed errors, but is unsuitable for representing large errors ((Chai & Draxler, 2014). It is more appropriate to use RMSE to describe normally distributed errors since it is sensitive to outliers (Chai & Draxler, 2014). The coefficient of determination R^2 provides information regarding the fit of the model but does not provide information regarding the residuals. Therefore, a single indicator emphasizes only one aspect of the error characteristics, whereas a combined indicator evaluation system is more appropriate for assessing the overall performance of the model (Chai & Draxler, 2014).

7.3 Results and discussion

7.3.1 The optimal Polynomial Regression model and fitting way for CIE L* values

The polynomial regression models fitted in different ways were used to investigate the relationship between the single-colour fading effect and the two-colour mixed fading effect of plasma-treated cotton fabrics. Equation (7.1) illustrated the relationship between the CIE L* values that needed to be explored when $i = 1$.

For the CIE L* values, the results of the fit were shown in Table 7.5. It could be seen that the optimal polynomial regression model was named $poly54$ and the fit way used should be LS. The optimal model had an R^2 of 0.9611 and an RMSE of 2.3019, and the values have been with superscript "*".

Table 7.5. The results of polynomial regression models fitted with different ways for the CIE L* values

Model names	R^2			RMSE		
	LS	LAR	Bisquare	LS	LAR	Bisquare
*poly*11	0.9235	0.9226	0.9199	2.9697	2.9871	3.0374
*poly*12	0.9309	0.9286	0.9297	2.8470	2.8943	2.8725
*poly*13	0.9314	0.9289	0.9296	2.8643	2.9154	2.9009
*poly*14	0.9321	0.9282	0.9299	2.8754	2.9564	2.9227
*poly*15	0.9373	0.9298	0.9400	2.7907	2.9526	2.7307
*poly*21	0.9260	0.9241	0.9259	2.9468	2.9842	2.9485
*poly*22	0.9348	0.9324	0.9309	2.7799	2.8297	2.8608
*poly*23	0.9382	0.9330	0.9383	2.7428	2.8578	2.7420
*poly*24	0.9463	0.9434	0.9418	2.5961	2.6632	2.7004
*poly*25	0.9470	0.9427	0.9431	2.6178	2.7215	2.7109
*poly*31	0.9334	0.9315	0.9322	2.8214	2.8619	2.8459
*poly*32	0.9459	0.9424	0.9464	2.5676	2.6484	2.5542
*poly*33	0.9462	0.9407	0.9463	2.5718	2.7006	2.5711
*poly*34	0.9537	0.9509	0.9501	2.4347	2.5073	2.5264
*poly*35	0.9562	0.9504	0.9488	2.4164	2.5707	2.6119
*poly*41	0.9364	0.9319	0.9363	2.7839	2.8792	2.7863
*poly*42	0.9494	0.9453	0.9483	2.5178	2.6184	2.5465
*poly*43	0.9528	0.9496	0.9499	2.4559	2.5385	2.5307
*poly*44	0.9543	0.9516	0.9497	2.4295	2.5014	2.5504
*poly*45	0.9578	0.9548	0.9525	2.3964	2.4798	2.5410
*poly*51	0.9402	0.9380	0.9359	2.7253	2.7738	2.8221
*poly*52	0.9556	0.9521	0.9544	2.3963	2.4875	2.4281
*poly*53	0.9580	0.9556	0.9553	2.3643	2.4312	2.4409
*poly*54	0.9611*	0.9557	0.9567	2.3019*	2.4562	2.4284
*poly*55	0.9611	0.9562	0.9559	2.3133	2.4550	2.4623

For the remaining polynomial regression models, the model with the name $poly55$ had a similar fit to the optimal $poly54$. The regression effects of the polynomial regression model tend to increase with increasing degree, as shown in Figure 7.1. As the degree of polynomial regression models increased, the RMSE of the models also showed a decreasing trend, as shown in Figure 7.2. The fitting way of LS was better than both LAR and Bisquare in general. This suggests that the relationship between the lightness levels of the fabric samples between the single-colour fading effect and the two-colour mixed fading effect was difficult to explain by a simple linear relationship. Instead, a polynomial regression model with a higher degree would provide a better regression effect.

Figure 7.1. The R^2 of polynomial regression models fitted with different ways for the CIE L* values

Figure 7.2. The RMSE of polynomial regression models fitted with different ways for the CIE L* values

Therefore, the relationship between the lightness levels of the fabric samples between the single-colour fading effect and the two-colour mixed fading effect could be expressed by the $poly54$ polynomial regression model with the fitting way of LS, as shown in Table 7.6. Equation (7.27) showed the estimated coefficients with 95% confidence bounds for the $poly54$ polynomial regression model. Figure 7.3 shows a plot of the fitted curve for the $poly54$ model and Figure 7.4 showed a plot of the residuals for the $poly54$ model. It could be seen that the $poly54$ model could roughly fit the relationship between the lightness levels of the fabric samples between the single-colour fading effect and the two-colour mixed fading effect, with most of the model predictions and the actual values having an error of 2 or less, but there were still a small number of errors between 4 and 5 in the predicted and actual values.

Table 7.6. Estimated coefficients with 95% confidence bounds for the $poly54$ model

Model names	The specific Equation	No.
CIE L*, $poly54$ model with the fitting way of LS	$f(x,y) = p_{00} + p_{10}x + p_{01}y + p_{20}x^2 + p_{11}xy + p_{02}y^2 + p_{30}x^3 + p_{21}x^2y + p_{12}xy^2 + p_{03}y^3 + p_{40}x^4 + p_{31}x^3y + p_{22}x^2y^2 + p_{13}xy^3 + p_{04}y^4 + p_{50}x^5 + p_{41}x^4y + p_{32}x^3y^2 + p_{23}x^2y^3 + p_{14}xy^4$ Where x is normalized by mean 59.32 and standard deviation 6.958, and where y is normalized by mean 69.86 and standard deviation 10.51. Coefficients with 95% confidence bounds are as follows. $p_{00} =$ 57.15 (54.34, 59.96) $p_{10} =$ 10.97 (6.988, 14.95) $p_{01} =$ 1.384 (-4.864, 7.632) $p_{20} =$ -13.05 (-19.31, -6.795) $p_{11} =$ -6.31 (-15.63, 3.007) $p_{02} =$ -4.789 (-9.484, -0.0928) $p_{30} =$ -4.668 (-8.053, -1.284) $p_{21} =$ 35.42 (21.53, 49.31) $p_{12} =$ -16.85 (-28.25, -5.452) $p_{03} =$ 1.853 (-5.478, 9.184) $p_{40} =$ 4.757 (0.9813, 8.533) $p_{31} =$ -4.187 (-16.62, 8.247) $p_{22} =$ -5.652 (-15.94, 4.638) $p_{13} =$ 8.221 (0.3614, 16.08) $p_{04} =$ 1.154 (-2.626, 4.934) $p_{50} =$ 1.603 (0.5031, 2.702) $p_{41} =$ -12.32 (-19.62, -5.022) $p_{32} =$ 18.32 (2.621, 34.02) $p_{23} =$ -15.16 (-30.51, 0.1871) $p_{14} =$ 5.955 (0.8418, 11.07)	(7.27)
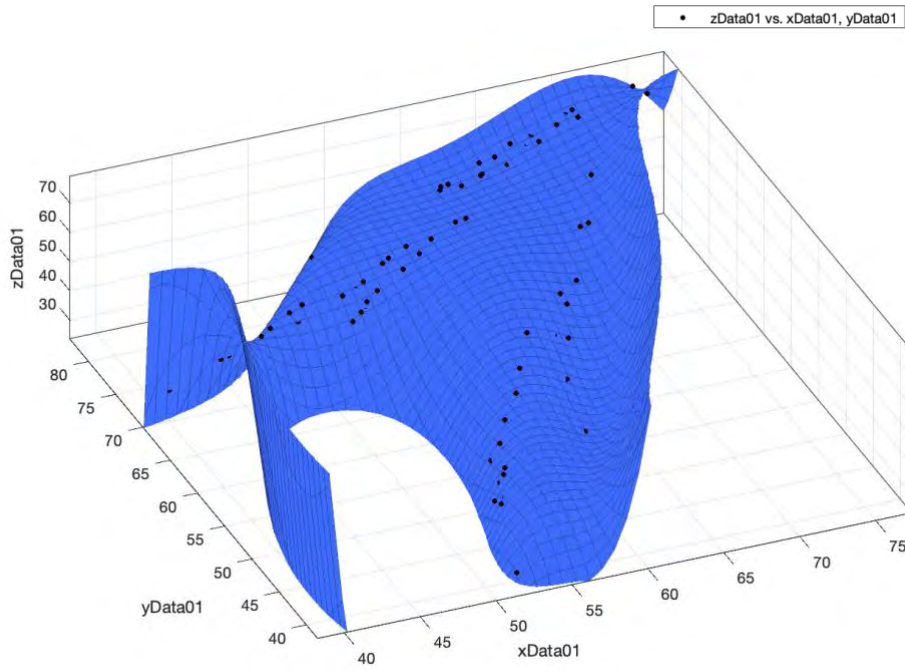
Figure 7.3. A plot of the fitted curve for the $poly54$ model about the relationship between CIE L* values
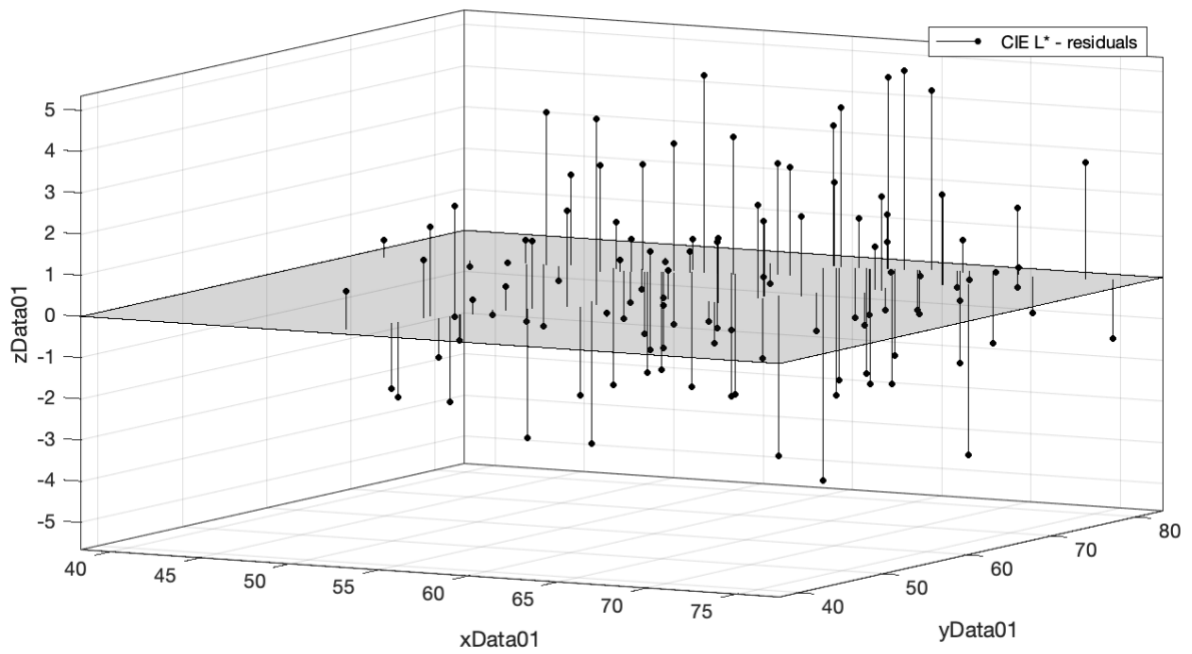
Figure 7.4. A residual plot for the $poly54$ model about the relationship between CIE L* values

Furthermore, the regression effects of the polynomial regression model with CIE L* values were low, i.e., 0.9611, which was not very close to 1. And the MAE of the $poly54$ model about the relationship between CIE L* values is 1.6796. This was partly due to the limited data set used for the models. In addition, it was possible that the CIE L* values reflect mainly the lightness levels of the fabric samples, whereas the relationship between the lightness levels of the single-colour fading effect and the two-colour mixed fading effect of the plasma-treated cotton fabrics was not highly closely related. The relationship between the monochrome fading effect and the two-colour mixed fading effect might be more reflected in the colour-related CIE a*, CIE b* values, or in the K/S values related to the dyeing level.

7.3.2 The optimal Polynomial Regression model and fitting way for CIE a* values

In order to investigate the relationship between the single-colour fading effect and the two-colour mixed fading effect of plasma-treated cotton fabrics, polynomial regression models were fitted in different ways. Equation (7.1) illustrated the relationship between the CIE a* values that needed to be explored when $i = 2$.

For the CIE a* values, the results of the fit were shown in Table 7.7. Based on the results, $poly53$ appeared to be the optimal polynomial regression model and LAR should be used to fit the data. R^2 and RMSE of this model are 0.9978 and 0.9861, respectively, and the values were superscripted with "*".

Table 7.7. The results of polynomial regression models fitted with different ways for the CIE a* values

Model names	R^2			RMSE		
	LS	LAR	Bisquare	LS	LAR	Bisquare
$poly11$	0.9218	0.9192	0.9147	5.5199	5.6106	5.7650
$poly12$	0.9785	0.9961	0.9810	2.9215	1.2396	2.7424
$poly13$	0.9884	0.9965	0.9906	2.1670	1.1881	1.9538
$poly14$	0.9907	0.9961	0.9912	1.9603	1.2634	1.9036
$poly15$	0.9928	0.9963	0.9933	1.7338	1.2441	1.6775
$poly21$	0.9812	0.9808	0.9837	2.7334	2.7624	2.5407
$poly22$	0.9844	0.9839	0.9852	2.4973	2.5385	2.4332
$poly23$	0.9911	0.9963	0.9922	1.9188	1.2367	1.7962
$poly24$	0.9955	0.9952	0.9954	1.3803	1.4314	1.3998
$poly25$	0.9962	0.9959	0.9961	1.2939	1.3407	1.2999
$poly31$	0.9870	0.9961	0.9922	2.2923	1.2569	1.7745
$poly32$	0.9927	0.9970	0.9933	1.7310	1.1156	1.6571
$poly33$	0.9928	0.9966	0.9933	1.7277	1.1810	1.6657
$poly34$	0.9963	0.9960	0.9964	1.2616	1.3102	1.2420
$poly35$	0.9967	0.9964	0.9967	1.2274	1.2687	1.2171
$poly41$	0.9872	0.9947	0.9915	2.2923	1.4774	1.8663
$poly42$	0.9941	0.9937	0.9944	1.5817	1.6352	1.5414
$poly43$	0.9963	0.9960	0.9965	1.2645	1.3123	1.2304
$poly44$	0.9963	0.9960	0.9967	1.2670	1.3218	1.2055
$poly45$	0.9971	0.9969	0.9973	1.1514	1.1923	1.1218
$poly51$	0.9874	0.9935	0.9911	2.2991	1.6498	1.9334
$poly52$	0.9943	0.9962	0.9945	1.5768	1.2846	1.5438
$poly53$	0.9971	0.9978*	0.9973	1.1465	0.9861*	1.1078
$poly54$	0.9971	0.9977	0.9972	1.1571	1.0207	1.1287
$poly55$	0.9971	0.9969	0.9973	1.1559	1.2023	0.9967

For the remaining polynomial regression models, with the exception of those named $poly11$, $poly12$ and $poly21$, which were relatively poorly fitted, all the models had similar regression

effects to the optimal $poly53$, with R^2 essentially at 0.98 or above. It means that the regression of the polynomial regression model was relatively poorly fitted when the degree of the model was below 2. However, it was well-fitted when the degree of the model was 2 and above, as shown in Figure 7.5. The RMSE of the model showed a similar trend of the regression effects, as shown in Figure 7.6. There was a large RMSE of 2 to 6 when the degree of the model was below 2, which indicated a poor fit. However, there was a smaller RMSE of 0.8 and 2 when the degree of the model was 2 and above, which indicated a more accurate model fit. It also suggests that the relationship between the single-colour fading effect and the two-colour mixed fading effect between the CIE a* values of the fabric samples is difficult to explain by a simple linear relationship. In contrast, a polynomial regression model with a higher degree, i.e., the degree of the model was 2 or more, would provide a better-fitted regression. In terms of fitting ways, LAR and Bisquare are better than LS in general. Moreover, the fitting methods LAR and Bisquare are closer, with LAR having better-fitted regression effects in most cases.
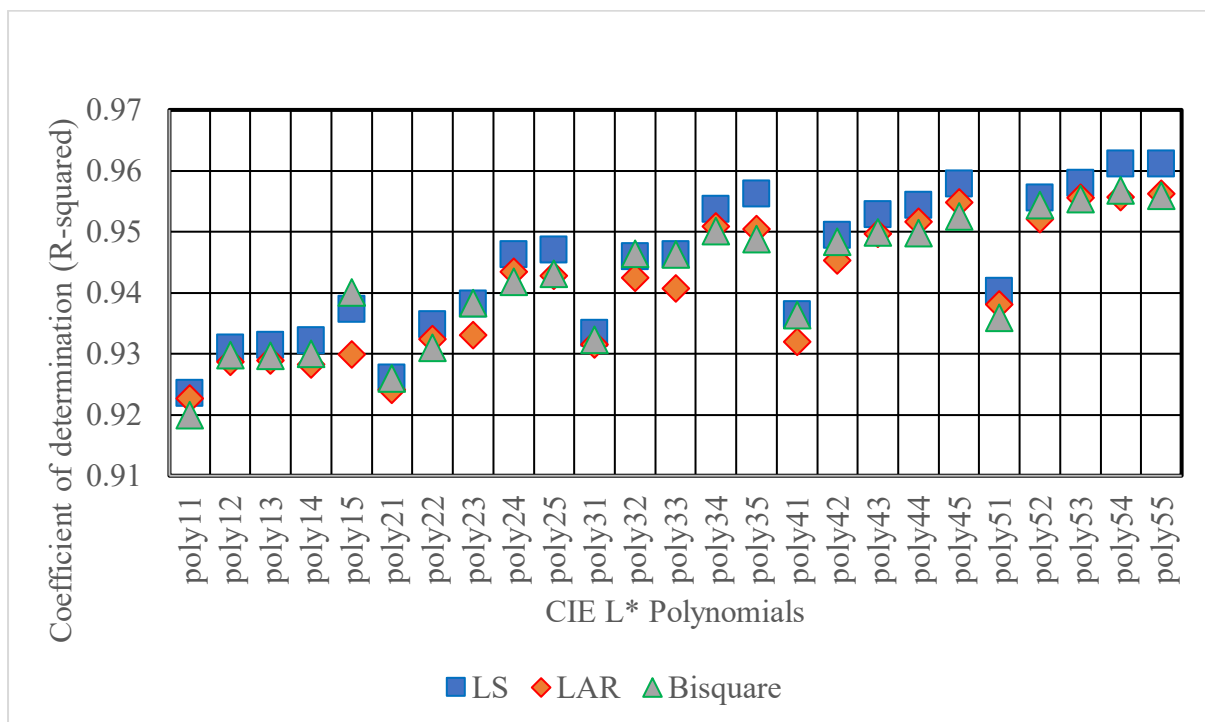
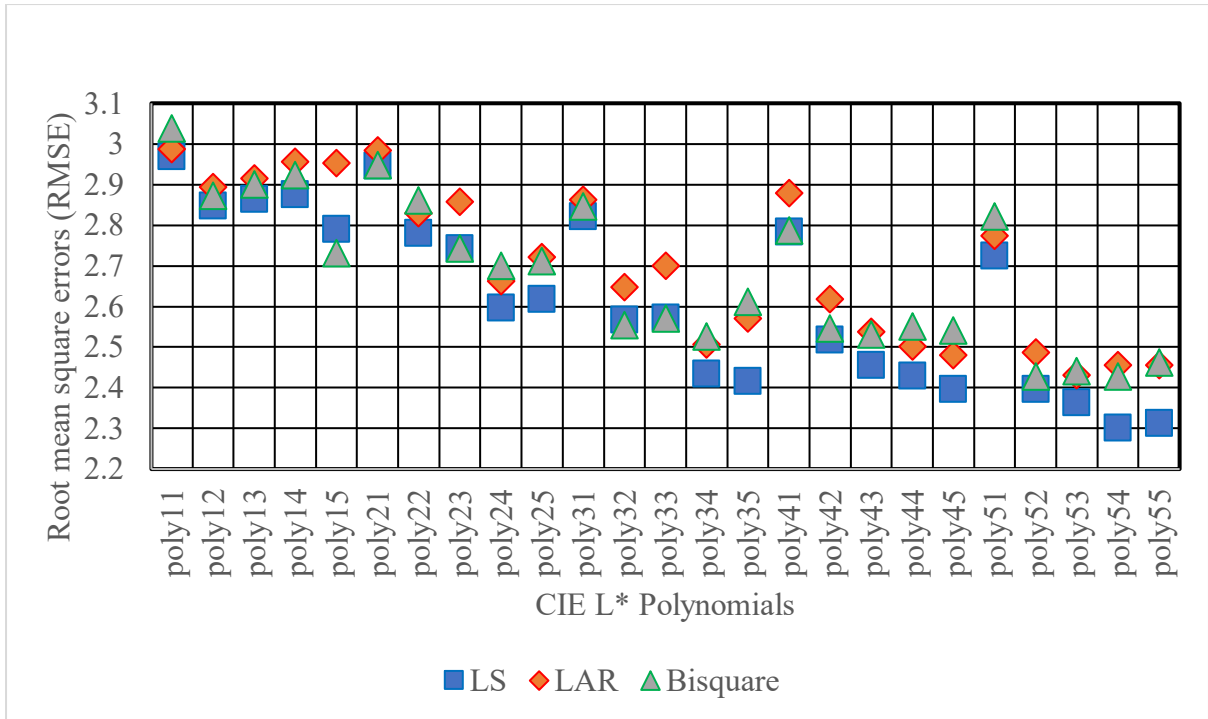Figure 7.5. The R^2 of polynomial regression models fitted with different ways for the CIE a*

values

Figure 7.6. The RMSE of polynomial regression models fitted with different ways for the

CIE a* values

Therefore, the relationship between the CIE a* values of the fabric samples for the single-colour fading effect and the two-colour mixed fading effect could be represented by the $poly53$ polynomial regression model with the fitting method LAR, as shown in Table 7.8. Equation (7.28) showed the estimated coefficients with 95% confidence bounds for the $poly53$ polynomial regression model. Figure 7.7 showed a plot of the fitted curve of the $poly53$ model and Figure 7.8 showed a plot of the residuals of the $poly53$ model. It could be seen that the $poly53$ model can roughly fit the relationship between the CIE a* values of fabric samples with the single-colour fading effect and the two-colour mixed fading effect, with most models having errors of 2 or less between the predicted and actual values. However, a small number of larger errors existed between the predicted and actual values, ranging between 3 and 4.

Table 7.8. Estimated coefficients with 95% confidence bounds for the $poly53$ model

Model names	The specific Equation	No.
CIE a*, $poly53$ model with the fitting way of LAR	$f(x,y) = p_{00} + p_{10}x + p_{01}y + p_{20}x^2 + p_{11}xy + p_{02}y^2 + p_{30}x^3 + p_{21}x^2y + p_{12}xy^2 + p_{03}y^3 + p_{40}x^4 + p_{31}x^3y + p_{22}x^2y^2 + p_{13}xy^3 + p_{50}x^5 + p_{41}x^4y + p_{32}x^3y^2 + p_{23}x^2y^3$ Where x is normalized by mean 30.06 and standard deviation 26.56, and where y is normalized by mean 11.69 and standard deviation 13.98. Coefficients with 95% confidence bounds are as follows. $p_{00} =$ 21.43 (19.47, 23.38) $p_{10} =$ 30.86 (22.59, 39.13) $p_{01} =$ -0.7957 (-5.839, 4.248) $p_{20} =$ -4.67 (-9.334, -0.005325) $p_{11} =$ 4.419 (-1.444, 10.28) $p_{02} =$ -12.25 (-14.74, -9.767) $p_{30} =$ -5.9 (-17.97, 6.172) $p_{21} =$ 25.04 (18.16, 31.92)	(7.28)

$p_{12} =$	-0.4626 (-3.918, 2.993)	
$p_{03} =$	-4.219 (-7.603, -0.8347)	
$p_{40} =$	1.067 (-2.79, 4.923)	
$p_{31} =$	6.251 (2.663, 9.839)	
$p_{22} =$	11.86 (8.537, 15.18)	
$p_{13} =$	-0.6708 (-3.294, 1.952)	
$p_{50} =$	-1.603 (-6.361, 3.154)	
$p_{41} =$	-10.37 (-14.03, -6.713)	
$p_{32} =$	-3.164 (-5.649, -0.6785)	
$p_{23} =$	-3.118 (-6.535, 0.2985)	
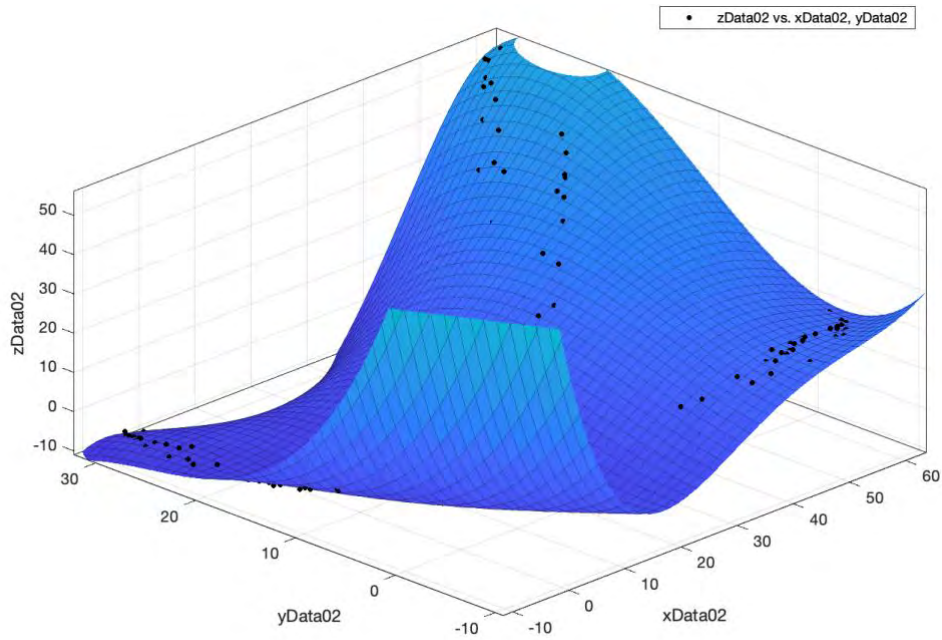
Figure 7.7. A plot of the fitted curve for the $poly53$ model about the relationship between CIE a* values

Figure 7.8. A residual plot for the $poly53$ model about the relationship between CIE a* values

Furthermore, the regression effects of the polynomial regression model with CIE a* values were high, i.e., 0.9978, which was very close to 1. Meanwhile, the MAE of the $poly53$ model about the relationship between CIE a* values is 0.7195. Although there was a limited data set used for the models, the relationship between the CIE a* values of the single-colour fading effect and the CIE a* values of the two-colour mixed fading effect of the plasma-treated cotton fabrics was still highly closely related. It is mainly because the CIE a* values reflect mainly the magnitude of red and green of the fabric samples, i.e., +a* indicates red and -a* indicates green (Hunt & Pointer, 2011), which is easily reflected in the relationship between the single-colour fading effect and the two-colour mixed fading effect. It also means that the CIE a* values for the two-colour mixed fading effect might be calculated from the corresponding CIE a* values for the single-colour fading effect through the $poly53$ model.

7.3.3 The optimal Polynomial Regression model and fitting way for CIE b* values

Several polynomial regression models were fitted in order to investigate the relationship between the single-colour fading effect and the two-colour mixed fading effect of plasma-treated cotton fabrics. Equation (7.1) illustrated the relationship between the CIE b* values that needed to be explored when $i = 3$.

For the CIE b* values, the results of the fit were shown in Table 7.9. Based on the results, $poly22$ appeared to be the optimal polynomial regression model and LAR should be used to fit the data. R^2 and RMSE of this model were 0.9968 and 1.0192, respectively, and the values were superscripted with "*".

Table 7.9. The results of polynomial regression models fitted with different ways for the CIE b* values

Model	R^2			RMSE		
names	LS	LAR	Bisquare	LS	LAR	Bisquare
$poly11$	0.9732	0.9730	0.9702	2.9004	2.9147	3.0589
$poly12$	0.9862	0.9855	0.9886	2.1033	2.1523	1.9096
$poly13$	0.9892	0.9967	0.9908	1.8777	1.0296	1.7323
$poly14$	0.9896	0.9957	0.9918	1.8593	1.1983	1.6539
$poly15$	0.9899	0.9948	0.9915	1.8504	1.3278	1.6987
$poly21$	0.9753	0.9706	0.9731	2.8102	3.0656	2.9335
$poly22$	0.9866	0.9968*	0.9887	2.0803	1.0192*	1.9120
$poly23$	0.9894	0.9956	0.9907	1.8796	1.2114	1.7577
$poly24$	0.9906	0.9947	0.9921	1.7943	1.3405	1.6471
$poly25$	0.9911	0.9941	0.9921	1.7676	1.4400	1.6673
$poly31$	0.9816	0.9797	0.9805	2.4486	2.5708	2.5239
$poly32$	0.9882	0.9951	0.9896	1.9782	1.2750	1.8632
$poly33$	0.9897	0.9894	0.9907	1.8621	1.8899	1.7696

*poly*34	0.9910	0.9943	0.9921	1.7695	1.4071	1.6629
*poly*35	0.9916	0.9938	0.9922	1.7466	1.5022	1.6787
*poly*41	0.9843	0.9832	0.9833	2.2834	2.3607	2.3570
*poly*42	0.9897	0.9943	0.9906	1.8749	1.4007	1.7960
*poly*43	0.9913	0.9945	0.9921	1.7463	1.3886	1.6603
*poly*44	0.9915	0.9944	0.9924	1.7309	1.4101	1.6336
*poly*45	0.9922	0.9939	0.9928	1.7052	1.5043	1.6334
*poly*51	0.9846	0.9838	0.9838	2.2827	2.3389	2.3395
*poly*52	0.9902	0.9935	0.9914	1.8628	1.5176	1.7396
*poly*53	0.9919	0.9940	0.9927	1.7131	1.4734	1.6319
*poly*54	0.9922	0.9939	0.9928	1.7043	1.5034	1.6302
*poly*55	0.9922	0.9938	0.9928	1.7091	1.5235	1.6387

For the remaining polynomial regression models, with the exception of those named $poly11$, $poly21, poly31, poly41$ and $poly51$, which were relatively poorly fitted, all the models had similar regression effects to the optimal $poly22$, with R^2 essentially at 0.985 or above. It means that the regression effects of the polynomial regression model were relatively poorly fitted when the degree of y in the model was below 2. However, it was well-fitted when the degree of y in the model was 2 and above, as shown in Figure 7.9. The RMSE of the model showed a similar trend to the regression effects, as shown in Figure 7.10. There was a large RMSE of 2 to 3 when the degree of y in the model was below 2, which indicated a poor fit. However, there was a smaller RMSE of 0.9 and 2 when the degree of y in the model was 2 and above, which indicated a more accurate model fit. It also suggests that the relationship between the single-colour fading effect and the two-colour mixed fading effect about the CIE b* values of the fabric samples was difficult to explain by a simple linear relationship. In contrast, a polynomial regression model with a higher degree, i.e., when the degree of y in the model was 2 or more, would provide a better-fitted regression. Meanwhile, the model was most appropriate when the degree of y in the model was 2. In terms of fitting ways, LAR and Bisquare were better than

LS in general. Moreover, the fitting method LAR had better-fitted regression effects than Bisquare in most cases.
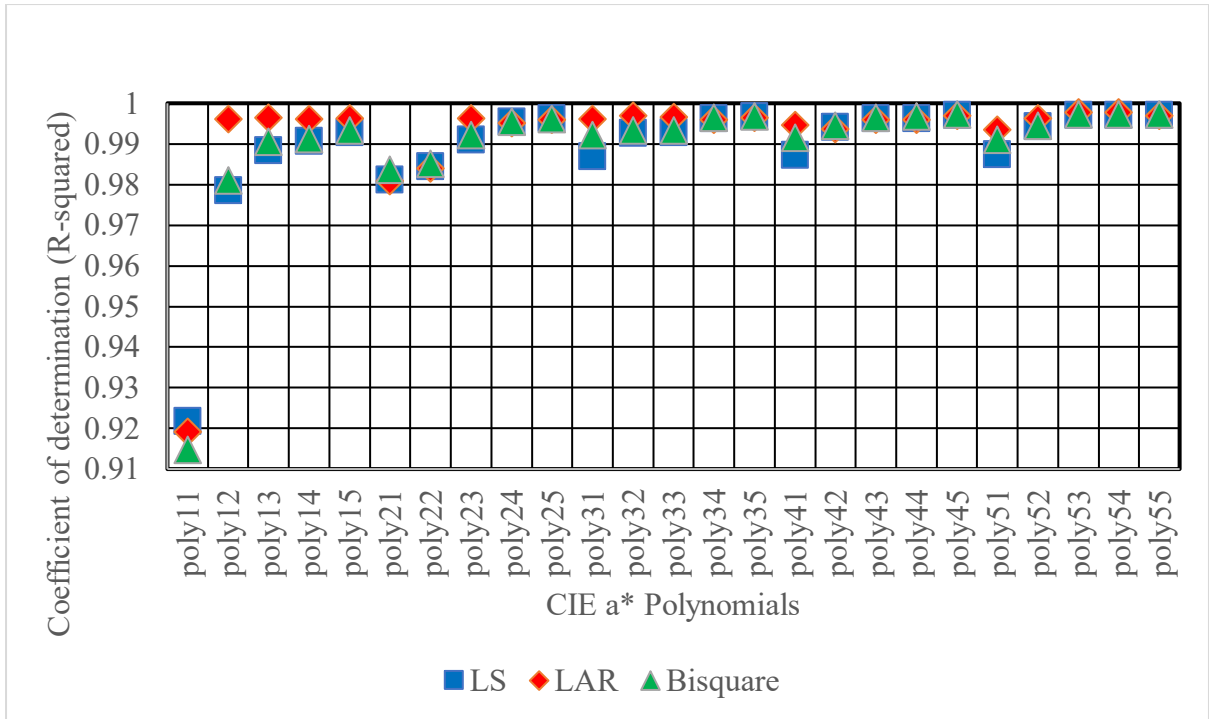

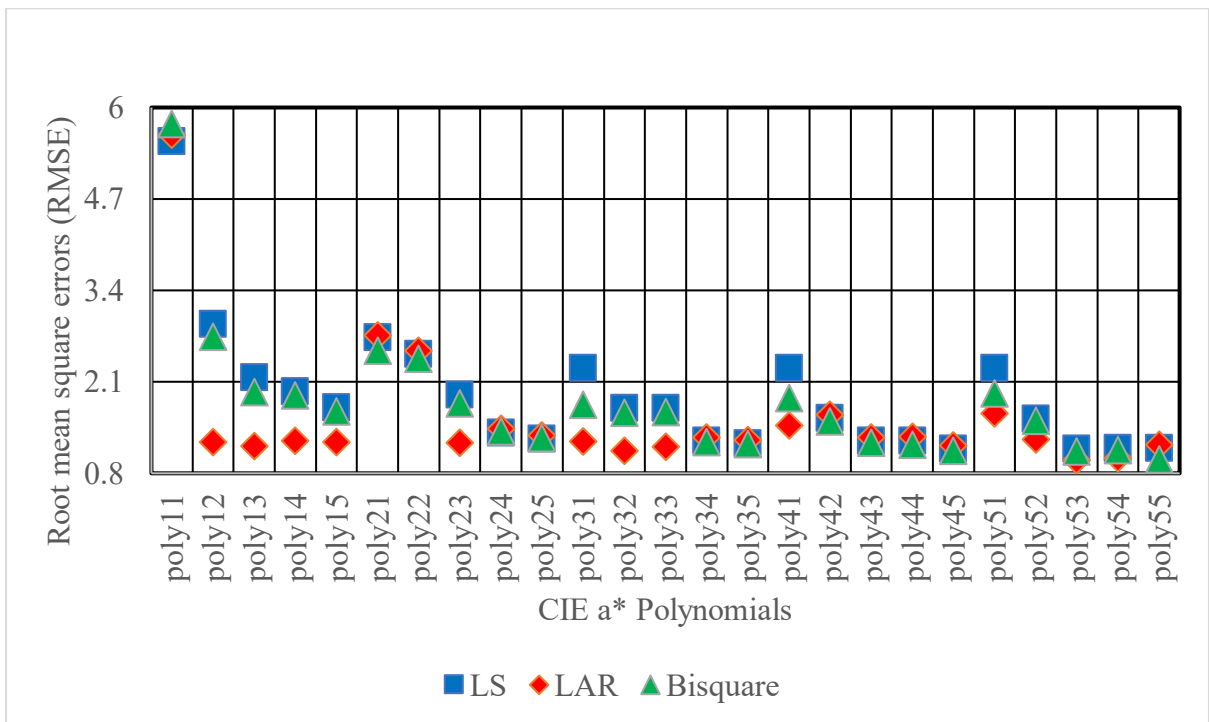Figure 7.9. The R^2 of polynomial regression models fitted with different ways for the CIE b* values

Figure 7.10. The RMSE of polynomial regression models fitted with different ways for the

CIE b* values

Therefore, the relationship between the CIE b* values of the fabric samples for the single-colour fading effect and the two-colour mixed fading effect could be represented by the $poly22$ polynomial regression model with the fitting method LAR, as shown in Table 7.10. Equation (7.29) showed the estimated coefficients with 95% confidence bounds for the $poly22$ polynomial regression model. Figure 7.11 showed a plot of the fitted curve of the $poly22$ model and Figure 7.12 showed a plot of the residuals of the $poly22$ model. It could be seen that the $poly22$ model can roughly fit the relationship between the CIE b* values of fabric samples with the single-colour fading effect and the two-colour mixed fading effect, with most models having an error of 2 or less between the predicted and actual values. However, a small number of larger errors existed between the predicted and actual values, ranging between 2 and 8.

141

Table 7.10. Estimated coefficients with 95% confidence bounds for the $poly22$ model

| Model names	The specific Equation	No.
CIE b*, $poly22$ model with the fitting way of LAR	$$f(x,y) = p_{00} + p_{10}\text{x} + p_{01}\text{y} + p_{20}x^2 + p_{11}xy + p_{02}y^2$$ Where x is normalized by mean -2.085 and standard deviation 9.093, and where y is normalized by mean 39.02 and standard deviation 37.93. Coefficients with 95% confidence bounds are as follows. $p_{00} =$ 11.51 (11.04, 11.97) $p_{10} =$ 1.858 (1.371, 2.345) $p_{01} =$ 15.56 (15.06, 16.07) $p_{20} =$ -0.6685 (-0.9627, -0.3743) $p_{11} =$ 0.3225 (-0.3831, 1.028) $p_{02} =$ -4.224 (-4.635, -3.814)	(7.29)
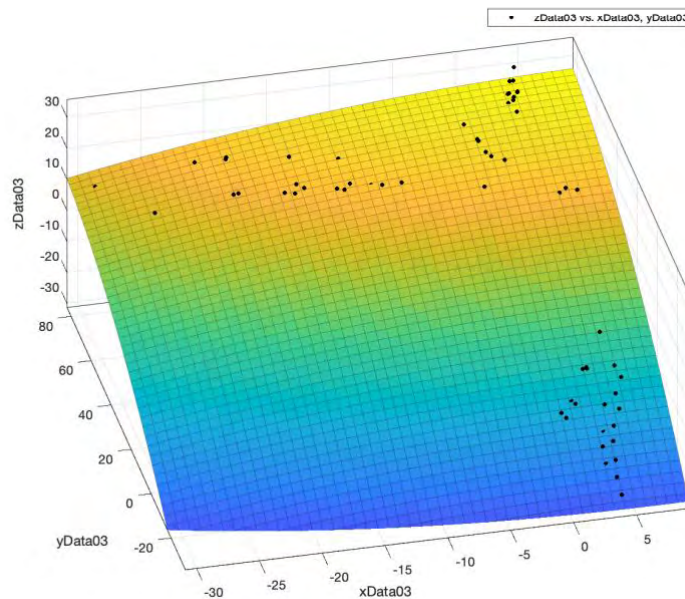
Figure 7.11. A plot of the fitted curve for the $poly22$ model about the relationship between CIE b* values
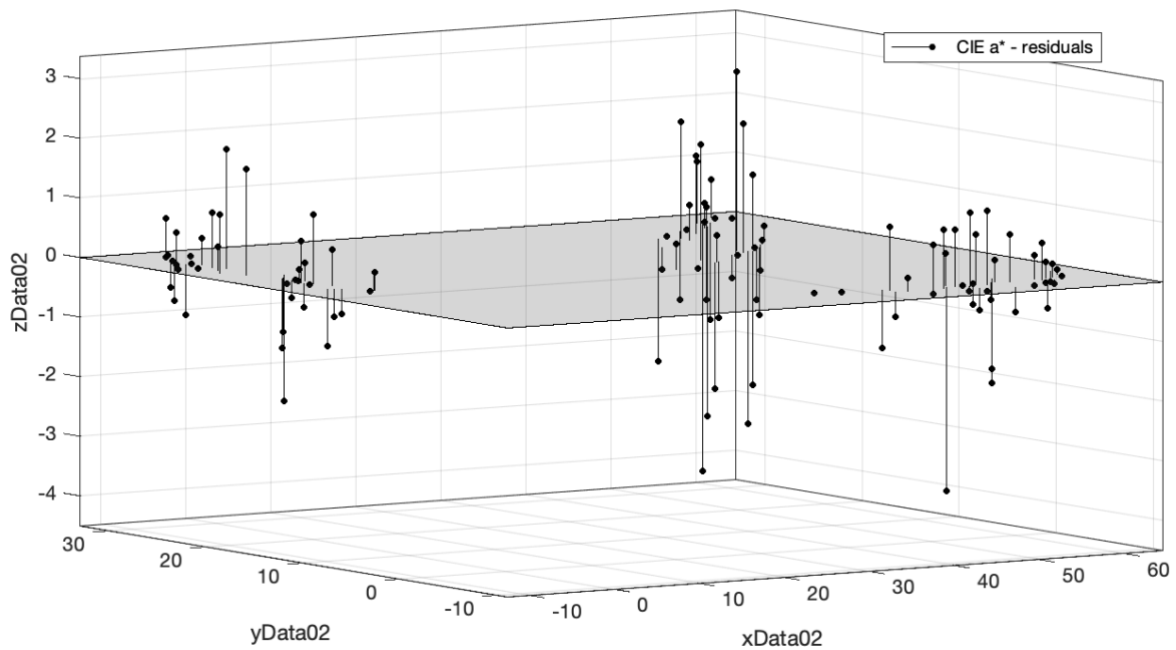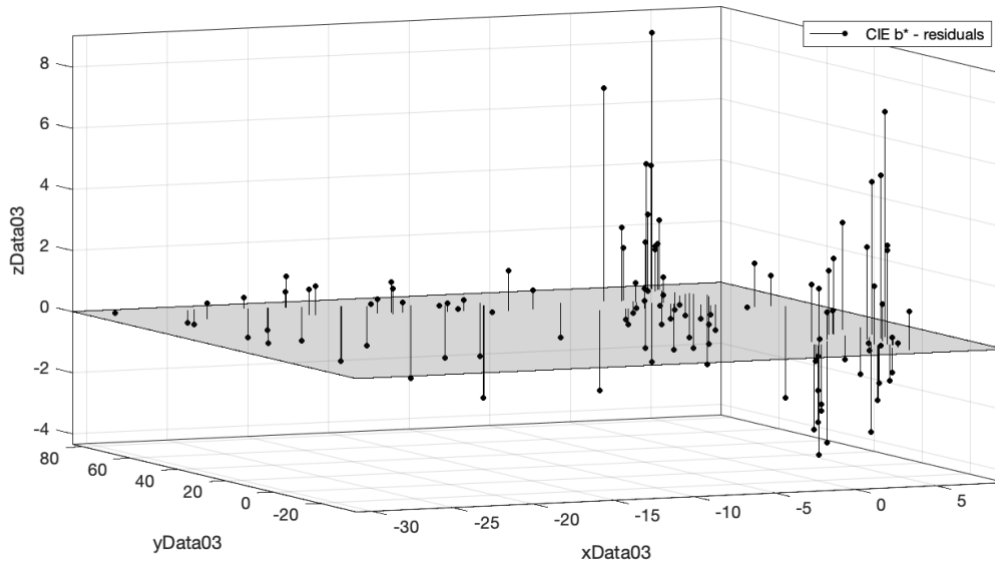
Figure 7.12. A residual plot for the $poly22$ model about the relationship between CIE b* values

Furthermore, the regression effects of the polynomial regression model with CIE b* values were high, i.e., 0.9968, which was very close to 1. Meanwhile, the MAE of the $poly22$ model about the relationship between CIE a* values was 1.4886. Although there was a limited data set used for the models, the relationship between the CIE b* values of the single-colour fading effect and the CIE b* values of the two-colour mixed fading effect of the plasma-treated cotton fabrics was still highly closely related. It was mainly because the degree of yellow and blue of a fabric sample was reflected by the CIE b* value, i.e. +b* values represent yellow and -b* values represent blue (Hunt & Pointer, 2011), which was easily reflected in the relationship between the single-colour fading effect and the two-colour mixed fading effect. Since the data set of $yData_{03}$ was CIE b* (RY1-RY38, RY1-RY38, RB1-RB38), which allowed for a better fitting regression when the degree of y in the model was 2 or higher. It also means that the CIE b* values for the two-colour mixed fading effect might be calculated from the corresponding CIE b* values for the single-colour fading effect through the $poly22$ model.

143

7.3.4 The optimal Polynomial Regression model and fitting way for K/S values

Several polynomial regression models were fitted to investigate the relationship between the single-colour fading effect and the two-colour mixed fading effect of plasma-treated cotton fabrics. Equation (7.1) illustrated the relationship between the K/S values that needed to be explored when $i = 4$.

For the K/S values, the results of the fit were shown in Table 7.11. Based on the results, $poly11$ appeared to be the optimal polynomial regression model and LAR should be used to fit the data. R^2 and RMSE of this model were 0.9922 and 3.8790, respectively, and the values were superscripted with "*".

Table 7.11. The results of polynomial regression models fitted with different ways for the K/S values

Model names	R^2			RMSE		
	LS	LAR	Bisquare	LS	LAR	Bisquare
$poly11$	0.8942	0.9922*	0.9185	14.3249	3.8790*	12.5724
$poly12$	0.8965	0.9814	0.9287	14.2980	6.0646	11.8653
$poly13$	0.9060	0.9717	0.9221	13.7552	7.5422	12.5203
$poly14$	0.9145	0.9123	0.9289	13.2406	13.4057	12.0752
$poly15$	0.9158	0.9566	0.9282	13.2661	9.5193	12.2505
$poly21$	0.8976	0.9816	0.9263	14.2229	6.0327	12.0628
$poly22$	0.8981	0.9755	0.9184	14.2495	6.9815	12.7549
$poly23$	0.9078	0.9617	0.9309	13.7499	8.8620	11.9004
$poly24$	0.9214	0.9561	0.9344	12.8794	9.6221	11.7643
$poly25$	0.9286	0.9526	0.9370	12.4633	10.1537	11.7078
$poly31$	0.9036	0.9710	0.9300	13.9272	7.6363	11.8694
$poly32$	0.9040	0.9601	0.9248	14.0310	9.0431	12.4202
$poly33$	0.9178	0.9616	0.9331	13.0473	8.9190	11.7681
$poly34$	0.9296	0.9555	0.9371	12.3145	9.7919	11.6350

*poly*35	0.9317	0.9495	0.9377	12.3750	10.6434	11.8181
*poly*41	0.9160	0.9651	0.9315	13.1221	8.4574	11.8507
*poly*42	0.9191	0.9548	0.9317	13.0702	9.7647	12.0069
*poly*43	0.9255	0.9529	0.9353	12.6660	10.0713	11.8044
*poly*44	0.9322	0.9550	0.9381	12.1448	9.8942	11.5988
*poly*45	0.9425	0.9390	0.9474	11.4793	11.8168	10.9729
*poly*51	0.9173	0.9574	0.9311	13.1471	9.4339	11.9968
*poly*52	0.9259	0.9508	0.9368	12.6906	10.3389	11.7206
*poly*53	0.9363	0.9529	0.9428	11.9531	10.2806	11.3287
*poly*54	0.9404	0.9536	0.9457	11.6848	10.3079	11.1485
*poly*55	0.9428	0.9546	0.9473	11.5045	10.2551	11.0460

For the remaining polynomial regression models, as the degree of the model was increasing, the regression effect of the model was decreasing. For example, when the degree of x or y in the model was 2 or more, the regression effect of the polynomial regression model was relatively poor because R^2 was essentially at 0.98 or below, as shown in Figure 7.13. The RMSE of the model showed a trend similar to the regression effect, as shown in Figure 7.14. When the degree of x or y in the model was 2 or more, there were large RMSEs of 5 to 15, which indicated a relatively poor fit. As far as the fitting approach is concerned, LAR overall outperforms Bisquare and LS. In addition, the Bisquare fitting method had a better regression effect than LS. Moreover, it also suggests that the relationship between the single-colour fading effect and the two-colour mixed fading effect between the K/S values of the fabric samples could be explained by a simple linear relationship. If a polynomial regression model of a high degree was used, it would instead lead to a decrease in the model fit.
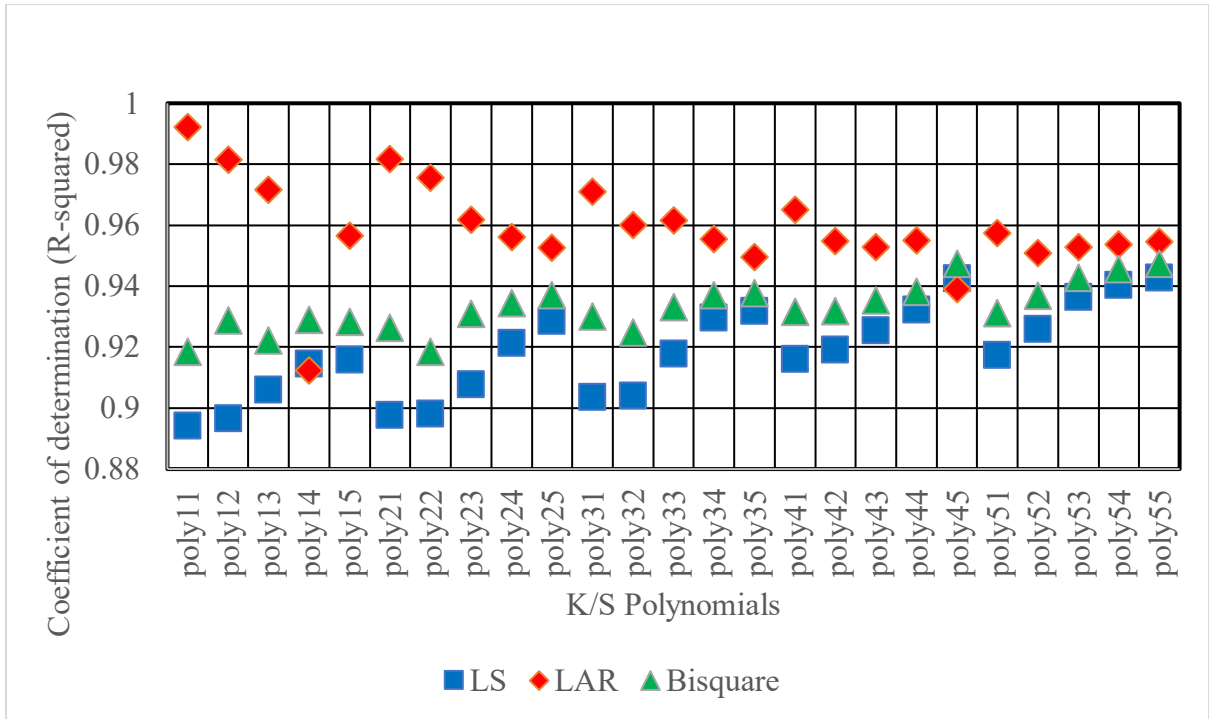
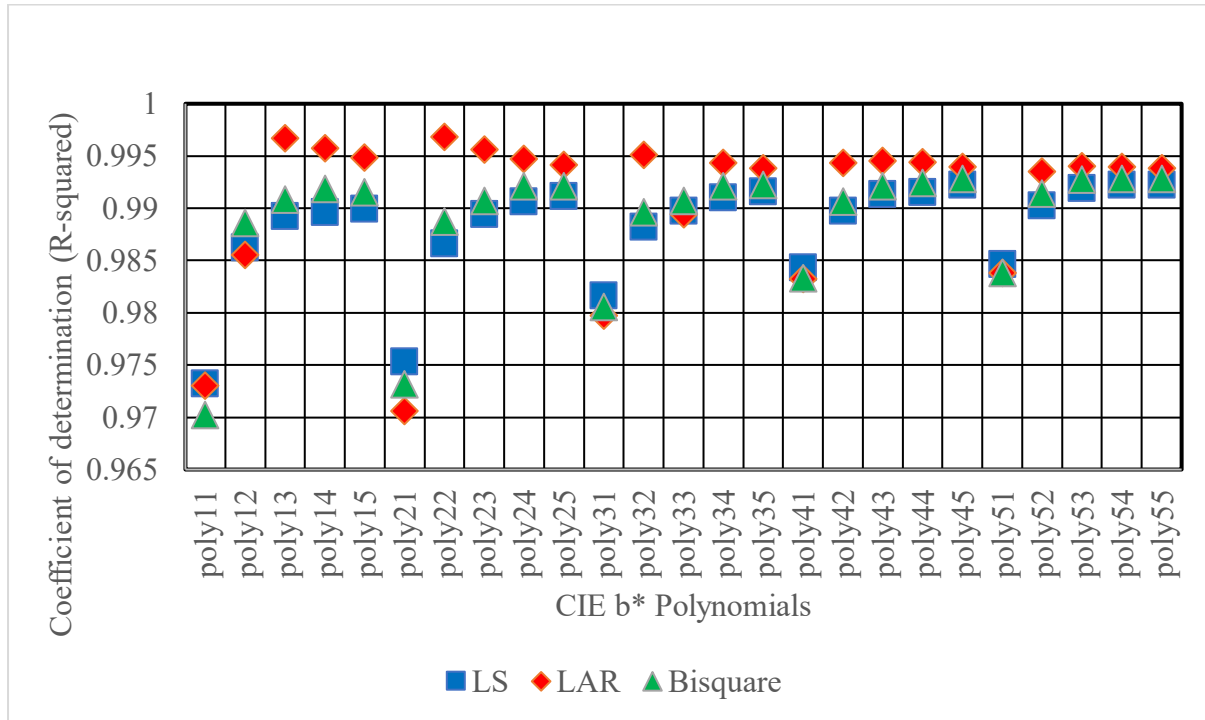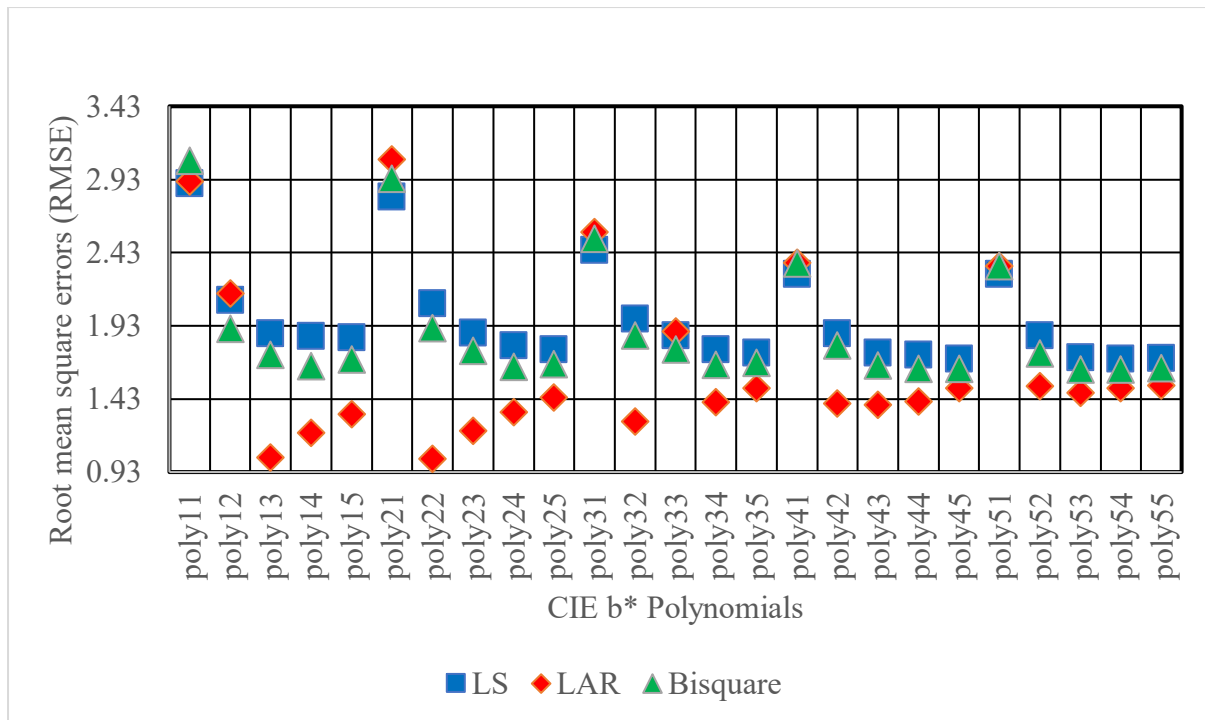Figure 7.13. The R^2 of polynomial regression models fitted with different ways for the K/S values
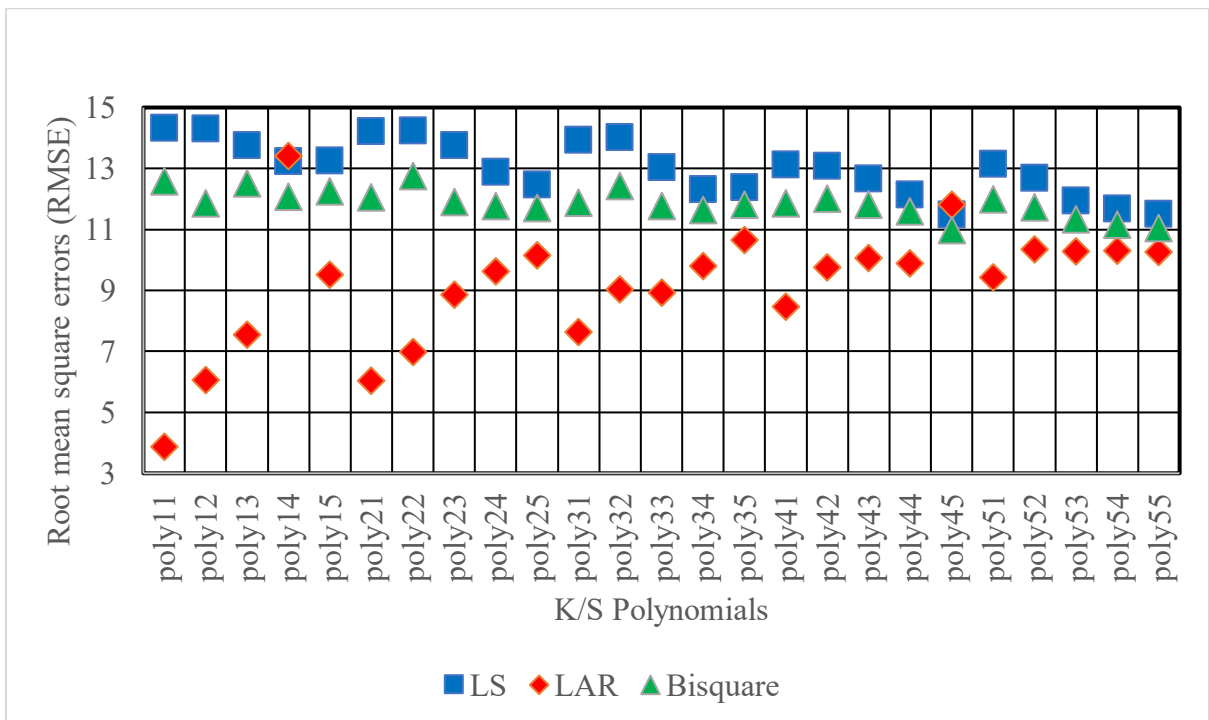
Figure 7.14. The RMSE of polynomial regression models fitted with different ways for the K/S values

Therefore, the relationship between the K/S values of the fabric samples for the single-colour fading effect and the two-colour mixed fading effect could be represented by the $poly11$ polynomial regression model with the fitting method LAR, as shown in Table 7.12. Equation (7.30) showed the estimated coefficients with 95% confidence bounds for the $poly11$ polynomial regression model. Figure 7.15 showed a plot of the fitted curve of the $poly11$ model and Figure 7.16 showed a plot of the residuals of the $poly11$ model. It could be seen that the $poly11$ model can roughly fit the relationship between the K/S values of fabric samples with the single-colour fading effect and the two-colour mixed fading effect, with most models having an error of 10 or less between the predicted and actual values. However, a small number of larger errors existed between the predicted and actual values, ranging between 20 and 60.

Table 7.12. Estimated coefficients with 95% confidence bounds for the $poly11$ model

| Model names	The specific Equation	No.
K/S, $poly11$ model with the fitting way of LAR	$$f(x,y) = p_{00} + p_{10}x + p_{01}y$$ Where x is normalized by mean 37.54 and standard deviation 20.2, and where y is normalized by mean 51.89 and standard deviation 33.58. Coefficients with 95% confidence bounds are as follows. p_{00} = 64.16 (63.44, 64.88) p_{10} = 43.83 (42.13, 45.54) p_{01} = -5.348 (-7.054, -3.642)	(7.30)
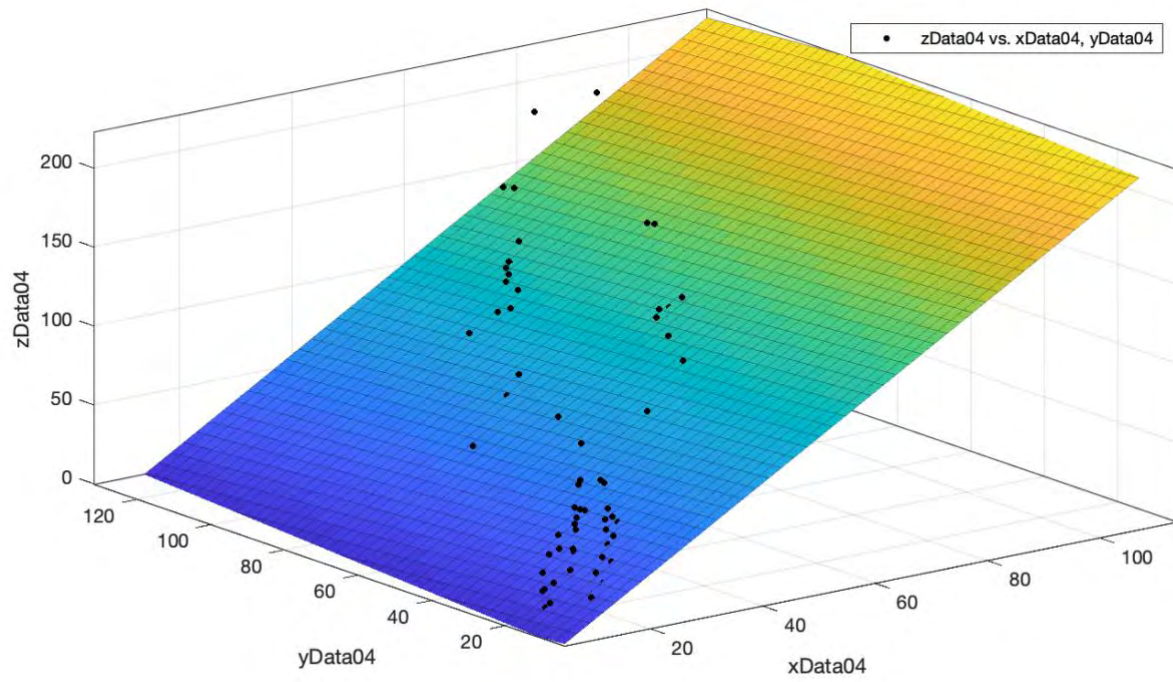
Figure 7.15. A plot of the fitted curve for the $poly11$ model about the relationship between K/S values
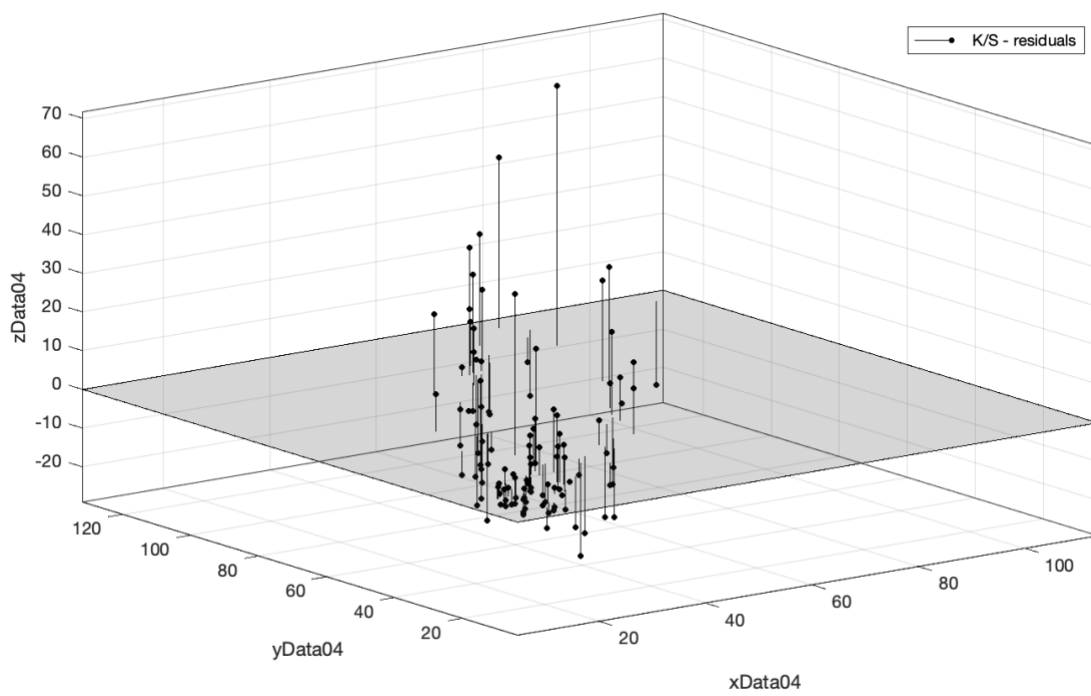
Figure 7.16. A residual plot for the $poly11$ model about the relationship between K/S values

Furthermore, the regression effects of the polynomial regression model with K/S values were high, i.e., 0.9922, which was very close to 1. The relationship between the K/S values of the single-colour fading effect and the K/S values of the two-colour mixed fading effect of the plasma-treated cotton fabrics was still highly closely related. The K/S values mainly reflect the dyeing performance, i.e., the shade of the surface colour of the fabric sample (Brinkworth, 1972). A higher K/S value indicates a darker surface colour, meaning better dyeing performance (Brinkworth, 1972). However, the MAE of the $poly11$ model about the relationship between K/S values was 10.0717, which might partly be due to the limited data set used for the model. Another possibility is that there are some errors in the measurement that cause some outliers in the model. It also means that the K/S values for the two-colour mixed fading effect might be calculated from the corresponding K/S values for the single-colour fading effect through the $poly11$ model, but there might be some errors in the predicted values.

7.3.5 Summary

In summary, the polynomial regression model could fit the relationship between the CIE L*a*b* values and K/S values of the fabric samples between the single-colour fading effect and the two-colour mixed fading effect. The corresponding models and fitting results were shown in Table 7.13.

Table 7.13. Fitting results of the polynomial regression models

	CIE L*	CIE a*	CIE b*	K/S
Model names	$poly54$	$poly53$	$poly22$	$poly11$
Fitting way	LS	LAR	LAR	LAR
R^2	0.9611	0.9978	0.9968	0.9922
RMSE	2.3019	0.9861	1.0192	3.8790
MAE	1.6796	0.7195	1.4886	10.0717

It could be seen that the relatively low R^2 of the polynomial regression model on the CIE L* values might reflect the fact that the relationship between the lightness levels of the single-colour fading effect and the two-colour mixed fading effect of the plasma-treated cotton fabrics was not highly relevant. In contrast, the R^2 of the polynomial regression models on CIE a* values, CIE b* values and K/S values were all higher than 0.99, indicating that the relationship between the single-colour fading effect and the two-colour mixed fading effect might be more reflected in the colour-related CIE a* and CIE b* values, or the K/S values related to the dyeing level.

As can be seen from Table 7.14, the CIE L* values of the two-colour mixed fading effect could be calculated from the corresponding CIE L* values of the single-colour fading effect by the $poly54$ model, but due to the relatively low regression effect of this polynomial regression model, large errors might occur in some values. For the CIE a* and CIE b* values, due to the low RMSE and MAE in their models, it means that the CIE a* and CIE b* values of the two-colour mixed fading effect could be calculated more accurately from the corresponding CIE a* and CIE b* values of the single-colour fading effect by the $poly53$ model and the $poly22$ model, respectively.

Table 7.14. Polynomial regression models for the CIE L*a*b* and K/S values

Model names	The specific Equation	No.
CIE L*, $poly54$ model with the fitting way of LS	$\begin{aligned} f(x,y) = {}& 57.15 + 10.97x + 1.384y - 13.05x^2 - 6.31xy \\ & - 4.789y^2 - 4.668x^3 + 35.42x^2y - 16.85xy^2 \\ & + 1.853y^3 + 4.757x^4 - 4.187x^3y - 5.652x^2y^2 \\ & + 8.221xy^3 + 1.154y^4 + 1.603x^5 - 12.32x^4y \\ & + 18.32x^3y^2 - 15.16x^2y^3 + 5.955xy^4 \end{aligned}$	(7.27)

	Where x is normalized by mean 59.32 and standard deviation 6.958, and where y is normalized by mean 69.86 and standard deviation 10.51.	
CIE a*, $poly53$ model with the fitting way of LAR	$$\begin{aligned} f(x,y) =\ & 21.43 + 30.86x - 0.7957y - 4.67x^2 + 4.419xy \\ & - 12.25y^2 - 5.9x^3 + 25.04x^2y - 0.4626xy^2 \\ & - 4.219y^3 + 1.067x^4 + 6.251x^3y + 11.86x^2y^2 \\ & - 0.6708xy^3 - 1.603x^5 - 10.37x^4y - 3.164x^3y^2 \\ & - 3.118x^2y^3 \end{aligned}$$ Where x is normalized by mean 30.06 and standard deviation 26.56, and where y is normalized by mean 11.69 and standard deviation 13.98.	(7.28)
CIE b*, $poly22$ model with the fitting way of LAR	$$\begin{aligned} f(x,y) =\ & 11.51 + 1.858x + 15.56y - 0.6685x^2 + 0.3225xy \\ & - 4.224y^2 \end{aligned}$$ Where x is normalized by mean -2.085 and standard deviation 9.093, and where y is normalized by mean 39.02 and standard deviation 37.93.	(7.29)
K/S, $poly11$ model with the fitting way of LAR	$$f(x,y) = 64.16 + 43.83x - 5.348y$$ Where x is normalized by mean 37.54 and standard deviation 20.2, and where y is normalized by mean 51.89 and standard deviation 33.58.	(7.30)

Moreover, the higher MAE and RMSE values of the $poly11$ model about the K/S values might be due to the limited data. Another possibility is that they are prone to some small deviations during the colour measurement process. Fabric characteristics, including uniformity of dyeing, the flatness of the fabric, structure and surface texture, might lead to some errors in the K/S values reflecting dyeing performance (Özkan et al., 2018; Tang et al., 2018). This also means that the K/S values of the two-colour mixed fading effect might be calculated from the

corresponding K/S values of the single-colour fading effect by the $poly11$ model, but there might be some errors in the predicted values.

7.4 Conclusions

In this study, polynomial regression models were used to investigate the relationship between the single-colour fading effect and the two-colour mixed fading effect of plasma-treated cotton fabrics. The colour characteristics of the two-colour mixed fading effect of plasma-treated cotton fabrics could be predicted based on the known single-colour fading effect of plasma-treated cotton fabrics in most cases.

It was found that the relatively low R^2 of the polynomial regression model regarding the CIE L* values might reflect the fact that the relationship between the lightness levels of the single-colour fading effect and the two-colour mixed fading effect of plasma-treated cotton fabrics is not highly relevant. In contrast, the R^2 of the polynomial regression models for CIE a* values, CIE b* values and K/S values were all above 0.99, suggesting that the relationship between the single-colour fading effect and the two-colour mixed fading effect might be more reflected in the colour-related CIE a* and CIE b* values, or in the K/S values related to the dyeing level.

For the polynomial regression models of CIE L*a*b* and K/S values, it was found that the CIE L* values for the two-colour mixed fading effect could be calculated from the corresponding CIE L* values for the single-colour fading effect by means of the $poly54$ model with the LS fitting way, but due to the relatively low regression effect of this polynomial regression model, large errors might occur in some values. Furthermore, for the CIE a* and CIE b* values, the fact that they both had low RMSE and MAE and that R^2 were all close to 1 means that the CIE a* and CIE b* values for the two-colour mixed fading effect could be

obtained more accurately from the corresponding CIE a* and CIE b* values for the single-colour fading effect by the $poly53$ and $poly22$ models with the LAR fitting way, respectively. In addition, the higher MAE and RMSE values for the $poly11$ model with the LAR fitting way about the K/S values might be caused by limited data. Another possibility is that they are influenced by fabric properties and are prone to some small deviations during the colour measurement phase. Although the K/S values for the two-colour mixed fading effect could be calculated from the corresponding K/S values for the single-colour fading effect by the $poly11$ model with the LAR fitting way, there might be some large errors in the predicted values.

Overall, the polynomial regression models provided a suitable fit between the single-colour fading effect and the two-colour mixed fading effect of plasma-treated cotton fabrics. It might be used as a reference for manufacturers of plasma-treated faded cotton fabrics to facilitate the development of intelligence and digitalisation within the cotton processing industry.

Chapter 8 Conclusions and Suggestions for Future Research

8.1 Conclusions

Plasma treatment, as a sustainable technology, can be used to complement traditional fading methods. However, the application of plasma treatment to industrial-scale fading results may suffer from inconsistent fading results as the mechanisms by which variations in plasma treatment parameters affect fading results remain unclear, meaning that plasma treatment parameters need to be continuously adjusted to obtain accurate fading results.

Given these challenges and complexities, our resolution involves harnessing the capabilities of artificial intelligence, particularly artificial neural networks, to delve into and comprehend the relationship between plasma treatment parameters and fading effects. The current investigation employed Bayesian regulated neural network (BRNN) models to simulate and forecast the influence of various plasma treatment parameters on cotton fabric fading effects. Our examination focused on reactive dyes, sulphur dyes, as well as reactive dyes of two colours, endeavouring to explore the specific correlations between plasma treatment parameters and the discolouration effects on cotton fabric. In this manner, we were able to adjust plasma treatment parameters based on projected fading effects, thereby optimizing industrial-scale production processes. Furthermore, we investigated whether polynomial regression models could approximate the relationship between single colour fading effects and two-colour mixed fading effects. These discoveries will enable manufacturers to predict and control the fading effects of cotton fabric with enhanced accuracy, consequently augmenting production efficiency and diminishing production costs.

In Chapter 4, the study focused on investigating the relationship between various plasma treatment parameters and the fading effect of cotton fabrics monochromatically dyed with

154

reactive dyes. The findings demonstrate that the BRNN model had the capability to accurately predict the colour measurements of yellow and red reactive dyed cotton fabrics after plasma fading treatment, while exhibiting a slight error in predicting the colour measurements of blue reactive dyed cotton fabrics after plasma fading treatment. Overall, the colour differences between the predicted and actual colours were small, with approximately 87.5% to 91.67% of the predicted colours falling within an acceptable range, indicating that the majority of the predictions were either acceptable or had imperceptible colour differences.

In Chapter 5, the research was conducted to investigate the correlation between various plasma treatment parameters and the fading effect of cotton fabrics dyed with monochromatic sulphur dyes. The results indicate that the BRNN model has the capability to precisely predict the colour measurements of yellow, red, and blue sulphur-dyed cotton fabrics after plasma fading treatment with negligible errors. In general, the discrepancy between the actual and predicted colours was minor, and the percentage of predicted colours within an acceptable range was approximately 95.83%, implying that most of the predictions were accurate or the colour differences were insignificant and difficult to discern.

In Chapter 6, as fashionable clothing may involve different colour combinations, the study investigates the correlation between various plasma treatment parameters and the fading effect of cotton fabrics dyed with a two-colour reactive dye mix. The results show that the BRNN model is able to accurately predict the fading effect of different combinations of plasma parameters on two-colour mixed dyed cotton fabrics, with over 80% of predicted colours falling within the acceptable range.

Furthermore, in Chapter 7, since two-colour dyestuffs are produced by mixing monochromatic dyestuffs in equal concentrations, the method of predicting the colour characteristics of the fading effect of two-colour plasma-treated cotton fabrics mixed from the known monochromatic fading effect of plasma-treated cotton fabrics is further explored. It was discovered that the relatively low R^2 of the polynomial regression model for the CIE L* values may indicate that the correlation between the lightness levels of the monochrome fading effect and the two-colour mixed fading effect of plasma-treated cotton fabrics is not high. Conversely, the R^2 of the polynomial regression models for the CIE a* values, CIE b* values, and K/S values were all above 0.99, indicating that the correlation between the monochrome fading effect and the two-colour mixed fading effect may be more reflected in the colour-related CIE a* and CIE b* values, or in the K/S values related to the dyeing level.

In summary, the BRNN model with 10-fold cross-validation constructed through a modular approach used in this thesis is an effective artificial intelligence technique that can simulate the relationship between the plasma treatment process and the fading effect on cotton fabrics. This provides a useful tool for dyers to adjust the parameter settings of the plasma machine before treating cotton fabrics with plasma, ultimately reducing the cost and time spent in the trial and error process. Additionally, the polynomial regression model can approximate the relationship between the single-colour fading effect and the two-colour mixed fading effect of plasma-treated cotton fabrics, which provides a valuable reference for manufacturers using artificial intelligence techniques in combination with plasma-treated fading.

One limitation of this study is that some errors still exist in the predicted values when compared to the actual values, particularly in the predicted K/S values. These errors may be attributed to

156

several factors, such as variations in colour measurements, fabric properties, a limited sample size, and random partitioning of the model training set.

8.2 Suggestions for Future Research

In future research, the following aspects will be further explored:

i) Improving the accuracy and stability of the model by increasing the sample size of cotton fabrics after plasma fading treatment.

ii) Exploring the use of different artificial intelligence techniques to further enhance the prediction accuracy and robustness of the model.

iii) Using the BRNN model to generate and predict various combinations of plasma treatment parameters to provide a detailed analysis of fading colour effects.

iv) Further utilizing artificial intelligence methods to reverse predict the correlation between fading effects and combinations of plasma treatment parameters, contributing to the development of intelligence and digitization in the field of garment fading.

v) Applying the model to the commercial side by analyzing cost and consumption (such as water, treatment time, oxygen concentration, etc.) to find the most economical way to achieve a specific fading effect.

vi) Integrating the relevant models into a client-side interface with a user-friendly design to facilitate use by dyers.

Appendix A

The arrangements for fading by plasma treatment of (1) reactive dyed fabric samples, (2) sulphur dyed fabric samples and (3) two-colour mixed dyed fabric samples are briefly described through Table A.1, Table A.2 and Table A.3.

Table A.1. Arrangement of fading of reactive dye-dyed fabric samples by plasma treatment

Types of fabric	No.	Colour Depth	Air (Oxygen) Concentration (%)	Water Content (%)	Treatment time (min)
RR/RB/RY	Control	1.5	0	0	0
	1	1.5	10	35	10
	2	1.5	10	35	20
	3	1.5	10	35	30
	4	1.5	10	45	10
	5	1.5	10	45	20
	6	1.5	10	45	30
	7	1.5	30	35	10
	8	1.5	30	35	20
	9	1.5	30	35	30
	10	1.5	30	45	10
	11	1.5	30	45	20
	12	1.5	30	45	30
	13	1.5	50	35	10
	14	1.5	50	35	20
	15	1.5	50	35	30
	16	1.5	50	45	10
	17	1.5	50	45	20
	18	1.5	50	45	30
	19	1.5	70	35	10
	20	1.5	70	35	20
	21	1.5	70	35	30
	22	1.5	70	45	10

	23	1.5	70	45	20
	24	1.5	70	45	30
RR/RB/RY	Control	2.5	0	0	0
	25	2.5	10	35	10
	26	2.5	10	35	20
	27	2.5	10	35	30
	28	2.5	10	45	10
	29	2.5	10	45	20
	30	2.5	10	45	30
	31	2.5	30	35	10
	32	2.5	30	35	20
	33	2.5	30	35	30
	34	2.5	30	45	10
	35	2.5	30	45	20
	36	2.5	30	45	30
	37	2.5	50	35	10
	38	2.5	50	35	20
	39	2.5	50	35	30
	40	2.5	50	45	10
	41	2.5	50	45	20
	42	2.5	50	45	30
	43	2.5	70	35	10
	44	2.5	70	35	20
	45	2.5	70	35	30
	46	2.5	70	45	10
	47	2.5	70	45	20
	48	2.5	70	45	30
RR/RB/RY	Control	0.5	0	0	0
	49	0.5	10	35	10
	50	0.5	10	35	20
	51	0.5	10	35	30
	52	0.5	10	45	10

	53	0.5	10	45	20
	54	0.5	10	45	30
	55	0.5	30	35	10
	56	0.5	30	35	20
	57	0.5	30	35	30
	58	0.5	30	45	10
	59	0.5	30	45	20
	60	0.5	30	45	30
	61	0.5	50	35	10
	62	0.5	50	35	20
	63	0.5	50	35	30
	64	0.5	50	45	10
	65	0.5	50	45	20
	66	0.5	50	45	30
	67	0.5	70	35	10
	68	0.5	70	35	20
	69	0.5	70	35	30
	70	0.5	70	45	10
	71	0.5	70	45	20
	72	0.5	70	45	30

Table A.2. Arrangement for fading of sulphur-dyed fabric samples by plasma treatment

Types of fabric	No.	Colour Depth	Air (Oxygen) Concentration (%)	Water Content (%)	Treatment time (min)
	Control	1.5	0	0	0
	1	1.5	10	35	10
	2	1.5	10	35	20
	3	1.5	10	35	30
SR/SB/SY	4	1.5	10	45	10
	5	1.5	10	45	20
	6	1.5	10	45	30
	7	1.5	30	35	10

	8	1.5	30	35	20
	9	1.5	30	35	30
	10	1.5	30	45	10
	11	1.5	30	45	20
	12	1.5	30	45	30
	13	1.5	50	35	10
	14	1.5	50	35	20
	15	1.5	50	35	30
	16	1.5	50	45	10
	17	1.5	50	45	20
	18	1.5	50	45	30
	19	1.5	70	35	10
	20	1.5	70	35	20
	21	1.5	70	35	30
	22	1.5	70	45	10
	23	1.5	70	45	20
	24	1.5	70	45	30
SR/SB/SY	Control	2.5	0	0	0
	25	2.5	10	35	10
	26	2.5	10	35	20
	27	2.5	10	35	30
	28	2.5	10	45	10
	29	2.5	10	45	20
	30	2.5	10	45	30
	31	2.5	30	35	10
	32	2.5	30	35	20
	33	2.5	30	35	30
	34	2.5	30	45	10
	35	2.5	30	45	20
	36	2.5	30	45	30
	37	2.5	50	35	10
	38	2.5	50	35	20

	39	2.5	50	35	30
	40	2.5	50	45	10
	41	2.5	50	45	20
	42	2.5	50	45	30
	43	2.5	70	35	10
	44	2.5	70	35	20
	45	2.5	70	35	30
	46	2.5	70	45	10
	47	2.5	70	45	20
	48	2.5	70	45	30
SR/SB/SY	Control	0.5	0	0	0
	49	0.5	10	35	10
	50	0.5	10	35	20
	51	0.5	10	35	30
	52	0.5	10	45	10
	53	0.5	10	45	20
	54	0.5	10	45	30
	55	0.5	30	35	10
	56	0.5	30	35	20
	57	0.5	30	35	30
	58	0.5	30	45	10
	59	0.5	30	45	20
	60	0.5	30	45	30
	61	0.5	50	35	10
	62	0.5	50	35	20
	63	0.5	50	35	30
	64	0.5	50	45	10
	65	0.5	50	45	20
	66	0.5	50	45	30
	67	0.5	70	35	10
	68	0.5	70	35	20
	69	0.5	70	35	30

	70	0.5	70	45	10
	71	0.5	70	45	20
	72	0.5	70	45	30

Table A.3. Arrangement for fading of two-colour mixed dyed fabric samples by plasma treatment

Types of fabric	No.	Colour Depth	Air (Oxygen) Concentration (%)	Water Content (%)	Treatment time (min)
RN/RG/RV	Control	0.5	0	0	0
	1	0.5	10	35	10
	2	0.5	10	35	20
	3	0.5	10	35	30
	4	0.5	10	45	10
	5	0.5	10	45	20
	6	0.5	10	45	30
	7	0.5	30	35	10
	8	0.5	30	35	20
	9	0.5	30	35	30
	10	0.5	30	45	10
	11	0.5	30	45	20
	12	0.5	30	45	30
	13	0.5	50	35	10
	14	0.5	50	35	20
	15	0.5	50	35	30
	16	0.5	50	45	10
	17	0.5	50	45	20
	18	0.5	50	45	30
RN/RG/RV	Control	1.5	0	0	0
	19	1.5	10	35	10
	20	1.5	10	35	20
	21	1.5	10	35	30
	22	1.5	10	45	10

	23	1.5	10	45	20
	24	1.5	10	45	30
	25	1.5	30	35	10
	26	1.5	30	35	20
	27	1.5	30	35	30
	28	1.5	30	45	10
	29	1.5	30	45	20
	30	1.5	30	45	30
	31	1.5	50	35	10
	32	1.5	50	35	20
	33	1.5	50	35	30
	34	1.5	50	45	10
	35	1.5	50	45	20
	36	1.5	50	45	30
RN/RG/RV	Control	3	0	0	0
	37	3	10	35	10
	38	3	10	35	20
	39	3	10	35	30
	40	3	10	45	10
	41	3	10	45	20
	42	3	10	45	30
	43	3	30	35	10
	44	3	30	35	20
	45	3	30	35	30
	46	3	30	45	10
	47	3	30	45	20
	48	3	30	45	30
	49	3	50	35	10
	50	3	50	35	20
	51	3	50	35	30
	52	3	50	45	10
	53	3	50	45	20

	54	3	50	45	30

References

Abd Jelil, R., Zeng, X., Koehl, L., & Perwuelz, A. (2013). Modeling plasma surface modification of textile fabrics using artificial neural networks. *Engineering Applications of Artificial Intelligence*, *26*(8), 1854-1864. https://doi.org/10.1016/j.engappai.2013.03.015

Abiodun, O. I., Jantan, A., Omolara, A. E., Dada, K. V., Umar, A. M., Linus, O. U., Arshad, H., Kazaure, A. A., Gana, U., & Kiru, M. U. (2019). Comprehensive review of artificial neural network applications to pattern recognition. *IEEE Access*, *7*, 158820-158846. https://doi.org/10.1109/ACCESS.2019.2945545

Agarwal, S., Singh, A. P., & Mathur, S. (2023). Removal of COD and color from textile industrial wastewater using wheat straw activated carbon: an application of response surface and artificial neural network modeling. *Environmental Science and Pollution Research*, 1-22. https://doi.org/10.1007/s11356-022-25066-2

Almodarresi, E. S. Y., Mokhtari, J., Almodarresi, S. M. T., Nouri, M., & Nateri, A. S. (2013). A scanner based neural network technique for color matching of dyed cotton with reactive dye. *Fibers and Polymers*, *14*(7), 1196-1202. https://doi.org/10.1007/s12221-013-1196-y

Atav, R., Yüksel, M. F., Özkaya, S., & Buğdaycı, B. (2022). The use of ozone technology for color stripping and obtaining vintage effect on reactive dyed cotton fabrics. *Journal of Natural Fibers*, *19*(13), 6648-6658. https://doi.org/10.1080/15440478.2021.1929653

Ben, F. A., & Jaouachi, B. (2021). Effects of ozone treatment on denim garment properties. *Coloration Technology*, *137*(6), 678-688. https://doi.org/10.1111/cote.12568

Berkner, L. V., & Marshall, L. (1965). On the origin and rise of oxygen concentration in the Earth's atmosphere. *Journal of Atmospheric Sciences*, *22*(3), 225-261. https://doi.org/10.1175/1520-0469(1965)022<0225:OTOARO>2.0.CO;2

Boominathan, S., V, K., & Balakrishanan, S. (2022). Optimization of process parameters on color strength and antimicrobial activities of cotton fabric dyed with Rubia cordifolia extract. *Journal of Natural Fibers*, *19*(7), 2414-2428. https://doi.org/10.1080/15440478.2020.1818347

Boukouvalas, D. T., Rosa, J. M., Belan, P. A., Tambourgi, E. B., Santana, J. C. C., & de Araújo, S. A. (2021). Optimization of cotton dyeing with reactive dyestuff using multiobjective evolutionary algorithms. *Chemometrics and Intelligent Laboratory Systems*, *219*, 1-9. https://doi.org/10.1016/j.chemolab.2021.104441

Brinkworth, B. (1972). Interpretation of the Kubelka-Munk coefficients in reflection theory. *Applied Optics*, *11*(6), 1434-1435. https://doi.org/10.1364/AO.11.001434

Bulut, M. O., & Sana, N. H. (2018). Modification of woolen fabric with plasma for a sustainable production. *Fibers and Polymers*, *19*(9), 1887-1897. https://doi.org/10.1007/s12221-018-8488-1

Carneiro, N., Souto, A. P., Silva, E., Marimba, A., Tena, B., Ferreira, H., & Magalhaes, V. (2001). Dyeability of corona‑treated fabrics. *Coloration Technology*, *117*(5), 298-302. https://doi.org/10.1111/j.1478-4408.2001.tb00079.x

Chai, T., & Draxler, R. R. (2014). Root mean square error (RMSE) or mean absolute error (MAE)?–Arguments against avoiding RMSE in the literature. *Geoscientific Model Development*, *7*(3), 1247-1250. https://doi.org/10.5194/gmd-7-1247-2014

Chakraborty, A., Kaur, P. D., & Chakraborty, J. (2019). Automation in colouration technology to predict dyeing parameters for desired shade and fastness. *Indian Journal of Fibre & Textile Research (IJFTR)*, *44*(4), 450-458. https://doi.org/10.56042/ijftr.v44i4.21976

Chan, C. M., Ko, T. M., & Hiraoka, H. (1996). Polymer surface modification by plasmas and photons. *Surface Science Reports*, *24*(1-2), 1-54. https://doi.org/10.1016/0167-5729(96)80003-3

Chaouch, S., Moussa, A., Ben Marzoug, I., & Ladhari, N. (2019a). Application of ant colony optimization to color matching of dyed cotton fabrics with direct dyestuffs mixtures. *Color Research & Application*, *44*(4), 556-567. https://doi.org/10.1002/col.22363

Chaouch, S., Moussa, A., Ben Marzoug, I., & Ladhari, N. (2019b). Colour recipe prediction using ant colony algorithm: principle of resolution and analysis of performances. *Coloration Technology*, *135*(5), 349-360. https://doi.org/10.1111/cote.12409

Chaouch, S., Moussa, A., Ben Marzoug, I., & Ladhari, N. (2020). Application of genetic algorithm to color recipe formulation using reactive and direct dyestuffs mixtures. *Color Research & Application*, *45*(5), 896-910. https://doi.org/10.1002/col.22533

Chaouch, S., Moussa, A., Ben Marzoug, I., & Ladhari, N. (2022). Study of C.I. Reactive Yellow 145, C.I. Reactive Red 238 and C.I. Reactive Blue 235 dyestuffs in order to use them in color formulation. Part 3: Application of ant colony and genetic algorithms for color recipe prediction. *The Journal of The Textile Institute*, 1-12. https://doi.org/10.1080/00405000.2022.2131353

Cheung, H., Kan, C. W., Yuen, C., Yip, J., & Law, M. (2013). Colour fading of textile fabric by plasma treatment. *Journal of Textiles*, *2013*, 1-4. https://doi.org/10.1155/2013/214706

Cheung, H. F. C. (2018). *Non-aqueous color fading effect on cotton with industrial application* [Doctoral dissertation, The Hong Kong Polytechnic University]. https://theses.lib.polyu.edu.hk/bitstream/200/9543/1/991022142754703411.pdf

Chicco, D., Warrens, M. J., & Jurman, G. (2021). The coefficient of determination R-squared is more informative than SMAPE, MAE, MAPE, MSE and RMSE in regression analysis evaluation. *PeerJ Computer Science*, *7*, 1-24. https://doi.org/10.7717/peerj-cs.623

Choudhury, T. A., Berndt, C., & Man, Z. (2015). Modular implementation of artificial neural network in predicting in-flight particle characteristics of an atmospheric plasma spray process. *Engineering Applications of Artificial Intelligence*, *45*, 57-70. https://doi.org/10.1016/j.engappai.2015.06.015

Coit, D. W., Jackson, B. T., & Smith, A. E. (1998). Static neural network process models: Considerations and case studies. *International Journal of Production Research*, *36*(11), 2953-2967. https://doi.org/10.1080/002075498192229

Correia, J., Mathur, K., Bourham, M., Oliveira, F. R., Siqueira Curto Valle, R. D. C., Valle, J. A. B., & Seyam, A.-F. M. (2021). Surface functionalization of greige cotton knitted fabric through plasma and cationization for dyeing with reactive and acid dyes. *Cellulose*, *28*(15), 9971-9990. https://doi.org/10.1007/s10570-021-04143-8

Dascalu, T., Acosta-Ortiz, S. E., Ortiz-Morales, M., & Compean, I. (2000). Removal of the indigo color by laser beam–denim interaction. *Optics and Lasers in Engineering*, *34*(3), 179-189. https://doi.org/10.1016/S0143-8166(00)00087-7

Doan, C. D., & Liong, S. Y. (2004, July 5-8). Generalization for multilayer neural network bayesian regularization or early stopping. Proceedings of Asia Pacific association of hydrology and water resources 2nd conference, Singapore.

Farooq, A., Ali, S., Abbas, N., Fatima, G. A., & Ashraf, M. A. (2013). Comparative performance evaluation of conventional bleaching and enzymatic bleaching with glucose oxidase on knitted cotton fabric. *Journal of Cleaner Production*, *42*, 167-171. https://doi.org/10.1016/j.jclepro.2012.10.021

Farooq, A., Irshad, F., Azeemi, R., & Iqbal, N. (2021). Prognosticating the shade change after softener application using artificial neural networks. *Autex Research Journal*, *21*(1), 79-84. https://doi.org/10.2478/aut-2020-0019

Farooq, A., Irshad, F., Azeemi, R., Nadeem, M., & Nasir, U. (2020). Development of shade prediction system to quantify the shade change after crease recovery finish application using artificial neural networks. *The Journal of The Textile Institute*, *112*(8), 1287-1294. https://doi.org/10.1080/00405000.2020.1812921

Furferi, R., Governi, L., & Volpe, Y. (2016). Color matching of fabric blends: Hybrid Kubelka-Munk+ artificial neural network based method. *Journal of Electronic Imaging*, *25*(6), 1-10. https://doi.org/10.1117/1.JEI.25.6.061402

Fushiki, T. (2011). Estimation of prediction error by using K-fold cross-validation. *Statistics and Computing*, *21*(2), 137-146. https://doi.org/10.1007/s11222-009-9153-8

Gadekar, M. R., & Ahammed, M. M. (2019). Modelling dye removal by adsorption onto water treatment residuals using combined response surface methodology-artificial neural network approach. *Journal of Environmental Management*, *231*, 241-248. https://doi.org/10.1016/j.jenvman.2018.10.017

Ghoranneviss, M., Moazzenchi, B., Shahidi, S., Anvari, A., & Rashidi, A. (2006). Decolorization of denim fabrics with cold plasmas in the presence of magnetic fields. *Plasma Processes and Polymers*, *3*(3), 316-321. https://doi.org/10.1002/ppap.200500061

Gotoh, K., & Yasukawa, A. (2011). Atmospheric pressure plasma modification of polyester fabric for improvement of textile-specific properties. *Textile Research Journal*, *81*(4), 368-378. https://doi.org/10.1177/0040517510387207

Griffin, L. D., & Sepehri, A. (2002). Performance of CIE94 for nonreference conditions. *Color Research and Application*, *27*(2), 108-115. https://doi.org/10.1002/col.10029

Haji, A., & Naebe, M. (2020). Cleaner dyeing of textiles using plasma treatment and natural dyes: A review. *Journal of Cleaner Production*, *265*, 1-13. https://doi.org/10.1016/j.jclepro.2020.121866

Haji, A., & Payvandy, P. (2020). Application of ANN and ANFIS in prediction of color strength of plasma-treated wool yarns dyed with a natural colorant. *Pigment & Resin Technology*, *49*(3), 171-180. https://doi.org/10.1108/PRT-10-2019-0089

Haji, A., Shahmoradi Ghaheh, F., & Indrie, L. (2022). Pomegranate fallen leaves as a source of natural dye for mordant‐free dyeing of wool. *Coloration Technology*, 1-6. https://doi.org/10.1111/cote.12651

Haji, A., & Vadood, M. (2021). Environmentally benign dyeing of polyester fabric with madder: modelling by artificial neural network and fuzzy logic optimized by genetic

algorithm. *Fibers and Polymers*, *22*(12), 3351-3357. https://doi.org/10.1007/s12221-021-1161-0

Hajipour, A., & Shams-Nateri, A. (2019). Improve neural network-based color matching of inkjet textile printing by classification with competitive neural network. *Color Research & Application*, *44*(1), 65-72. https://doi.org/10.1002/col.22246

Hasanzadeh, M., Moieni, T., & Moghadam, B. H. (2013). Modification of PET fabrics by hyperbranched polymer: a comparative study of artificial neural networks (ANN) and statistical approach. *Journal of Polymer Engineering*, *33*(5), 445-452. https://doi.org/10.1515/polyeng-2012-0145

Heggie, D., Wardman, R., & Luo, M. (1996). A comparison of the colour differences computed using the CIE94, CMC (l: c) and BFD (l: c) formulae. *Journal of the Society of Dyers and Colourists*, *112*(10), 264-269. https://doi.org/10.1111/j.1478-4408.1996.tb01755.x

Hemingray, C., & Westland, S. (2016). A novel approach to using neural networks to predict the colour of fibre blends. *Coloration Technology*, *132*(4), 297-303. https://doi.org/10.1111/cote.12220

Hodson, T. O. (2022). Root mean square error (RMSE) or mean absolute error (MAE): when to use them or not. *Geoscientific Model Development Discussions*, 1-10. https://doi.org/10.5194/gmd-2022-64

Hossain, I., Choudhury, I. A., Mamat, A. B., & Hossain, A. (2017). Predicting the colour properties of viscose knitted fabrics using soft computing approaches. *The Journal of the Textile Institute*, *108*(10), 1689-1699. https://doi.org/10.1080/00405000.2017.1279004

Hossain, I., Hossain, A., & Choudhury, I. A. (2015). Color strength modeling of viscose/Lycra blended fabrics using a fuzzy logic approach. *Journal of Engineered Fibers and Fabrics*, *10*(1), 158-168. https://doi.org/10.1177/155892501501000117

Hossain, I., Hossain, A., & Choudhury, I. A. (2016). Dyeing process parameters optimisation and colour strength prediction for viscose/lycra blended knitted fabrics using Taguchi method. *The Journal of The Textile Institute*, *107*(2), 154-164. https://doi.org/10.1080/00405000.2015.1018669

Hossain, I., Hossain, A., Choudhury, I. A., & Mamun, A. A. (2016). Fuzzy knowledge based expert system for prediction of color strength of cotton knitted fabrics. *Journal of Engineered Fibers and Fabrics*, *11*(3), 33-44. https://doi.org/10.1177/155892501601100306

Hu, L., Zhou, X., Chen, J., Zhang, X., Chen, G., Chang, W., Ye, A., Yi, H., & Yi, C. (2021). Investigation of color fading and fabric-touch test for jeans through ozonation. *Ozone: Science & Engineering*, *43*(3), 276-283. https://doi.org/10.1080/01919512.2020.1796584

Hung, O., Chan, C., Kan, C. W., Yuen, C., & Song, L. (2014). Artificial neural network approach for predicting colour properties of laser-treated denim fabrics. *Fibers and Polymers*, *15*(6), 1330-1336. https://doi.org/10.1007/s12221-014-1330-5

Hung, O., Song, L., Chan, C., Kan, C. W., & Yuen, C. (2011). Using artificial neural network to predict colour properties of laser-treated 100% cotton fabric. *Fibers and Polymers*, *12*(8), 1069-1076. https://doi.org/10.1007/s12221-011-1069-1

Hunt, R. W. G., & Pointer, M. R. (2011). Relations between Colour Stimuli. In M. A. Kriss (Ed.), *Measuring colour* (pp. 41-57). John Wiley & Sons.

Hwang, J. P., Kim, S., & Park, C. K. (2015). Development of a color matching algorithm for digital transfer textile printing using an artificial neural network and multiple regression. *Textile Research Journal*, *85*(10), 1076-1082. https://doi.org/10.1177/0040517515569525

Ibrahim, N., El-Zairy, E., Barakat, S., & Eid, B. M. (2022). Eco-Friendly Surface Modification and Multifunctionalization of Cotton Denim Fabric. *Egyptian Journal of Chemistry*, *65*(13), 39-51. https://doi.org/10.21608/EJCHEM.2022.147161.6382

Ibrahim, N. A., & Eid, B. M. (2020). Plasma treatment technology for surface modification and functionalization of cellulosic fabrics. In M. Shahid & R. Adivarekar (Eds.), *Advances in Functional Finishing of Textiles* (pp. 275-287). Springer. https://doi.org/10.1007/978-981-15-3669-4_12

Ibrahim, N. A., Hashem, M. M., Eid, M. A., Refai, R., El-Hossamy, M., & Eid, B. M. (2010). Eco-friendly plasma treatment of linen-containing fabrics. *The Journal of The Textile Institute*, *101*(12), 1035-1049. https://doi.org/10.1080/00405000903205467

Jang, J. (1993). ANFIS: adaptive-network-based fuzzy inference system. *IEEE Transactions on Systems, Man, and Cybernetics*, *23*(3), 665-685. https://doi.org/10.1109/21.256541

Jawahar, M., Narasimhan Kannan, C. B., & Kondamudi Manobhai, M. (2015). Artificial neural networks for colour prediction in leather dyeing on the basis of a tristimulus system. *Coloration Technology*, *131*(1), 48-57. https://doi.org/10.1111/cote.12123

Jee, J. G., Kim, M. B., & Lee, C. H. (2005). Pressure swing adsorption processes to purify oxygen using a carbon molecular sieve. *Chemical Engineering Science*, *60*(3), 869-882. https://doi.org/10.1016/j.ces.2004.09.050

Jelil, R. A. (2015). A review of low-temperature plasma treatment of textile materials. *Journal of Materials Science*, *50*(18), 5913-5943. https://doi.org/10.1007/s10853-015-9152-4

Jung, Y., & Hu, J. (2015). A K-fold averaging cross-validation procedure. *Journal of nonparametric statistics*, *27*(2), 167-179. https://doi.org/10.1080/10485252.2015.1010532

Kan, C. W. (2014). *A novel green treatment for textiles: Plasma treatment as a sustainable technology*. CRC Press. https://doi.org/10.1201/b17328

Kan, C. W., Cheung, H. F., & Chan, Q. (2016). A study of plasma-induced ozone treatment on the colour fading of dyed cotton. *Journal of Cleaner Production*, *112*(4), 3514-3524. https://doi.org/10.1016/j.jclepro.2015.10.100

Kan, C. W., Cheung, H. F., & Kooh, F. M. (2017). An investigation of color fading of sulfur-dyed cotton fabric by plasma treatment. *Fibers and Polymers*, *18*(4), 767-772. https://doi.org/10.1007/s12221-017-6934-0

Kan, C. W., Lam, C.-F., Chan, C.-K., & Ng, S.-P. (2014). Using atmospheric pressure plasma treatment for treating grey cotton fabric. *Carbohydrate Polymers*, *102*, 167-173. https://doi.org/10.1016/j.carbpol.2013.11.015

Kan, C. W., & Song, L. (2016). An artificial neural network model for prediction of colour properties of knitted fabrics induced by laser engraving. *Neural Processing Letters*, *44*(3), 639-650. https://doi.org/10.1007/s11063-015-9485-7

Kan, C. W., Yuen, C., & Cheng, C. (2010). Technical study of the effect of CO_2 laser surface engraving on the colour properties of denim fabric. *Coloration Technology*, *126*(6), 365-371. https://doi.org/10.1111/j.1478-4408.2010.00270.x

Kan, C. W., & Yuen, C. W. (2012). Effect of atmospheric pressure plasma treatment on the desizing and subsequent colour fading process of cotton denim fabric. *Coloration Technology*, *128*(5), 356-363. https://doi.org/10.1111/j.1478-4408.2012.00388.x

Kan, C. W., & Yuen, C. W. M. (2007). Plasma technology in wool. *Textile Progress*, *39*(3), 121-187. https://doi.org/10.1080/00405160701628839

Ke, G., Mulla, M. S., Peng, F., & Chen, S. (2023). Dyeing properties of natural Gardenia on the lyocell fabric pretreated with tannic acid. *Cellulose*, *30*(1), 611-624. https://doi.org/10.1007/s10570-022-04896-w

Khan, H., Ahmad, N., Yasar, A., & Shahid, R. (2010). Advanced Oxidative Decolorization of Red Cl-5B: Effects of Dye Concentration, Process Optimization and Reaction Kinetics. *Polish Journal of Environmental Studies*, *19*(1), 83-92. http://www.pjoes.com/pdf-88359-22217?filename=Advanced%20Oxidative.pdf

Lam, Y., Kan, C. W., & Yuen, C. (2011). Effect of plasma pretreatment on the wrinkle-resistance properties of cotton fibers treated with a 1, 2, 3, 4-butanetetracarboxylic acid–sodium hypophosulfite system with titanium dioxide as a cocatalyst. *Journal of Applied Polymer Science*, *120*(3), 1403-1410. https://doi.org/10.1002/app.32960

Leroux, F., Perwuelz, A., Campagne, C., & Behary, N. (2006). Atmospheric air-plasma treatments of polyester textile structures. *Journal of Adhesion Science and Technology*, *20*(9), 939-957. https://doi.org/10.1163/156856106777657788

Li, F., Chen, C., & Mao, Z. (2022). A novel approach for recipe prediction of fabric dyeing based on feature-weighted support vector regression and particle swarm optimisation. *Coloration Technology*, *138*(5), 495-508. https://doi.org/10.1111/cote.12607

Li, J., Shi, W., & Yang, D. (2020). Color difference classification of dyed fabrics via a kernel extreme learning machine based on an improved grasshopper optimization algorithm. *Color Research & Application*, *46*(2), 388-401. https://doi.org/10.1002/col.22581

Li, P. F., Ning, Y. W., & Jing, J. F. (2017). Research on the detection of fabric color difference based on T-S fuzzy neural network. *Color Research & Application*, *42*(5), 609-618. https://doi.org/10.1002/col.22113

Li, P. F., Wang, J., & Jing, J. F. (2015). Application of improved back propagation algorithm in color difference detection of fabric. *Color Research & Application*, *40*(3), 311-317. https://doi.org/10.1002/col.21895

Liu, X., & Yang, D. (2021). Color constancy computation for dyed fabrics via improved marine predators algorithm optimized random vector functional-link network. *Color Research & Application*, *46*(5), 1066-1078. https://doi.org/10.1002/col.22653

Liu, Y. H., To, C. K. M., Ngai, M. K., Kan, C. W., & Chua, H. (2019). Atmospheric pressure plasma-induced decolorisation of cotton knitted fabric dyed with reactive dye. *Coloration Technology*, *135*(6), 516-528. https://doi.org/10.1111/cote.12441

Liu, Z., & Liang, Y. (2018). The spectral characterizing model based on optimized RBF neural network for digital textile printing. In P. Zhao, Y. Ouyang, M. Xu, L. Yang, & Y. Ren

173

(Eds.), *Applied Sciences in Graphic Communication and Packaging* (Vol. 477, pp. 55-60). Springer. https://doi.org/10.1007/978-981-10-7629-9_7

Lu, J., Behbood, V., Hao, P., Zuo, H., Xue, S., & Zhang, G. (2015). Transfer learning using computational intelligence: A survey. *Knowledge-Based Systems*, *80*, 14-23. https://doi.org/10.1016/j.knosys.2015.01.010

Marasco, S., Marano, G. C., & Cimellaro, G. P. (2022). Evolutionary polynomial regression algorithm combined with robust bayesian regression. *Advances in Engineering Software*, *167*, 1-14. https://doi.org/10.1016/j.advengsoft.2022.103101

MathWorks. (2022a). *Least-Squares Fitting*. Retrieved 11st January 2023 from https://ww2.mathworks.cn/help/curvefit/least-squares-fitting.html?requestedDomain=en

MathWorks. (2022b). *Polynomial Models*. Retrieved 10th January from https://www.mathworks.com/help/curvefit/polynomial.html

Maulud, D., & Abdulazeez, A. M. (2020). A review on linear regression comprehensive in machine learning. *Journal of Applied Science and Technology Trends*, *1*(4), 140-147. https://doi.org/10.38094/jastt1457

Melgosa, M. (2000). Testing CIELAB‐based color‐difference formulas. *Color Research & Application*, *25*(1), 49-55. https://doi.org/10.1002/(SICI)1520-6378(200002)25:1<49::AID-COL7>3.0.CO;2-4

Minaker, S. A., Mason, R. H., & Chow, D. R. (2021). Optimizing Color Performance of the Ngenuity 3-Dimensional Visualization System. *Ophthalmology Science*, *1*(3), 1-9. https://doi.org/10.1016/j.xops.2021.100054

Mitrović, T., Ristić, M., Perić-Grujić, A., & Lazović, S. (2020). ANN prediction of the efficiency of the decolourisation of organic dyes in wastewater by plasma needle. *Journal of the Serbian Chemical Society*, *85*(6), 831-844. https://doi.org/10.2298/JSC191004002M

Morent, R., De Geyter, N., Verschuren, J., De Clerck, K., Kiekens, P., & Leys, C. (2008). Non-thermal plasma treatment of textiles. *Surface and Coatings Technology*, *202*(14), 3427-3449. https://doi.org/10.1016/j.surfcoat.2007.12.027

Mundadaa, P., & Brighub, U. (2016). Remediation of textile effluent using siliceous materials: A review with a proposed alternative. *Adsorption*, *3*(1), 1-5. https://doi.org/10.1016/S0960-8524(00)00080-8

Nateri, A. S., Hajipour, A., Balarak, S., & Khayati, G. (2017). Prediction of the concentration of dye and nanosilver particle on silk fabric using artificial neural network. *Pigment & Resin Technology*, *46*(6), 433-439. https://doi.org/10.1108/PRT-11-2016-0114

Nobbs, J. H. (1985). Kubelka—Munk theory and the prediction of reflectance. *Review of Progress in Coloration and Related Topics*, *15*(1), 66-75. https://doi.org/10.1111/j.1478-4408.1985.tb03737.x

Omerogullari Basyigit, Z., Eyupoglu, C., Eyupoglu, S., & Merdan, N. (2023). Investigation and Feed-Forward Neural Network-Based Estimation of Dyeing Properties of Air Plasma Treated Wool Fabric Dyed with Natural Dye Obtained from Hibiscus Sabdariffa. *Coloration Technology*, 1-13. https://doi.org/10.1111/cote.12665

Ondogan, Z., Pamuk, O., Ondogan, E. N., & Ozguney, A. (2005). Improving the appearance of all textile products from clothing to home textile using laser technology. *Optics & Laser Technology*, *37*(8), 631-637. https://doi.org/10.1016/j.optlastec.2004.10.001

Ortiz-Morales, M. n., Poterasu, M., Acosta-Ortiz, S. E., Compean, I., & Hernandez-Alvarado, M. R. (2003). A comparison between characteristics of various laser-based denim fading processes. *Optics and Lasers in Engineering*, *39*(1), 15-24. https://doi.org/10.1016/S0143-8166(02)00073-8

Ostertagova, E., & Ostertag, O. (2012). Forecasting using simple exponential smoothing method. *Acta Electrotechnica et Informatica*, *12*(3), 62-66. https://doi.org/10.2478/v10198-012-0034-2

Özkan, İ., Baykal, P. D., & Özdemir, H. (2018). Effects of intermingled yarn surface characteristics on knitted fabric's color parameters. *Tekstil ve Mühendis*, *25*(112), 327-334. https://doi.org/10.7216/1300759920182511206

Paul, R. (2015). Denim and jeans: an overview. In R. Paul (Ed.), *Denim* (pp. 1-11). Woodhead Publishing. https://doi.org/10.1016/B978-0-85709-843-6.00001-9

Peran, J., & Ercegović Ražić, S. (2020). Application of atmospheric pressure plasma technology for textile surface modification. *Textile Research Journal*, *90*(9-10), 1174-1197. https://doi.org/10.1177/0040517519883954

Periyasamy, A. P., & Periyasami, S. (2023). Critical Review on Sustainability in Denim: A Step toward Sustainable Production and Consumption of Denim. *ACS Omega*, 1-15. https://doi.org/10.1021/acsomega.2c06374

Radetic, M., Jovancic, P., Puac, N., & Petrovic, Z. L. (2007, July). Environmental impact of plasma application to textiles. Journal of Physics: Conference Series, https://doi.org/10.1088/1742-6596/71/1/012017

Radetić, M., Jovančić, P., Puač, N., Petrović, Z. L., & Šaponjić, Z. (2009). Plasma-induced decolorization of indigo-dyed denim fabrics related to mechanical properties and fiber surface morphology. *Textile Research Journal*, *79*(6), 558-565. https://doi.org/10.1177/0040517508095612

Rahaman, G. A., Parkkinen, J., & Hauta-Kasari, M. (2020). A novel approach to using spectral imaging to classify dyes in colored fibers. *Sensors*, *20*(16), 1-14. https://doi.org/10.3390/s20164379

Robinson, T., McMullan, G., Marchant, R., & Nigam, P. (2001). Remediation of dyes in textile effluent: a critical review on current treatment technologies with a proposed alternative. *Bioresource Technology*, *77*(3), 247-255. https://doi.org/10.1016/S0960-8524(00)00080-8

Rodriguez, J. D., Perez, A., & Lozano, J. A. (2009). Sensitivity analysis of k-fold cross validation in prediction error estimation. *IEEE transactions on pattern analysis and machine intelligence*, *32*(3), 569-575. https://doi.org/10.1109/TPAMI.2009.187

Rosa, J. M., Guerhardt, F., Ribeiro Júnior, S. E. R., Belan, P. A., Lima, G. A., Santana, J. C. C., Berssaneti, F. T., Tambourgi, E. B., Vanale, R. M., & Araújo, S. A. d. (2021). Modeling and optimization of reactive cotton dyeing using response surface methodology combined with artificial neural network and particle swarm techniques. *Clean Technologies and Environmental Policy*, *23*(8), 2357-2367. https://doi.org/10.1007/s10098-021-02142-8

Şahin, C., Balcı, O., Işık, M., & Gökenç, İ. (2022). Artificial neural networks approach for prediction of CIELab values for yarn after dyeing and finishing process. *The Journal of The Textile Institute*, 1-10. https://doi.org/10.1080/00405000.2022.2124629

Samanta, K., Basak, S., & Chattopadhyay, S. (2017). Environmentally friendly denim processing using water-free technologies. In K. Samanta, S. Basak, & S. Chattopadhyay (Eds.), *Sustainability in Denim* (pp. 319-348). Woodhead Publishing. https://doi.org/10.1016/B978-0-08-102043-2.00012-5

Shaffer, K. J., McLean, T. M., Waterland, M. R., Wenzel, M., & Plieger, P. G. (2012). Structural characterisation of difluoro-boron chelates of quino [7, 8-h] quinoline. *Inorganica Chimica Acta*, *380*, 278-283. https://doi.org/10.1016/j.ica.2011.09.046

Sharma, G., Wu, W., & Dalal, E. N. (2005). The CIEDE2000 color‑difference formula: Implementation notes, supplementary test data, and mathematical observations. *Color Research and Application*, *30*(1), 21-30. https://doi.org/10.1002/col.20070

Shen, J., & Zhou, X. (2017). Spectrophotometric colour matching algorithm for top‑dyed mé lange yarn, based on an artificial neural network. *Coloration Technology*, *133*(4), 341-346. https://doi.org/10.1111/cote.12285

Sircar, S. (2002). Pressure swing adsorption. *Industrial & Engineering Chemistry Research*, *41*(6), 1389-1392. https://doi.org/10.1021/ie0109758

Specht, D. F. (1991). A general regression neural network. *IEEE Transactions on Neural Networks*, *2*(6), 568-576. https://doi.org/10.1109/72.97934

Srikrishnan, M., & Jyoshitaa, S. (2022). An Overview of Preparation, Processes for Sustainable Denim Manufacturing. In S. M. Subramanian (Ed.), *Sustainable Approaches in Textiles and Fashion* (pp. 119-131). Springer. https://doi.org/10.1007/978-981-19-0538-4_5

Stegmaier, T., Linke, M., Dinkelmann, A., Von Arnim, V., & Planck, H. (2009). Environmentally friendly plasma technologies for textiles. In R. S. Blackburn (Ed.), *Sustainable textiles: Life cycle and environmental impact* (Vol. I, pp. 155-178). Woodhead Publishing. https://doi.org/10.1533/9781845696948.1.155

Stone, M. H. (1948). The generalized Weierstrass approximation theorem. *Mathematics Magazine*, *21*(5), 237-254. https://doi.org/10.2307/3029337

Tang, A. Y. L., Lee, C. H., Wang, Y., & Kan, C. W. (2018). Dyeing properties of cotton with reactive dye in nonane nonaqueous reverse micelle system. *ACS omega*, *3*(3), 2812-2819. https://doi.org/10.1021/acsomega.8b00032

Tonks, L., & Langmuir, I. (1929). A general theory of the plasma of an arc. *Physical Review*, *34*(6), 876. https://doi.org/10.1103/PhysRev.34.876

Vadood, M., & Haji, A. (2022a). Application of ANN Weighted by Optimization Algorithms to Predict the Color Coordinates of Cellulosic Fabric in Dyeing with Binary Mix of Natural Dyes. *Coatings*, *12*(10), 1-14. https://doi.org/10.3390/coatings12101519

Vadood, M., & Haji, A. (2022b). A hybrid artificial intelligence model to predict the color coordinates of polyester fabric dyed with madder natural dye. *Expert Systems with Applications*, *193*, 1-8. https://doi.org/10.1016/j.eswa.2022.116514

Venkatraman, P. D., & Liauw, C. M. (2019). Use of a carbon dioxide laser for environmentally beneficial generation of distressed/faded effects on indigo dyed denim fabric: Evaluation of colour change, fibre morphology, degradation and textile properties.

Optics & Laser Technology, *111*, 701-713. https://doi.org/10.1016/j.optlastec.2018.09.004

Voss, C. (2005). Applications of pressure swing adsorption technology. *Adsorption*, *11*(Suppl 1), 527-529. https://doi.org/10.1007/s10450-005-5979-3

Wong, T. T. (2015). Performance evaluation of classification algorithms by k-fold and leave-one-out cross validation. *Pattern Recognition*, *48*(9), 2839-2846. https://doi.org/10.1016/j.patcog.2015.03.009

Xie, G., Xu, Y., Yu, Z., & Sun, Y. (2020). An algorithm for online detection of colour differences in warp knitted fabrics. *The Journal of The Textile Institute*, *113*(1), 159-165. https://doi.org/10.1080/00405000.2020.1866280

Xie, G., Xu, Y., Yu, Z., & Sun, Y. (2021). An intelligent defect detection system for warp-knitted fabric. *Textile Research Journal*, *92*(9-10), 1394-1404. https://doi.org/10.1177/00405175211060084

Yadav, S., & Shukla, S. (2016, Feb 27-28). Analysis of k-fold cross-validation over hold-out validation on colossal datasets for quality classification. 2016 IEEE 6th International Advance Computing Conference (IACC), Bhimavaram, India. https://doi.org/10.1109/IACC37532.2016

Yu, C., Cao, W., Liu, Y., Shi, K., & Ning, J. (2021). Evaluation of a novel computer dye recipe prediction method based on the PSO-LSSVM models and single reactive dye database. *Chemometrics and Intelligent Laboratory Systems*, *218*, 1-7. https://doi.org/10.1016/j.chemolab.2021.104430

Yu, C., Xi, Z., Lu, Y., Tao, K., & Yi, Z. (2020). K/S value prediction of cotton fabric using PSO-LSSVM. *Textile Research Journal*, *90*(23-24), 2581-2591. https://doi.org/10.1177/0040517520924750

Zhang, J., & Yang, C. (2014). Evaluation model of color difference for dyed fabrics based on the support vector machine. *Textile Research Journal*, *84*(20), 2184-2197. https://doi.org/10.1177/0040517514537372

Zhang, J., Zhang, X., Wu, J., & Xiao, C. (2021). Dyeing recipe prediction of cotton fabric based on hyperspectral colour measurement and an improved recurrent neural network. *Coloration Technology*, *137*(2), 166-180. https://doi.org/10.1111/cote.12516

Zhang, J., Zheng, Z., Zhang, Y., Feng, J., & Li, J. (2008). Low-temperature plasma-induced degradation of aqueous 2, 4-dinitrophenol. *Journal of Hazardous Materials*, *154*(1-3), 506-512. https://doi.org/10.1016/j.jhazmat.2007.10.053

Zhang, J. x., Zhang, P., Wu, X. l., Zhou, Z. y., & Yang, C. (2017). Illumination compensation in textile colour constancy, based on an improved least‑squares support vector regression and an improved GM (1, 1) model of grey theory. *Coloration Technology*, *133*(2), 128-134. https://doi.org/10.1111/cote.12243

Zhang, X., & Zhou, Z. (2022). Classifying colour differences in dyed fabrics using an improved hunger games search optimised random vector functional link. *Journal of Engineered Fibers and Fabrics*, *17*, 1-11. https://doi.org/10.1177/15589250221111508

Zhang, Y., & Yang, Y. (2015). Cross-validation for selecting a model selection procedure. *Journal of Econometrics*, *187*(1), 95-112. https://doi.org/10.1016/j.jeconom.2015.02.006

Zhong, D., Liu, Y. H., Cheung, N. T., Kan, C. W., & Chua, H. (2018). A parameter study of the effect of a plasma-induced ozone colour-fading process on sulphur-dyed cotton fabric. *Processes*, *6*(7), 1-10. https://doi.org/10.3390/pr6070081

Zhou, Z., Gao, X., Zhang, J., Zhu, Z., & Hu, X. (2019). A novel hybrid model using the rotation forest-based differential evolution online sequential extreme learning machine for illumination correction of dyed fabrics. *Textile Research Journal*, *89*(7), 1180-1197. https://doi.org/10.1177/0040517518764020

Zhou, Z., Gao, X., Zhu, Z., & Hu, X. (2019). Illumination correction of dyed fabrics method using rotation forest‑based ensemble particle swarm optimization and sparse least squares support vector regression. *Color Research & Application*, *44*(1), 73-87. https://doi.org/10.1002/col.22262

Zhou, Z., Liu, D., Zhang, J., Zhu, Z., Yang, D., & Jiang, L. (2021). Colour difference classification for dyed fabrics based on differential evolution with dynamic parameter selection to optimise the output regularisation extreme learning machine. *Fibres & Textiles in Eastern Europe*, *3*(147), 97-102. https://doi.org/10.5604/01.3001.0014.7794

Zhou, Z., Wang, C., Zhang, J., & Zhu, Z. (2019). Color difference classification of solid color printing and dyeing products based on optimization of the extreme learning machine of the improved whale optimization algorithm. *Textile Research Journal*, *90*(2), 135-155. https://doi.org/10.1177/0040517519859933

Zhou, Z., Xu, R., Wu, D., Zhu, Z., & Wang, H. (2016). Illumination correction of dyed fabrics approach using Bagging-based ensemble particle swarm optimization–extreme learning machine. *Optical Engineering*, *55*(9), 1-12. https://doi.org/10.1117/1.OE.55.9.093102

Zille, A., Oliveira, F. R., & Souto, A. P. (2015). Plasma treatment in textile industry. *Plasma Processes And Polymers*, *12*(2), 98-131. https://doi.org/10.1002/ppap.201400052